Adventures in Structural Design Using Theoretical, Computational, and Experimental Fracture Mechanics

Roberto Ballarini

Leonard Case Jr. Professor of Engineering
Case Western Reserve University

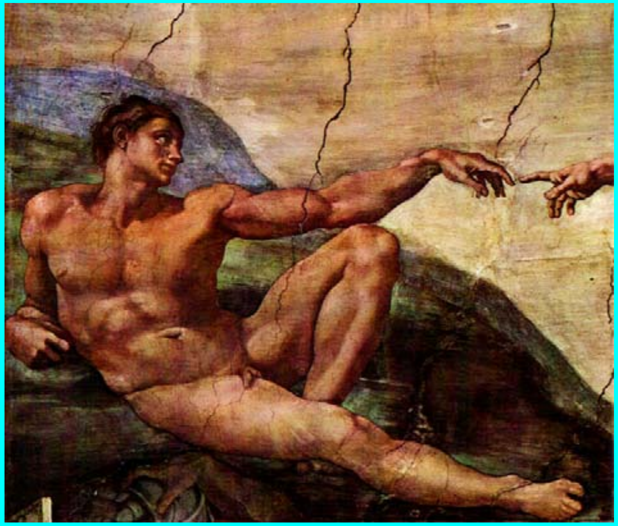

University of Minnesota
April 10, 2006

Theme
What I enjoy and have been doing.

- Mechanism-based design guidelines.
- Exploration and modeling of failure mechanisms.
- Whatever it takes experimentation.

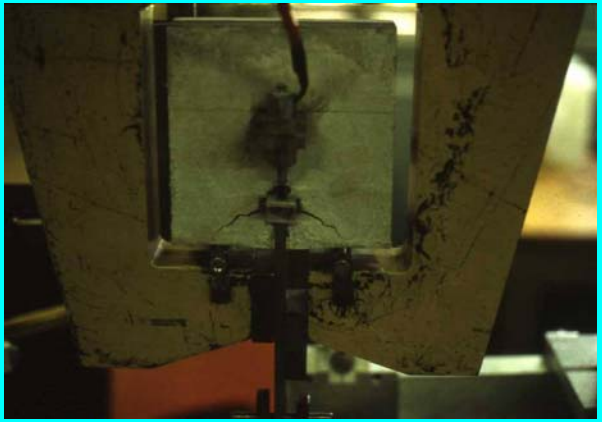

Design of anchor bolts

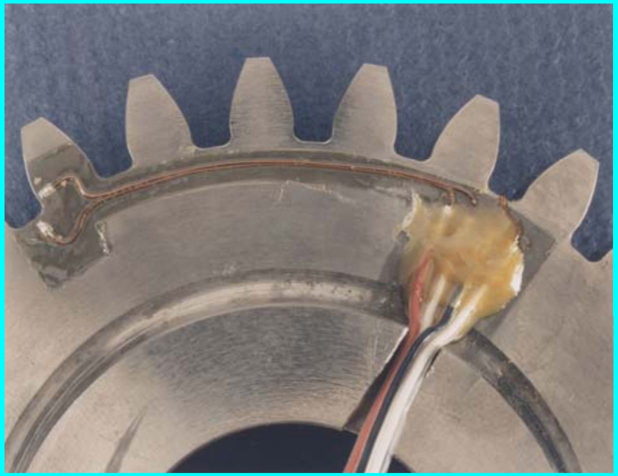

Design guidelines for spur gears

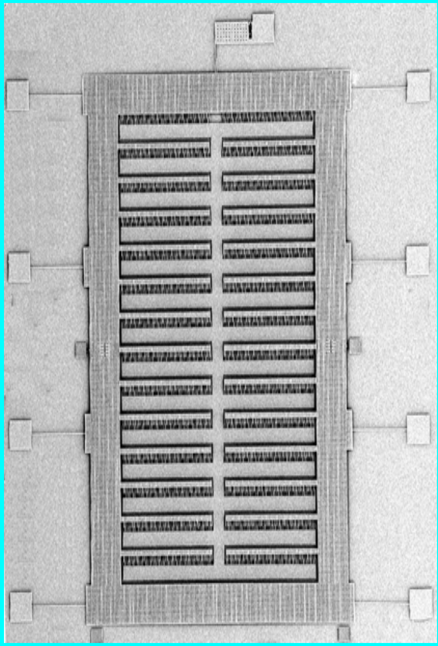

Fatigue of MEMS materials/structures

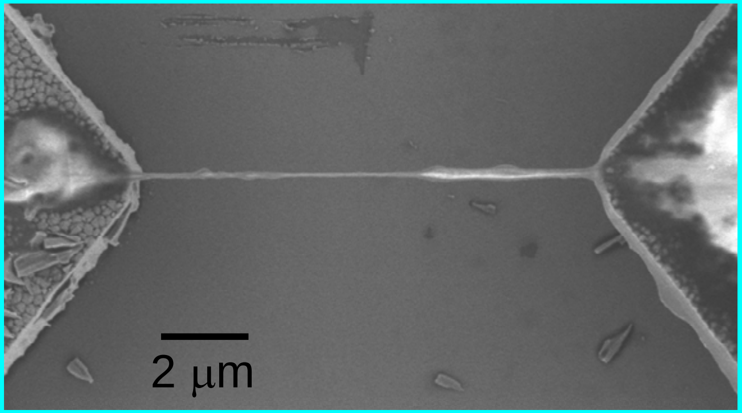

Mechanical testing of nanofibers

Linear Elastic Fracture Mechanics

Stress field near crack tip

$$\sigma_{ij} = \frac{K_I}{\sqrt{2\pi r}} f_{ij}^{I}(\theta) + \frac{K_{II}}{\sqrt{2\pi r}} f_{ij}^{II}(\theta)$$

Initiation criterion

$$F\left(K_I, K_{II}, K_{III}\right) = F_{critical}$$

Direction of growth

$$K_{II}^{local} = 0$$

K_I = mode I stress intensity factor

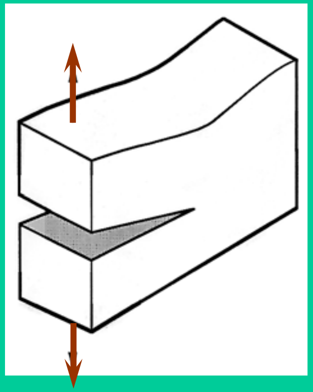

K_{II} = mode II stress intensity factor

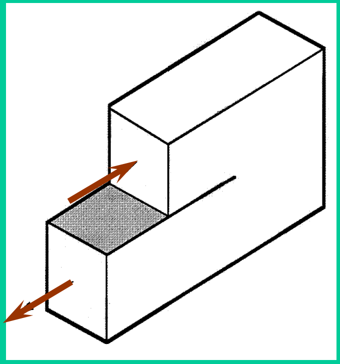

CRACK GROWTH MECHANISMS

Fast fracture

$$K_I = F(a/b)\sigma\sqrt{\pi a} = K_I^{cr}$$

High cycle fatigue

$$\frac{da}{dN} = C\left(\Delta K_I\right)^m$$

Stress corrosion

$$\frac{da}{dt} = DK_I^n$$

ANCHOR BOLTS

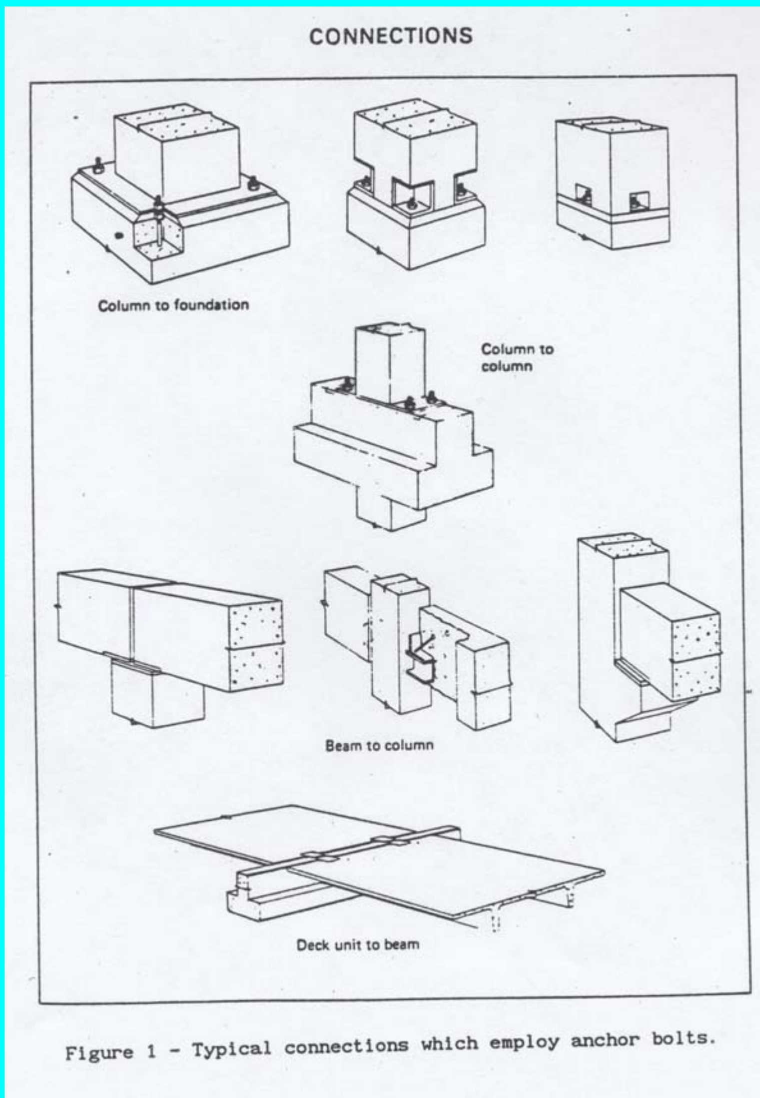

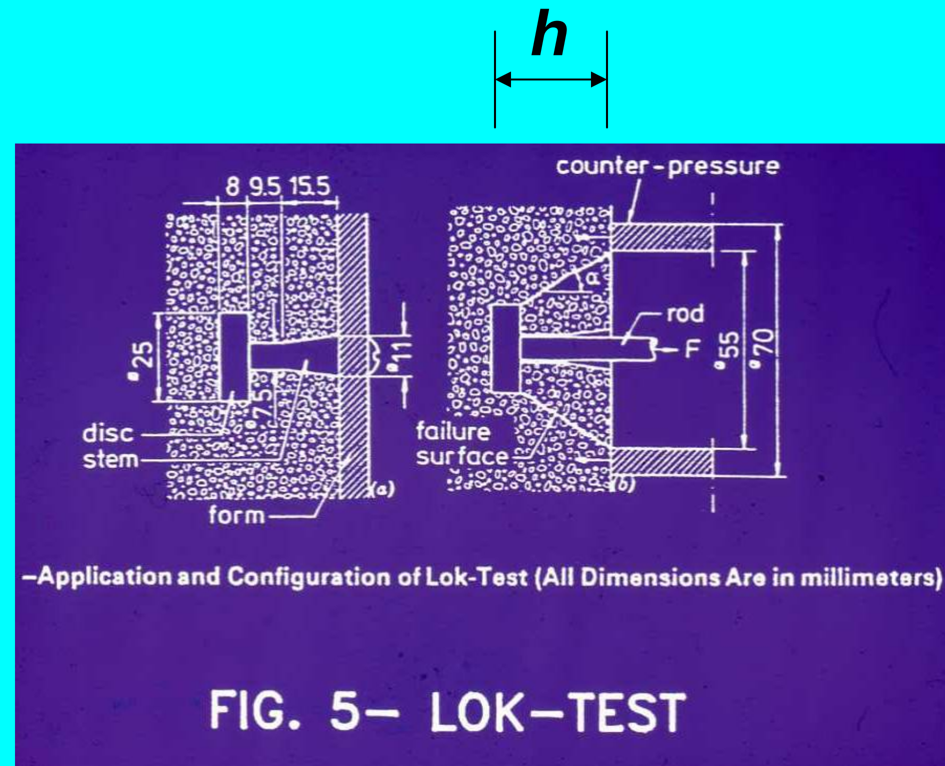

ACI Code:

$$P_u \approx f_t h^2$$

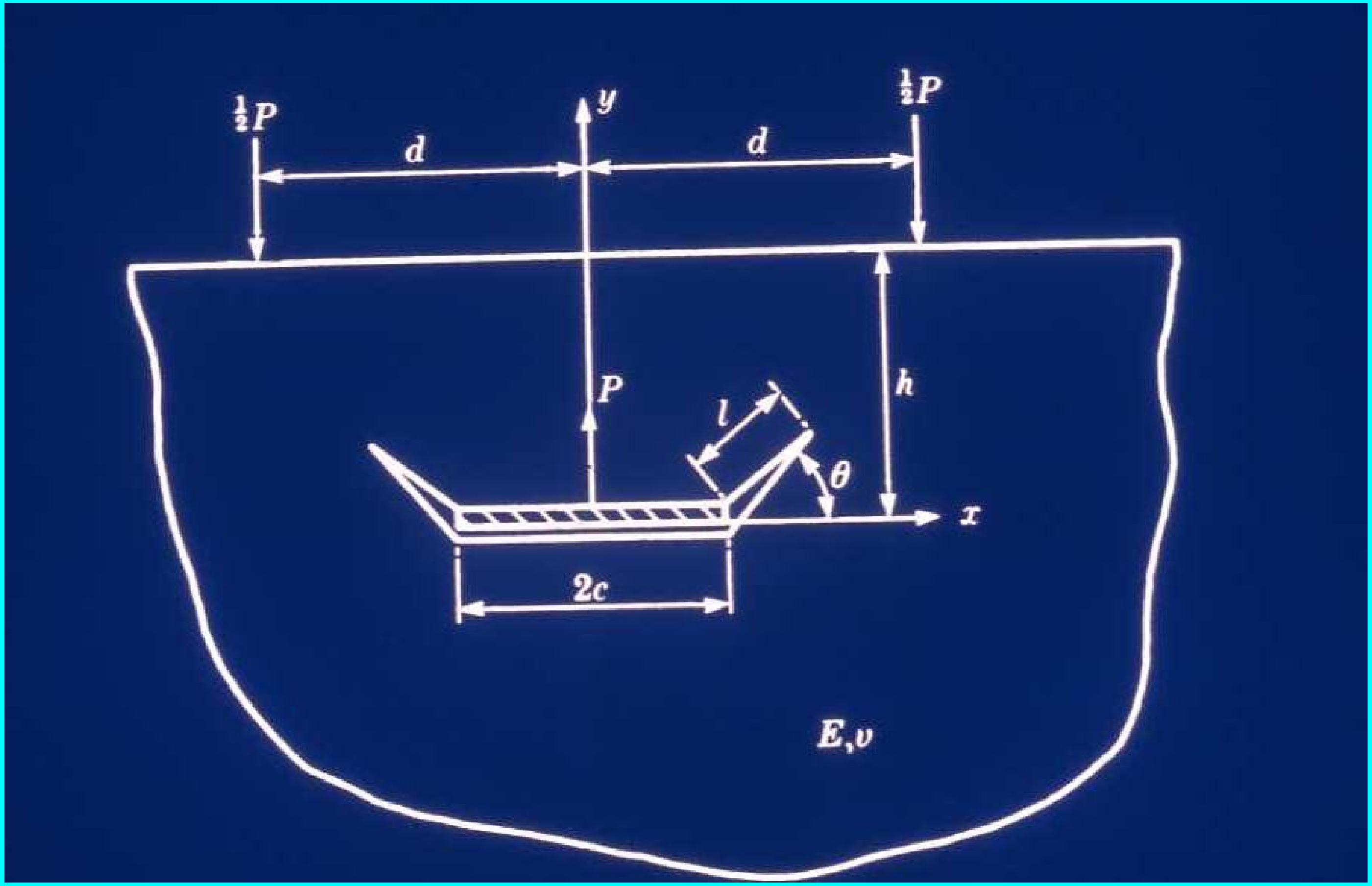

Ballarini *et al., Proc. Roy. Soc. Lond.,1985*

$$P_u \approx K_{Ic} h^{3/2} = \sqrt{EG_f}\, h^{3/2}$$

$$\alpha(\xi) = \frac{-1}{2\pi(\kappa+1)} \frac{\partial}{\partial \xi} (F_x + \mathrm{i} F_y),$$

$$\beta(\xi) = \frac{\mu e^{\mathrm{i}\theta}}{\pi \mathrm{i}(\kappa+1)} \frac{\partial}{\partial \xi} \{[u_r] + \mathrm{i}[v_\theta]\},$$

$$\psi(\tau) = \frac{\mu e^{\mathrm{i}\theta}}{\pi \mathrm{i}(\kappa+1)} \frac{\partial}{\partial \tau} \{[u_r] + \mathrm{i}[v_\theta]\},$$

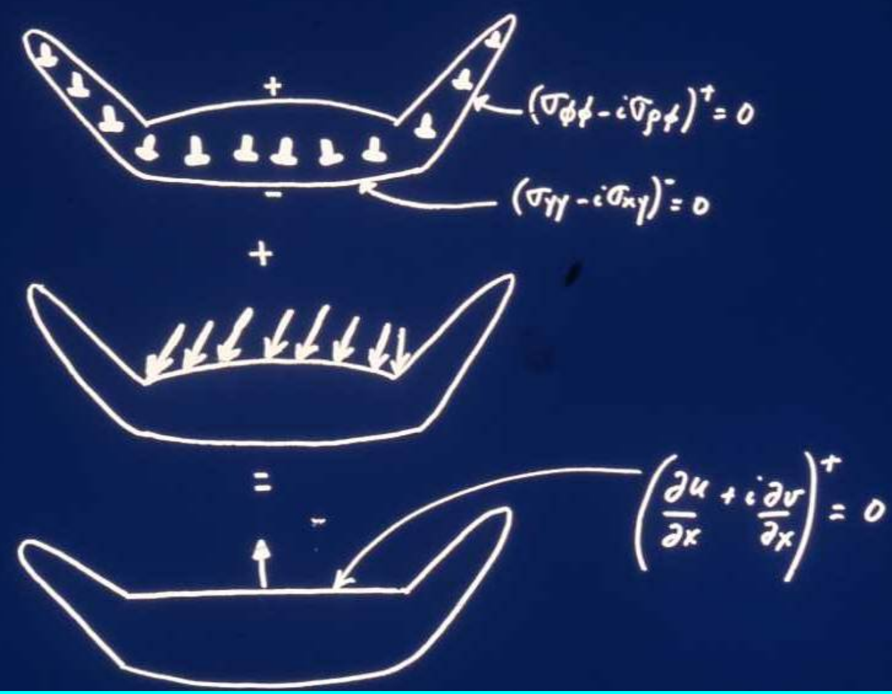

$$\int_0^c \alpha(\xi) \left\{\frac{\kappa-1}{\xi-x} + K_1(x,\xi) - K_2(x,-\xi)\right\} d\xi + \int_0^c \overline{\alpha(\xi)} \left\{K_2(x,\xi) - K_1(x,-\xi)\right\} d\xi$$

$$+ \pi i\ (\kappa+1)\ \alpha\ (x) + \int_0^c \beta(\rho) \left\{\frac{-2}{\rho-x} + K_3(x,\rho) - K_4(x,-\rho)\right\} d\rho$$

$$+ \int_0^c \overline{\beta(\rho)} \left\{K_4(x,\rho) - K_3(x,-\rho)\right\} d\rho$$

$$+ \int_0^\ell \psi(\tau)\ K_9(x,\tau)\ d\tau + \int_0^\ell \overline{\psi(\tau)}\ K_{10}\ (x,\tau)\ d\tau + f_1(x) = 0 \qquad -c \le x \le c$$

$$\int_0^c \alpha(\xi) \left\{K_{13}(t,\xi) - K_{14}(t,-\xi)\right\} d\xi + \int_0^c \overline{\alpha(\xi)} \left\{K_{14}\ (t,\xi) - K_{13}(t,-\xi)\right\} d\xi$$

$$+ \int_0^c \beta(\xi) \left\{K_{15}(t,\xi) - K_{16}(t,-\xi)\right\} d\xi + \int_0^c \overline{\beta(\xi)} \left\{K_{16}(t,\xi) - K_{15}(t,-\xi)\right\} d\xi$$

$$+ 2 \int_0^\ell \frac{\psi(\tau) d\tau}{(t-\tau)e^{i\theta}} + \int_0^\ell \psi(\xi)\ K_{17}(t,\tau)\ d\tau \quad + \int_0^\ell \overline{\psi(\tau)}\ K_{18}(t,\tau)\ d\tau + f_3(t) = 0 \qquad 0 \le t \le \ell$$

$$\int_0^c \alpha(\xi) \left\{\frac{-2\kappa}{\xi-x} + K_5(x,\xi) - K_6(x,-\xi)\right\} d\xi + \int_0^c \overline{\alpha(\xi)} \left\{K_6(x,\xi) - K_5(x,-\xi)\right\} d\xi$$

$$+ \int_0^c \beta(\rho) \left\{\frac{1-\kappa}{\rho-x} + K_7(x,\rho) - K_8(x,-\rho)\right\} d\rho + \int_0^c \overline{\beta(\rho)} \left\{K_8(x,\rho) - K_7(x,-\rho)\right\} d\rho$$

$$-\pi i\ (\kappa+1)\ \beta\ (x) + \int_0^\ell \psi(\tau)\ K_{11}(x,\tau)\ d\tau + \int_0^\ell \overline{\psi(\tau)}\ K_{12}(x,\tau)\ d\tau$$

$$+ f_2(x) = 0 \qquad -c \le x \le c$$

$$\int_0^c \left[\alpha(\xi) - \overline{\alpha(\xi)}\right] d\xi = \frac{P}{2\pi i(\kappa+1)}$$

$$\int_0^c \left[\beta(\xi) - \overline{\beta(\xi)}\right] d\xi + \int_0^\ell \left[\psi(\tau) - \overline{\psi(\tau)}\right] d\tau = 0$$

Stress intensity factor analysis

$$\frac{K\sqrt{c}}{P}$$

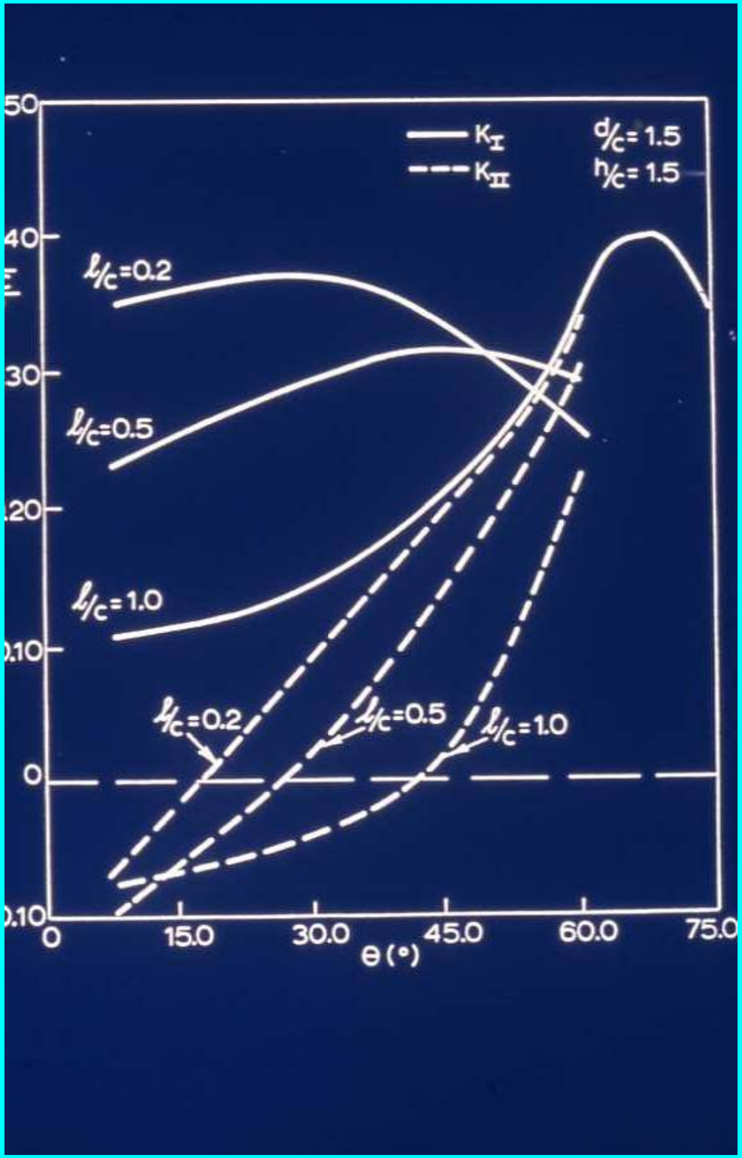

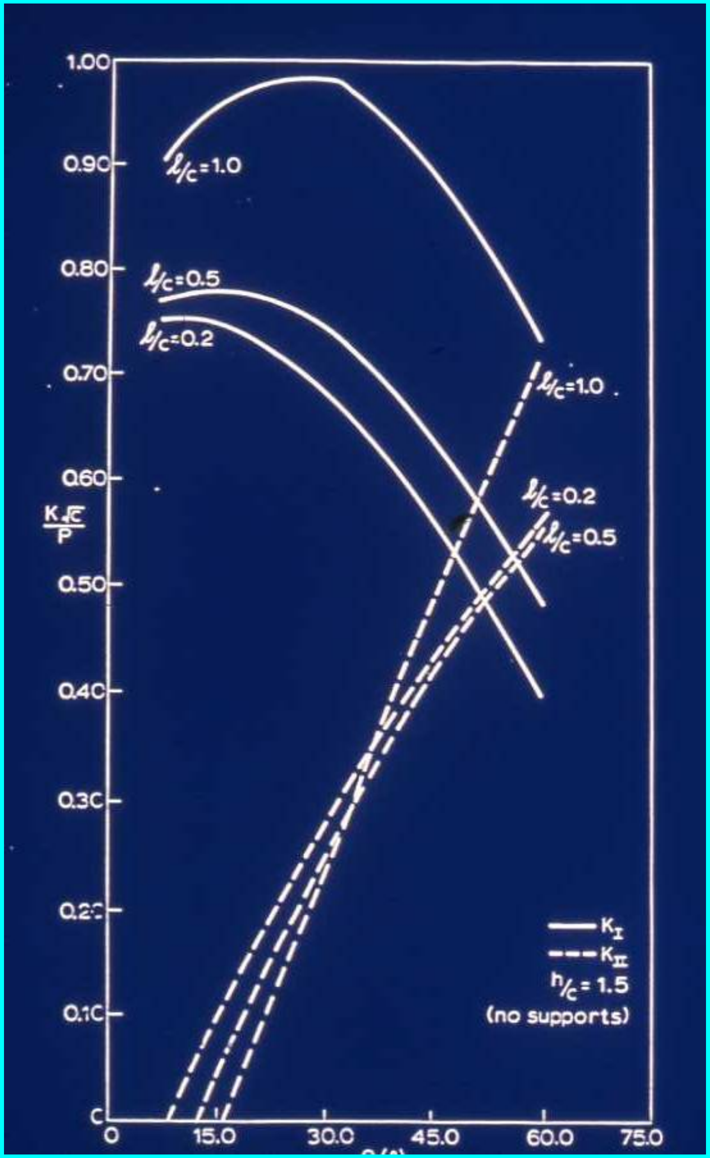

θ

Design Curve

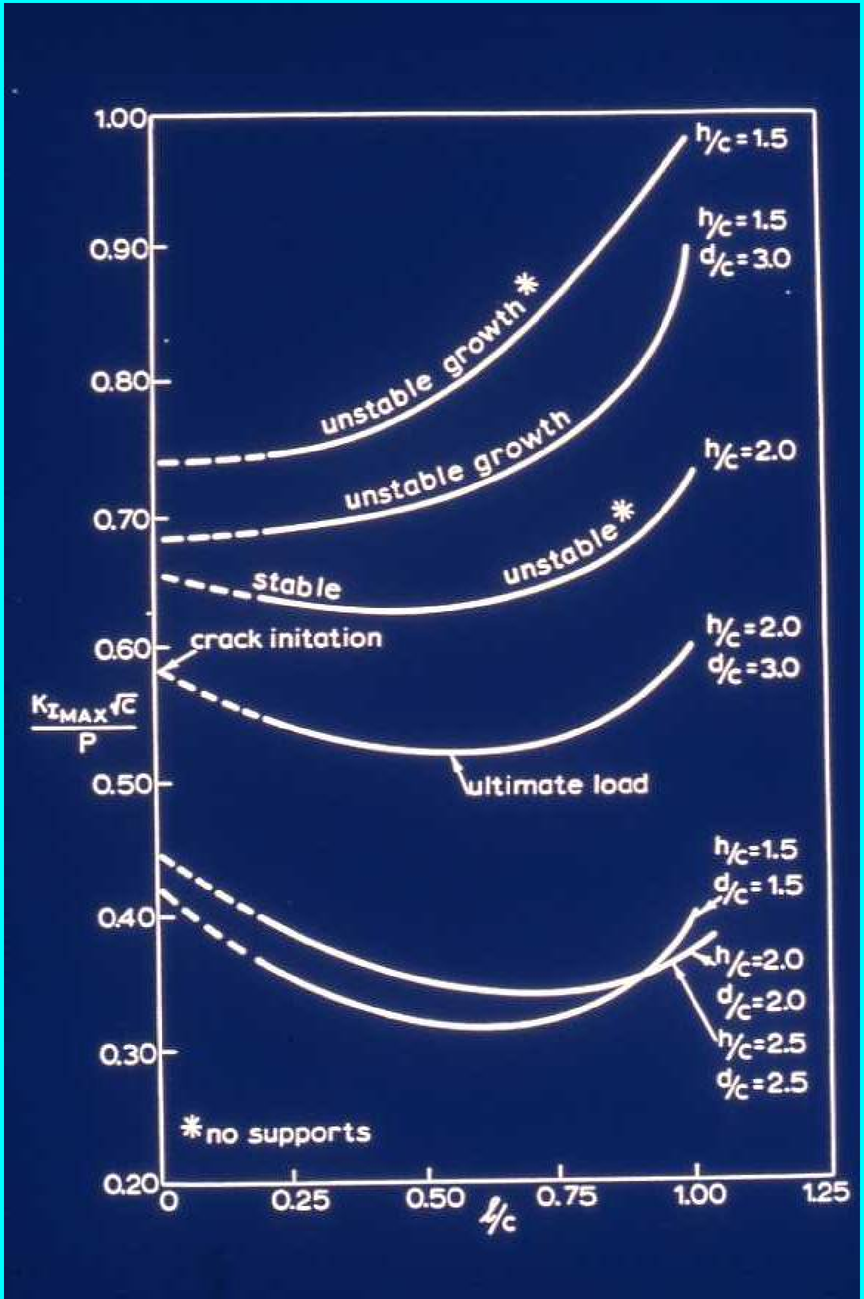

Crack Paths

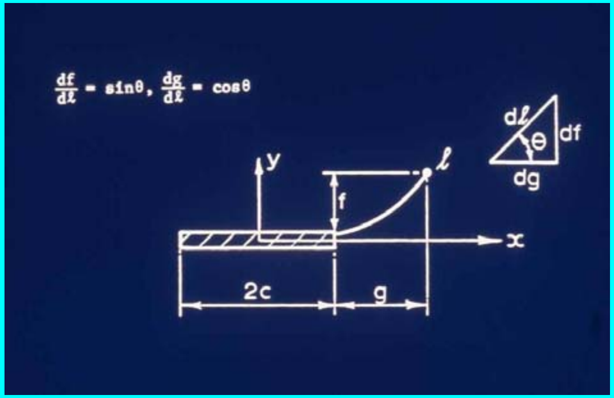

$\frac{df}{d\ell} = \sin\theta, \frac{dg}{d\ell} = \cos\theta$
y
x
f
g
2c
ℓ
$d\ell$
θ
df
dg

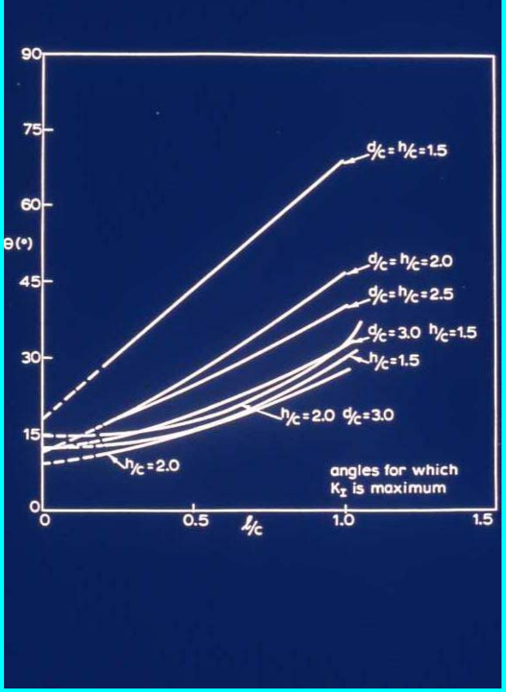

θ(°)
ℓ/c
d/c = h/c = 1.5
d/c = h/c = 2.0
d/c = h/c = 2.5
d/c = 3.0 h/c = 1.5
h/c = 1.5
h/c = 2.0 d/c = 3.0
h/c = 2.0
angles for which
K_I is maximum

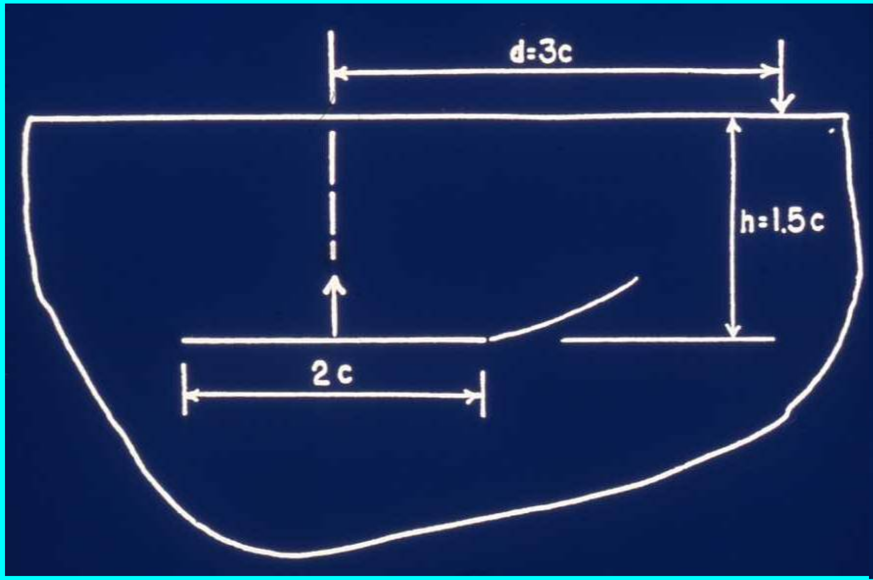

d=3c
h=1.5c
2c

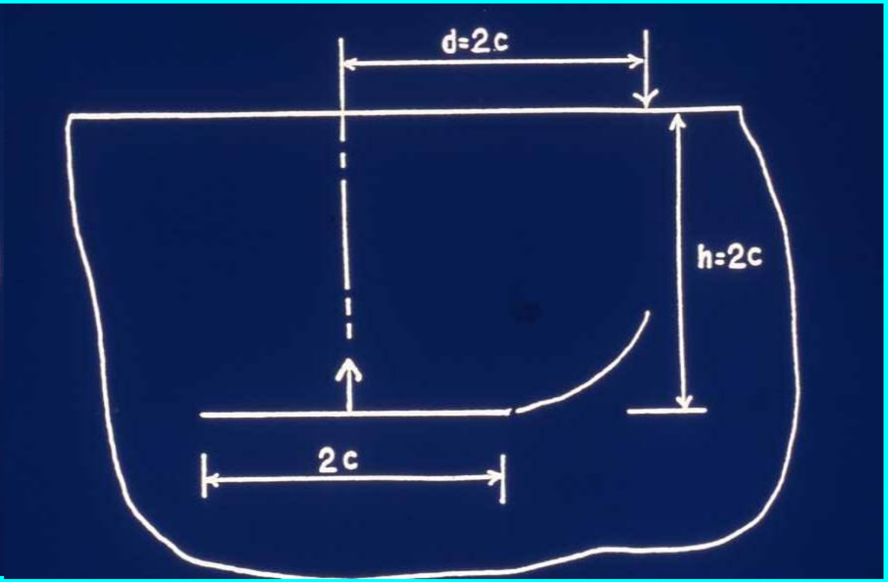

d=2c
h=2c
2c

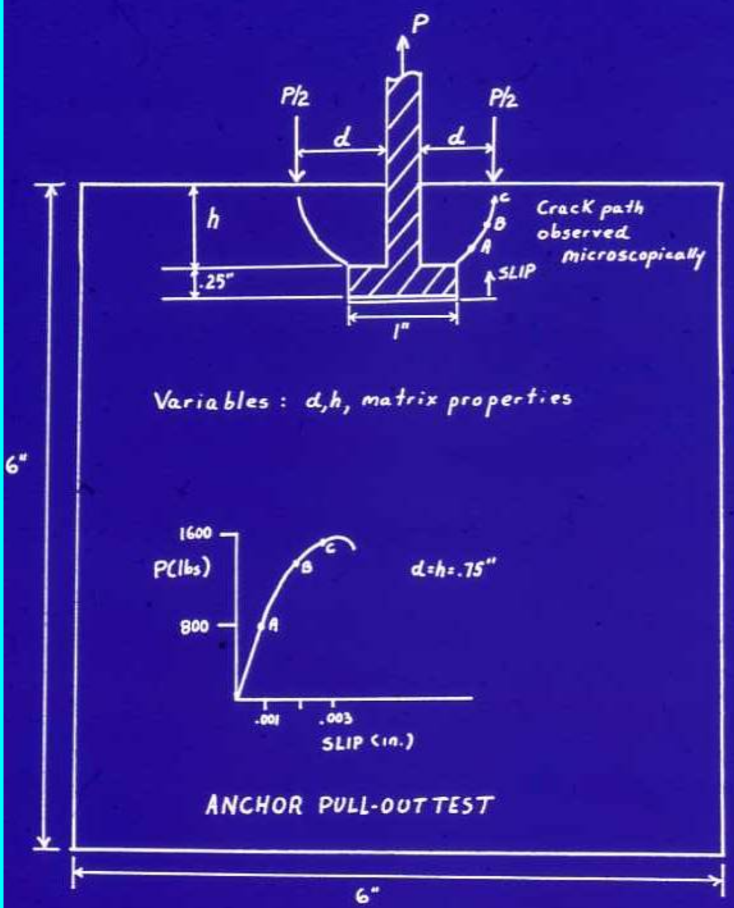

FIG. 6— CONFIGURATION OF 2-D

PULL—OUT TEST

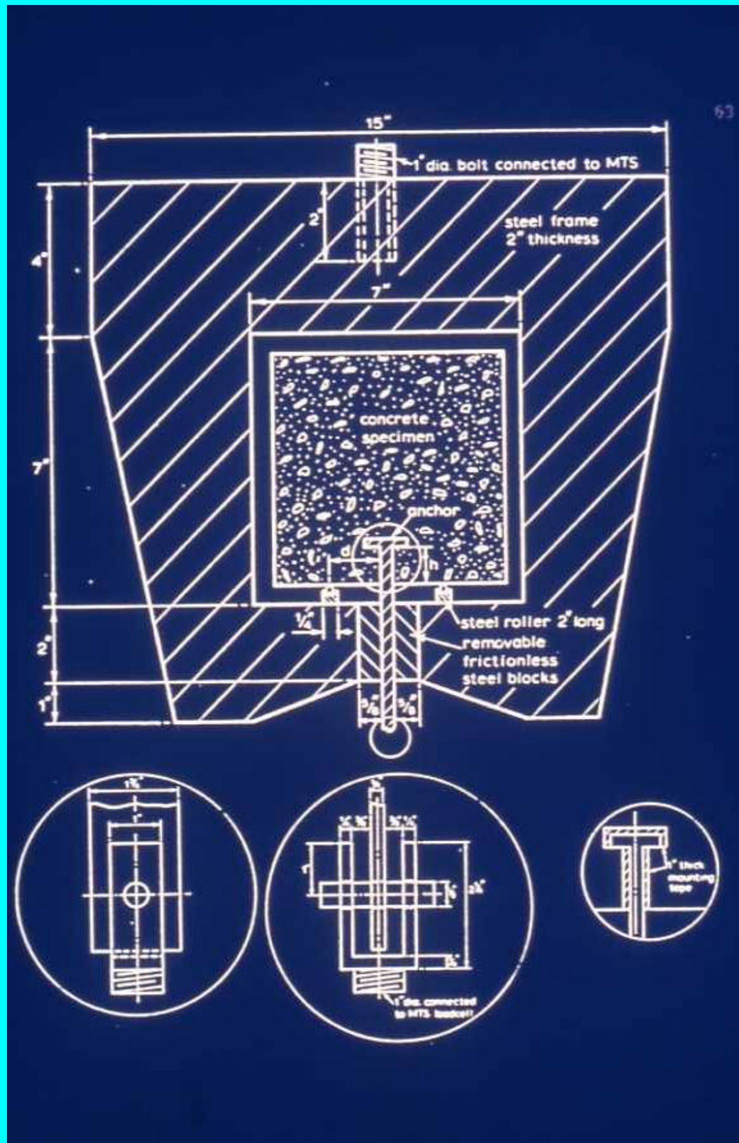
15"
1" dia. bolt connected to MTS
2"
steel frame
2" thickness
4"
7"
7"
concrete specimen
anchor
d
h
steel roller 2" long
removable
frictionless
steel blocks
2"
1"
1/4"

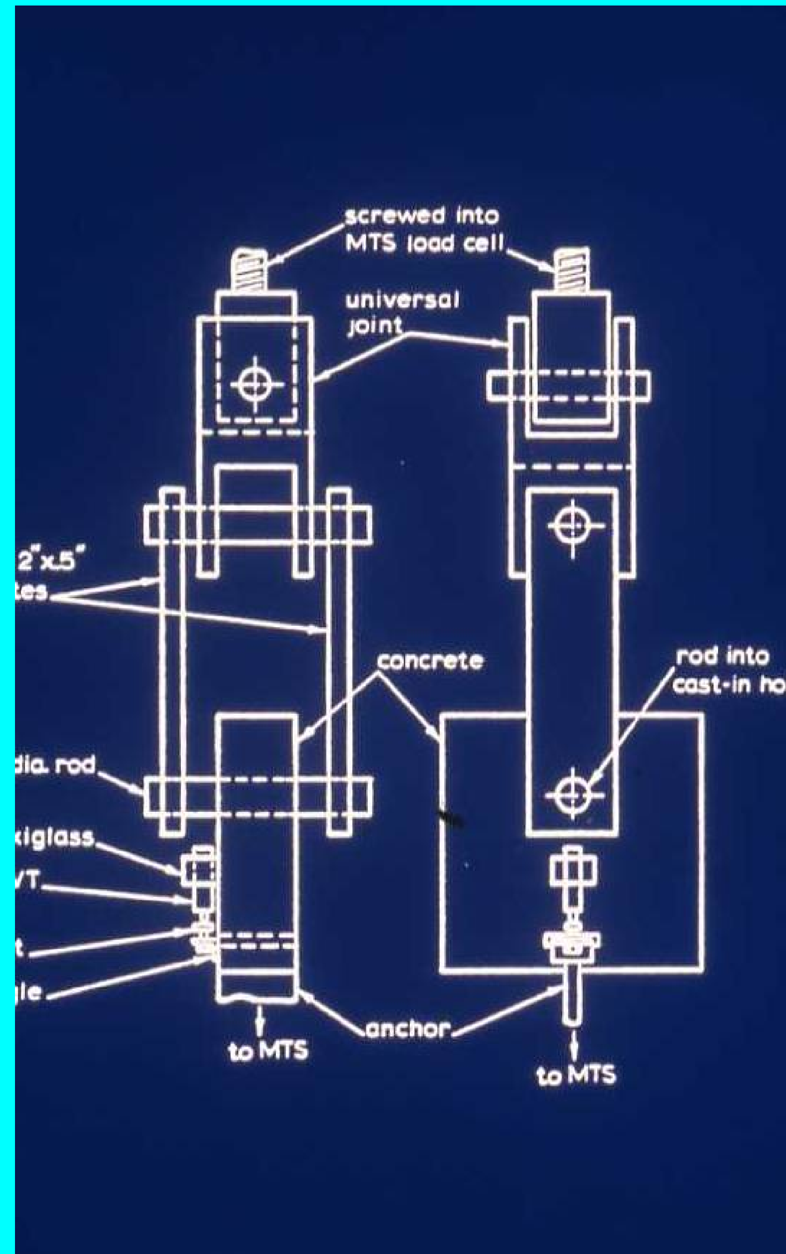
screwed into
MTS load cell
universal
joint
2"x.5"
concrete
rod into
anchor
to MTS
to MTS

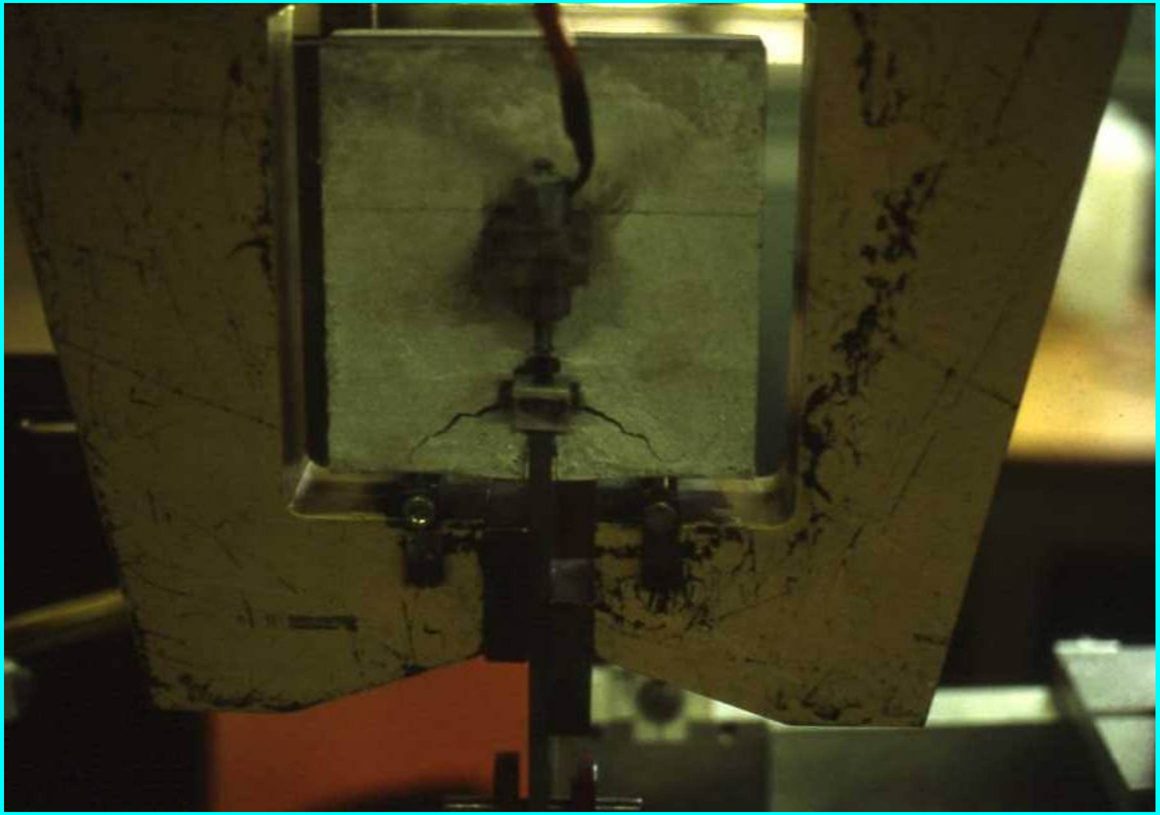
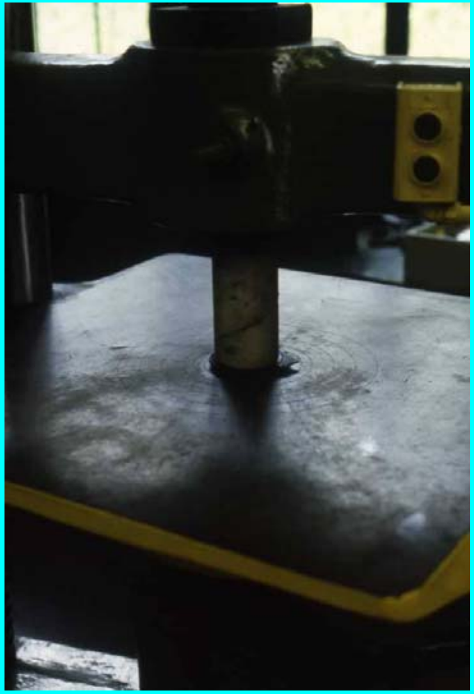

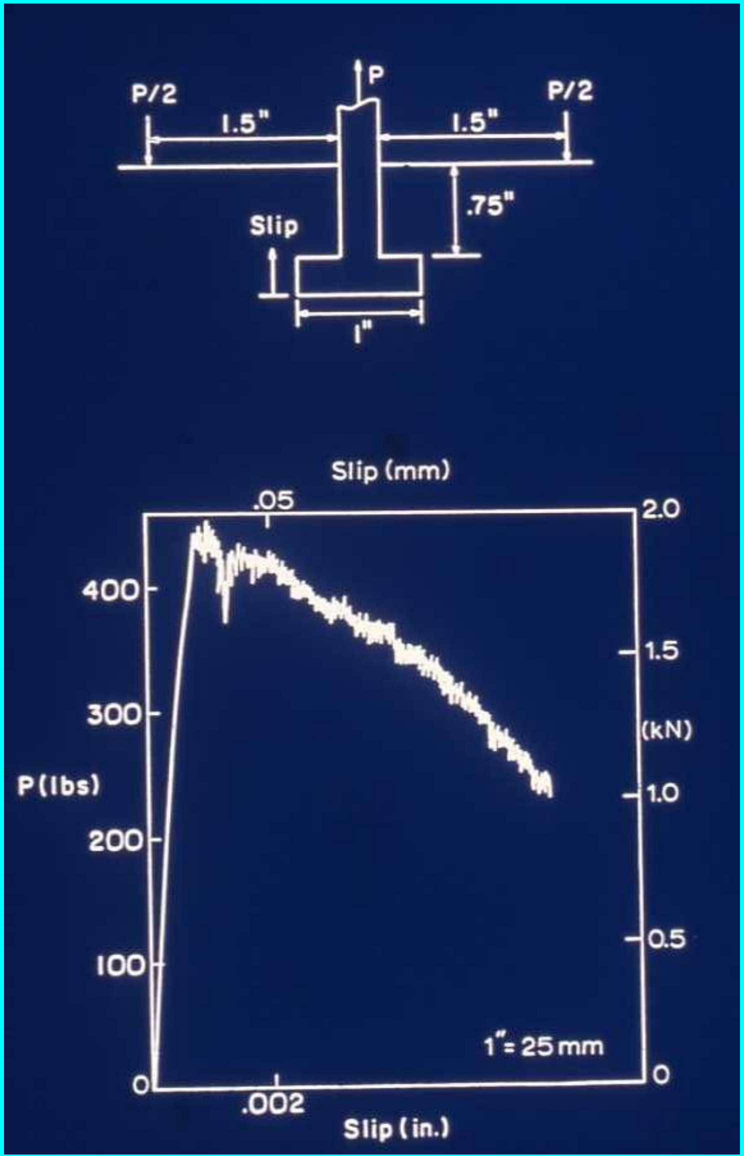
P
P/2
P/2
1.5"
1.5"
.75"
Slip
1"
Slip (mm)
.05
2.0
400
1.5
300
(kN)
P (lbs)
1.0
200
0.5
100
1" = 25 mm
0
0
.002
Slip (in.)

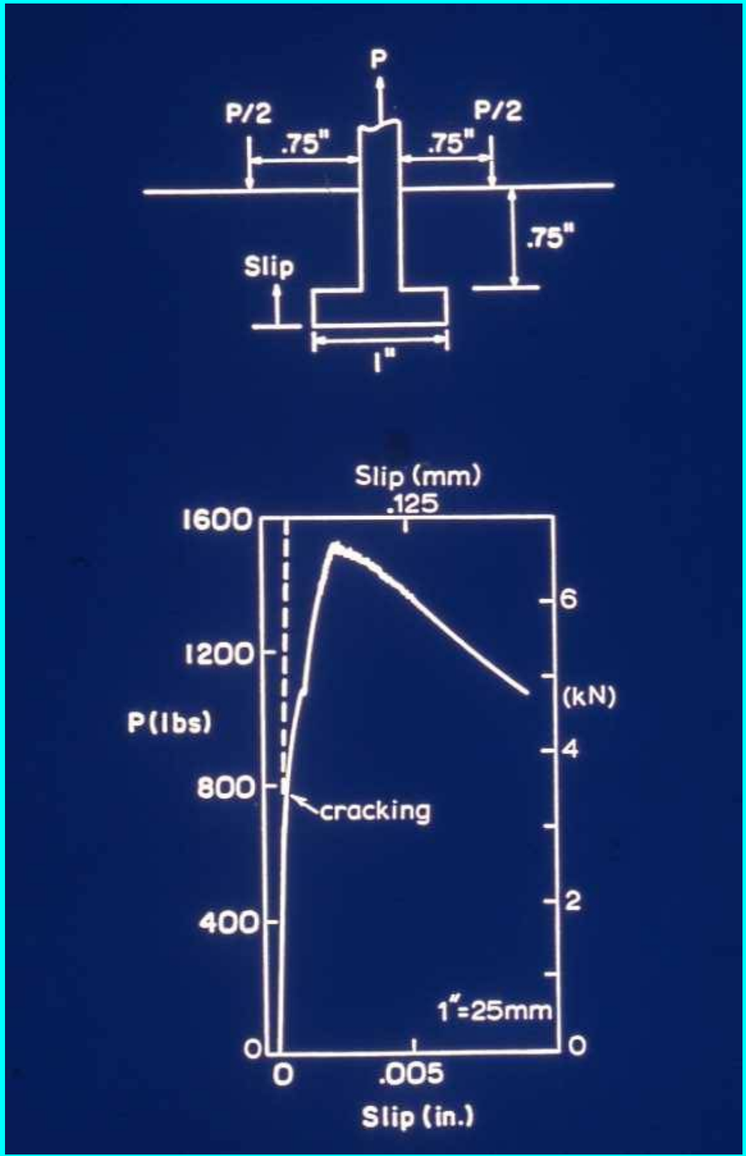
P
P/2
P/2
.75"
.75"
.75"
Slip
1"
Slip (mm)
.125
1600
6
1200
(kN)
P (lbs)
4
800
cracking
2
400
1"=25mm
0
0
0
.005
Slip (in.)

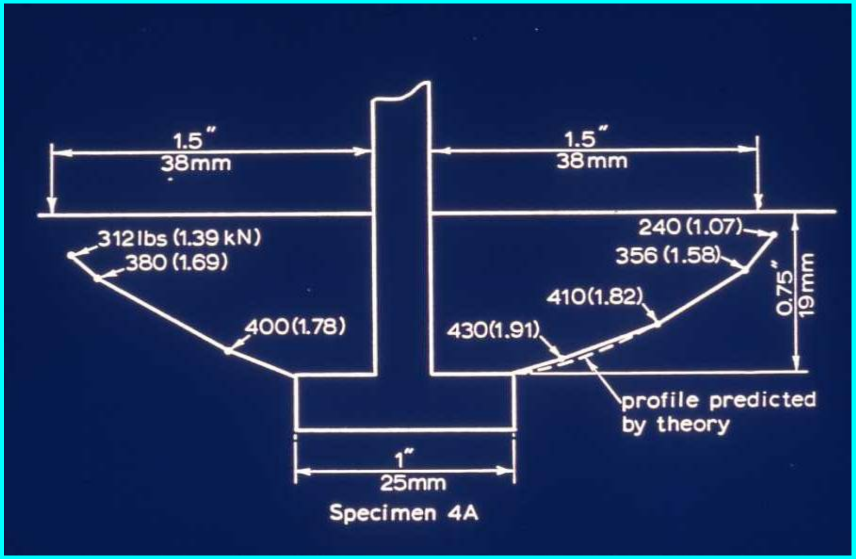
1.5″
38mm
1.5″
38mm
312 lbs (1.39 kN)
380 (1.69)
400 (1.78)
240 (1.07)
356 (1.58)
410 (1.82)
430 (1.91)
0.75″
19mm
profile predicted by theory
1″
25mm
Specimen 4A

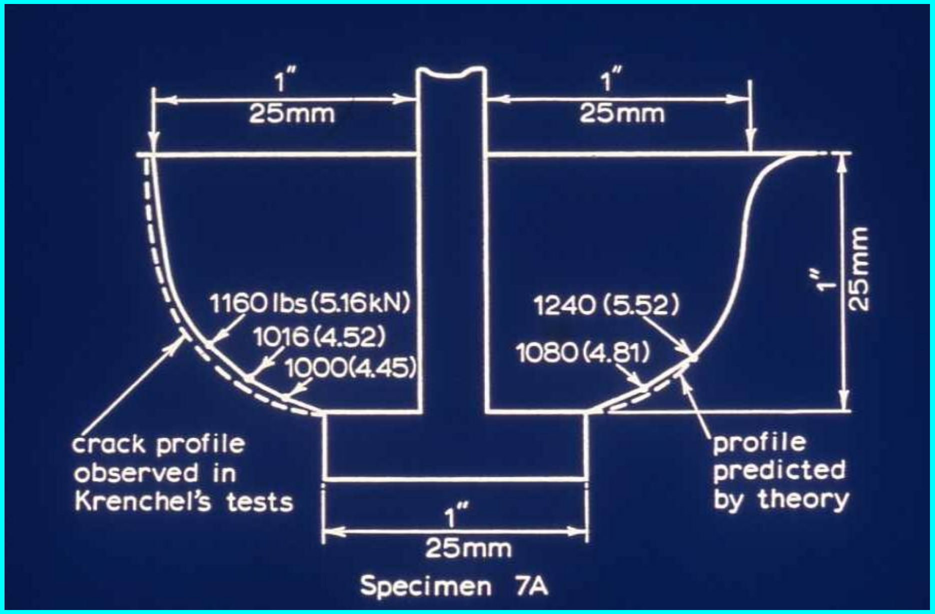
1″
25mm
1″
25mm
1160 lbs (5.16 kN)
1016 (4.52)
1000 (4.45)
1240 (5.52)
1080 (4.81)
1″
25mm
crack profile observed in Krenchel's tests
profile predicted by theory
1″
25mm
Specimen 7A

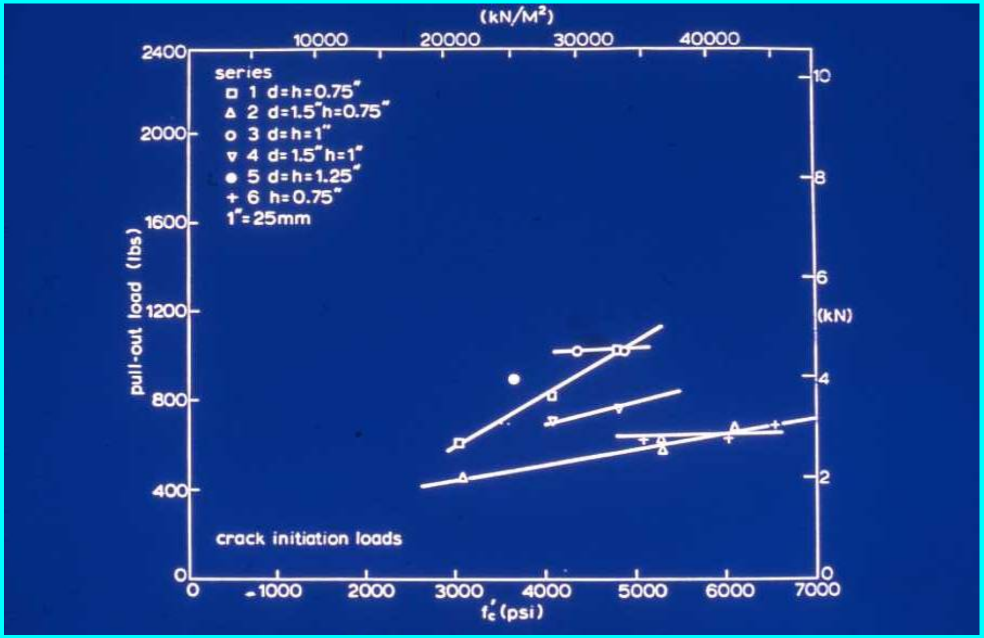
(kN/M²)
10000
20000
30000
40000
2400
2000
1600
1200
800
400
0
series
1 d=h=0.75"
2 d=1.5" h=0.75"
3 d=h=1"
4 d=1.5" h=1"
5 d=h=1.25"
6 h=0.75"
1"=25mm
pull-out load (lbs)
10
8
6
(kN)
4
2
0
crack initiation loads
0
1000
2000
3000
4000
5000
6000
7000
f'c (psi)

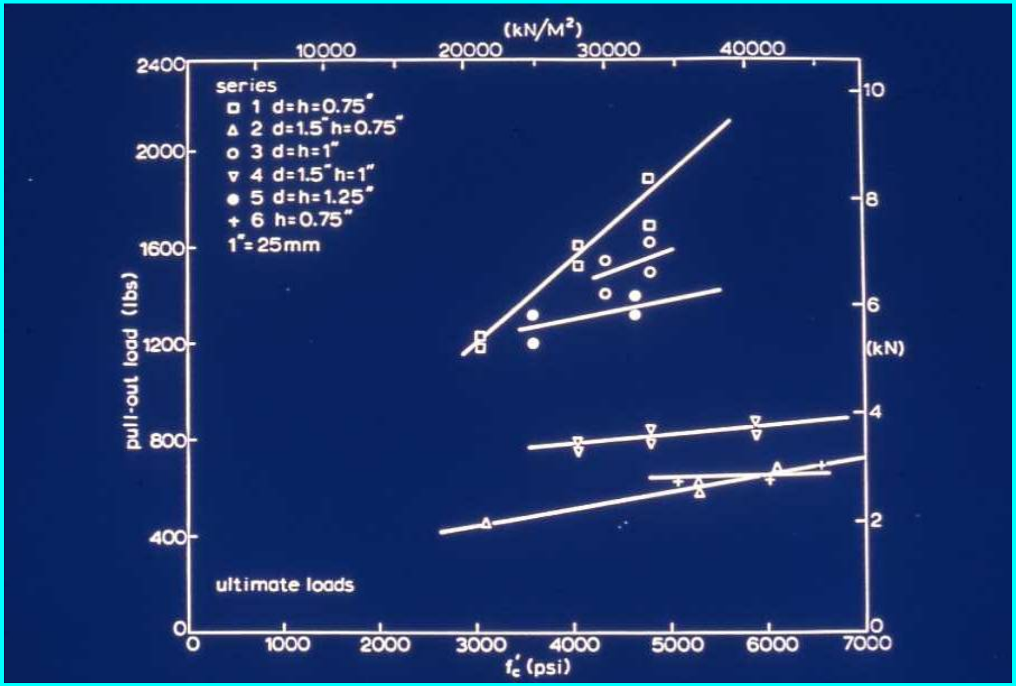
(kN/M²)
10000
20000
30000
40000
2400
2000
1600
1200
800
400
0
series
1 d=h=0.75"
2 d=1.5" h=0.75"
3 d=h=1"
4 d=1.5" h=1"
5 d=h=1.25"
6 h=0.75"
1"=25mm
pull-out load (lbs)
10
8
6
(kN)
4
2
0
ultimate loads
0
1000
2000
3000
4000
5000
6000
7000
f'c (psi)

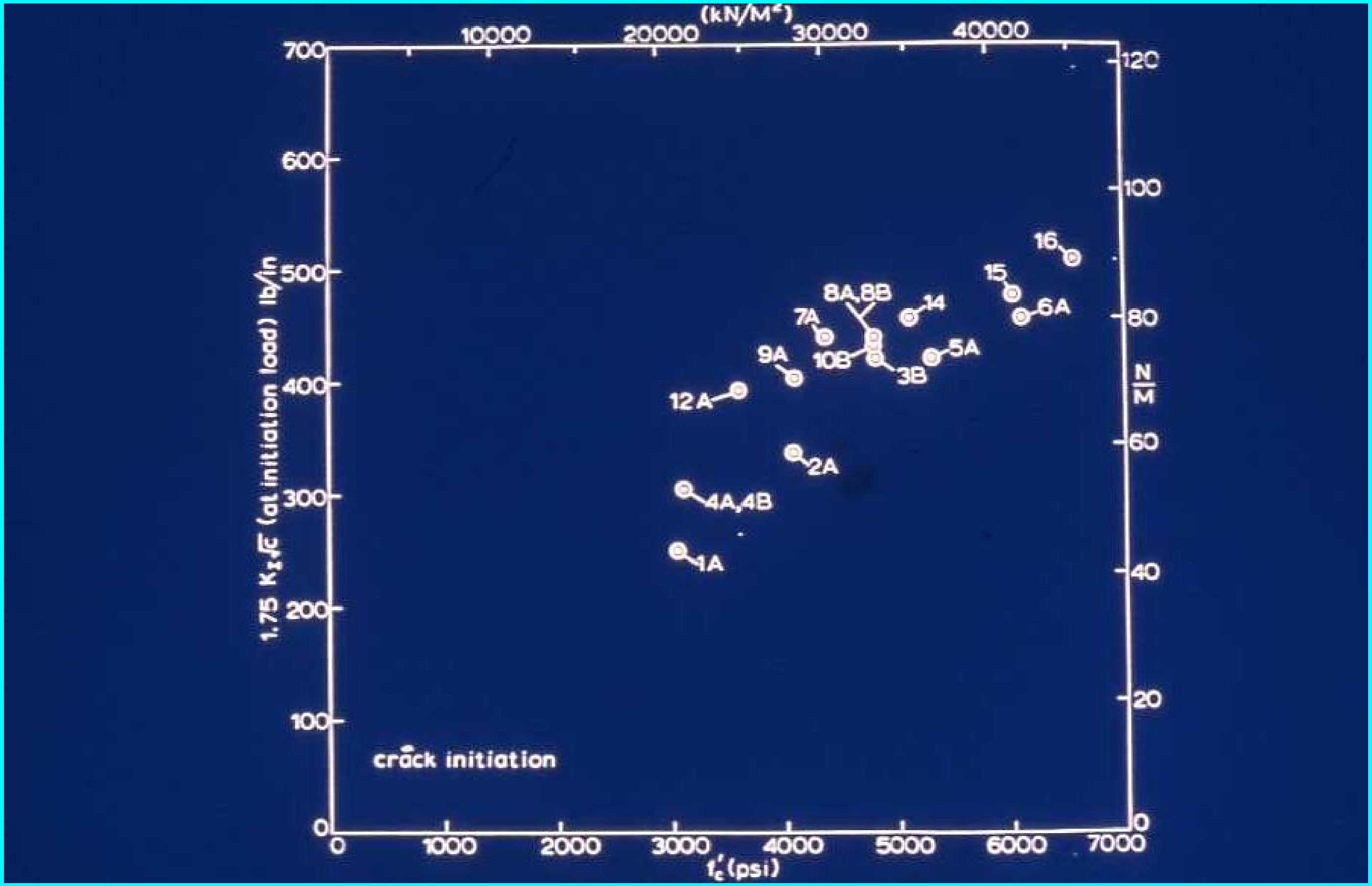

(kN/M²)
10000
20000
30000
40000
700
600
500
400
300
200
100
0
1.75 K_I√c (at initiation load) lb/in
120
100
80
60
40
20
0
N/M
16
15
6A
8A,8B
14
7A
5A
9A
10B
3B
12A
2A
4A,4B
1A
crack initiation
0
1000
2000
3000
4000
5000
6000
7000
f'c (psi)

Results of RILEM Round-Robin Tests

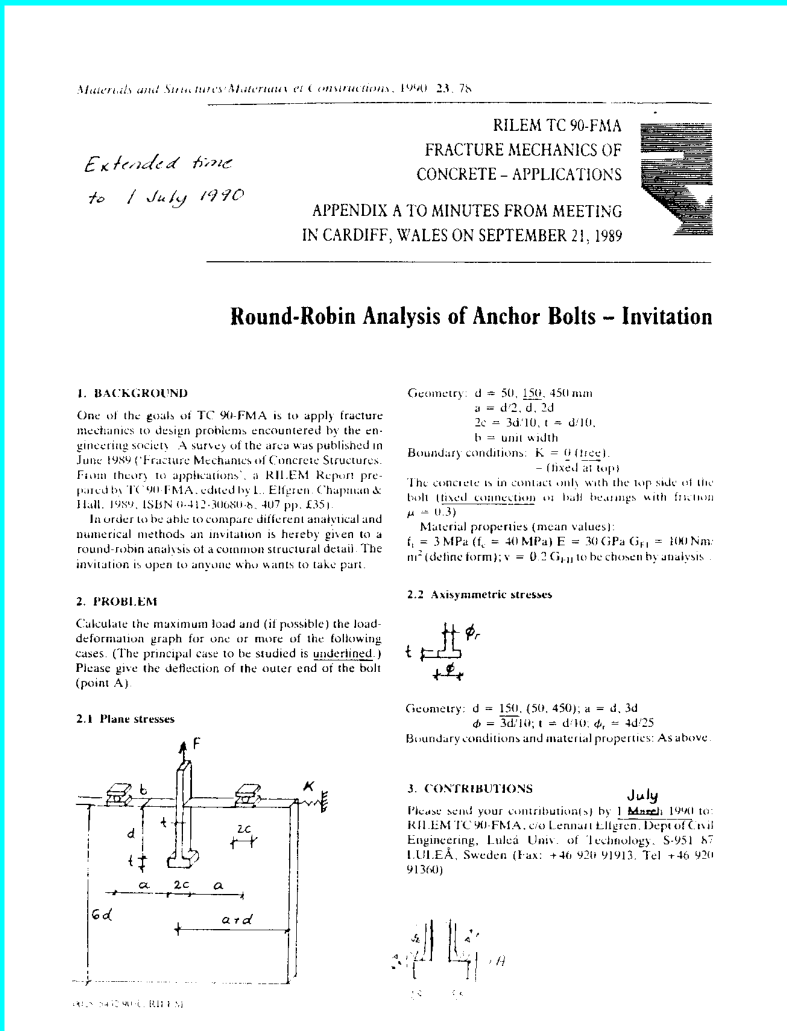

Materials and Structures/Matériaux et Constructions, 1990, 23, 78

Extended time to 1 July 1990

RILEM TC 90-FMA
FRACTURE MECHANICS OF CONCRETE – APPLICATIONS

APPENDIX A TO MINUTES FROM MEETING IN CARDIFF, WALES ON SEPTEMBER 21, 1989

Round-Robin Analysis of Anchor Bolts – Invitation

1. BACKGROUND

One of the goals of TC 90-FMA is to apply fracture mechanics to design problems encountered by the engineering society. A survey of the area was published in June 1989 ('Fracture Mechanics of Concrete Structures. From theory to applications', a RILEM Report prepared by TC 90-FMA, edited by L. Elfgren, Chapman & Hall, 1989, ISBN 0-412-30680-8, 407 pp. £35).

In order to be able to compare different analytical and numerical methods an invitation is hereby given to a round-robin analysis of a common structural detail. The invitation is open to anyone who wants to take part.

2. PROBLEM

Calculate the maximum load and (if possible) the load-deformation graph for one or more of the following cases. (The principal case to be studied is underlined.) Please give the deflection of the outer end of the bolt (point A).

2.1 Plane stresses

Geometry: d = 50, 150, 450 mm
a = d/2, d, 2d
2c = 3d/10, t = d/10,
b = unit width

Boundary conditions: K = 0 (free).
– (fixed at top)

The concrete is in contact only with the top side of the bolt (fixed connection or ball bearings with friction $\mu = 0.3$)

Material properties (mean values):
f_t = 3 MPa (f_c = 40 MPa) E = 30 GPa G_{FI} = 100 Nm/m² (define form); v = 0.2 G_{FII} to be chosen by analysis.

2.2 Axisymmetric stresses

Geometry: d = 150, (50, 450); a = d, 3d
ϕ = 3d/10; t = d/10; ϕ_r = 4d/25

Boundary conditions and material properties: As above.

3. CONTRIBUTIONS

Please send your contribution(s) by 1 ~~March~~ July 1990 to: RILEM TC 90-FMA, c/o Lennart Elfgren, Dept of Civil Engineering, Luleå Univ. of Technology, S-951 87 LULEÅ, Sweden (Fax: +46 920 91913, Tel +46 920 91360)

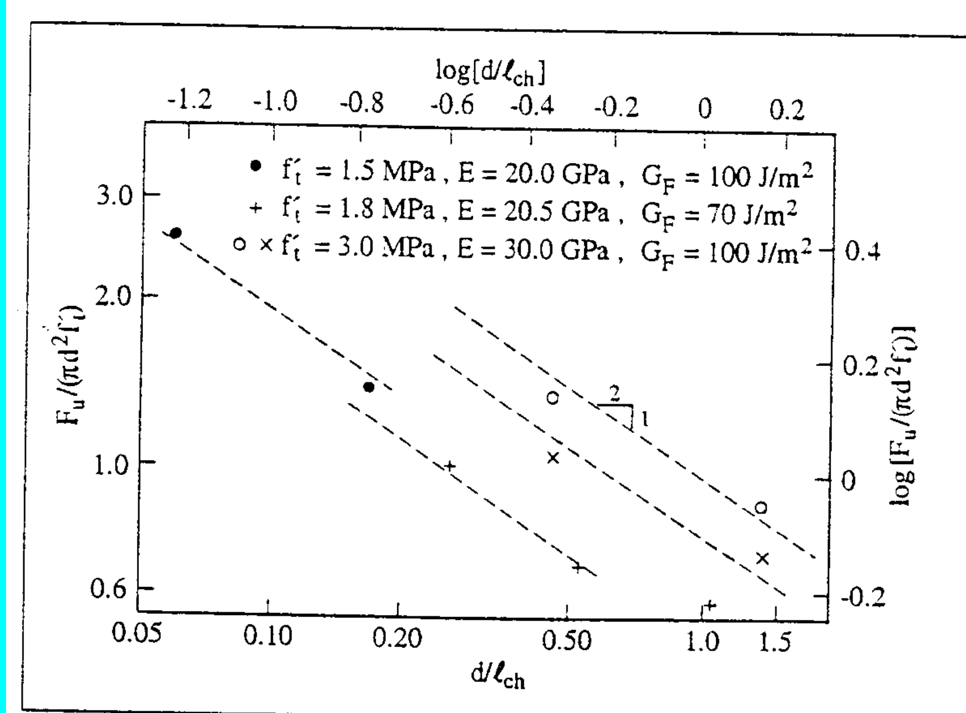

Fig. 3 – Results of pull-out tests on headed anchors can be reasonably accurately predicted by LEFM. Broken lines represent LEFM predictions for varying d/ℓ_{ch} [3].

Ultimate Load Capacities of Plane and Axisymmetric Headed Anchors

By Amy Vogel[1] and Roberto Ballarini[2]

Abstract: A finite-element-based linear elastic fracture mechanics analysis of the pullout of headed anchors is presented. The anchor is modeled as a vertically loaded crack of diameter c, embedded at a depth d, with a rigid upper surface, and traction-free lower surface. The fracture toughness and Poisson's ratio of the surrounding matrix are K_{Ic} and ν, respectively. For selected values of d/c, the mode-I stress intensity factor is calculated for each increment of the crack growth, which emanates from the edge of the anchor, and follo
zero mode-II stress intensity factor. The stress intensity factors are used to calculate the ultim
is written as $P_u = g(d/c, \nu)d^{3/2}K_{Ic}$. For $\nu = 0.2$ and relatively large values of d/c, $g = 2.8$ for axi
and $g = 1.2$ for plane strain anchors.

$$P_u \propto f_t d^2$$

$$P = f(c/d,\ l/d,\ \nu)d^{3/2}K_{Ic}$$

$$P_u = f_{\max}(c/d,\ l/d,\ \nu)d^{3/2}K_{Ic} \equiv g(d/c,\ \nu)d^{3/2}K_{Ic}$$

INTRODUCTION

Consider a headed anchor of diameter c, embedded within a concrete matrix at a depth d. The formula given in the American Concrete Institute code ("Code" 1989) for its tensile (pullout) capacity can be written, in terms of the concrete tensile strength f_t, as follows:

$$P_u \propto f_t d^2 \tag{1}$$

It is well known (Ozbolt and Eligehausen 1993) that (1), which is based on the assumption that pullout is resisted by a nominal stress acting along an assumed failure surface, is unconservative for relatively large d. This is not surprising, because it is not based on a rational analysis that treats the discrete cracking that dominates the failure process. Over the past 15 years improved design formulas have been developed through linear and nonlinear fracture mechanics; these have been recently summarized by Karihaloo (1996). As discussed by Ozbolt and Eligehausen (1993), for large embedment depths there is very little difference between the predictions of the linear and nonlinear fracture models. Therefore, we limit the subsequent discussion to linear elastic fracture mechanics (LEFM).

Consider the idealized headed anchor geometry shown in Fig. 1. The model consists of an anchor, embedded at a depth $d = 1$, modeled as an infinitesimally thin crack of diameter c, whose upper surface is restrained in all directions and whose lower surface is traction-free. It does not include the thickness of the anchor, nor its stem; these could be easily incorporated but are not expected to significantly affect the ultimate load capacity. The length of the extension from the edge of the anchor is l. A unit load is applied through a prescribed uniform stress along the bottom surface.

In LEFM, it is typically assumed that a crack will propagate when the mode-I stress intensity factor K_I reaches a value equal to the fracture toughness K_{Ic} along a path that is associated with zero mode-II stress intensity factor K_{II}. Linearity and dimensional consistency demand that the load associated with an equilibrium crack length l is of the form

$$P = f(c/d,\ l/d,\ \nu)d^{3/2}K_{Ic} \tag{2}$$

where ν = Poisson's ratio. The ultimate load corresponds to the crack length that maximizes f; that is

$$P_u = f_{\max}(c/d,\ l/d,\ \nu)d^{3/2}K_{Ic} \equiv g(d/c,\ \nu)d^{3/2}K_{Ic} \tag{3}$$

Numerical values of g have been presented for plane strain by Ballarini et al. (1985) and for the axisymmetric configuration by Karihaloo (1996) and Eligehausen and Sawade (1989). Eli-

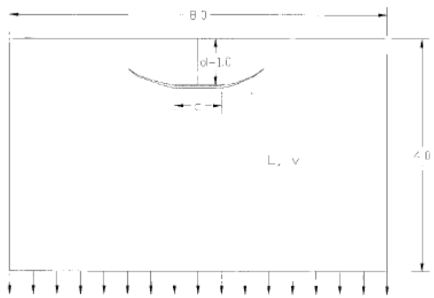

FIG. 1. Schematic of Headed Anchor Bolt Model

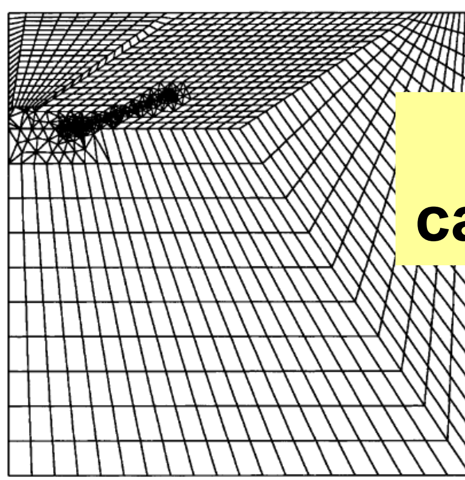

FIG. 2. Finite-Element Discretization of Anchor Bolt Model, $d/c = 1$

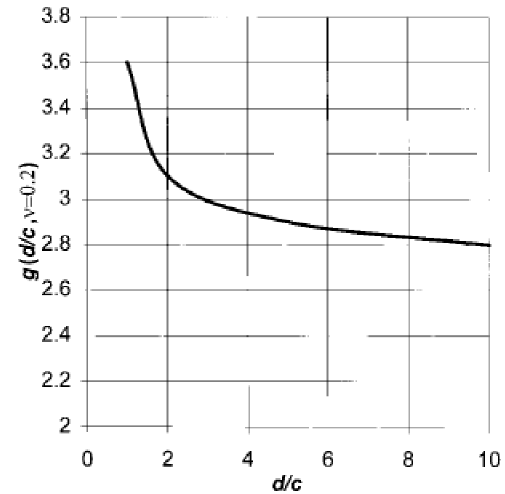

Now an undergrad can do these calculations

[1]Dept. of Civ. Engrg., Case Western Reserve Univ., Cleveland, OH 44106-7201.
[2]Prof., Dept. of Civ. Engrg., Case Western Reserve Univ., Cleveland, OH.

Note. Associate Editor: Gilles Pijaudier-Cabot. Discussion open until April 1, 2000. To extend the closing date one month, a written request must be filed with the ASCE Manager of Journals. The manuscript for this paper was submitted for review and possible publication on February 2, 1999. This paper is part of the *Journal of Engineering Mechanics*, Vol. 125, No. 11, November, 1999. ©ASCE, ISSN 0733-9399/99/0011-1276–1279/$8.00 + $.50 per page. Paper No. 20164.

Spur Gears

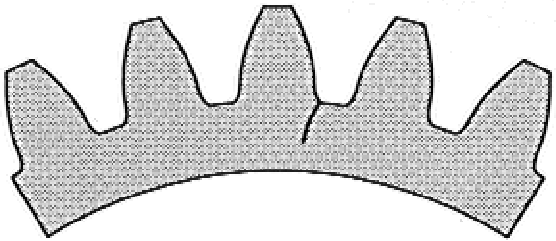

Thin rim - catastrophic rim fracture

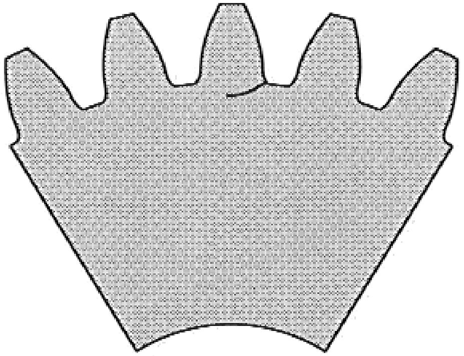

Thick rim - “benign” tooth fracture

- Thin-rim gears desired for reduced weight.
- Stress fields and failure characteristics significantly different for thin-rim gears compared to conventional gears.
- Designed according to standards published by AGMA.
- Catastrophic failures have occurred in thin-rim gears.

Objectives

Develop fracture mechanics-based design guidelines to prevent rim fracture failure modes in gear tooth bending fatigue.

Definition of Backup Ratio (m_B)

$$m_B = \frac{b}{h}$$

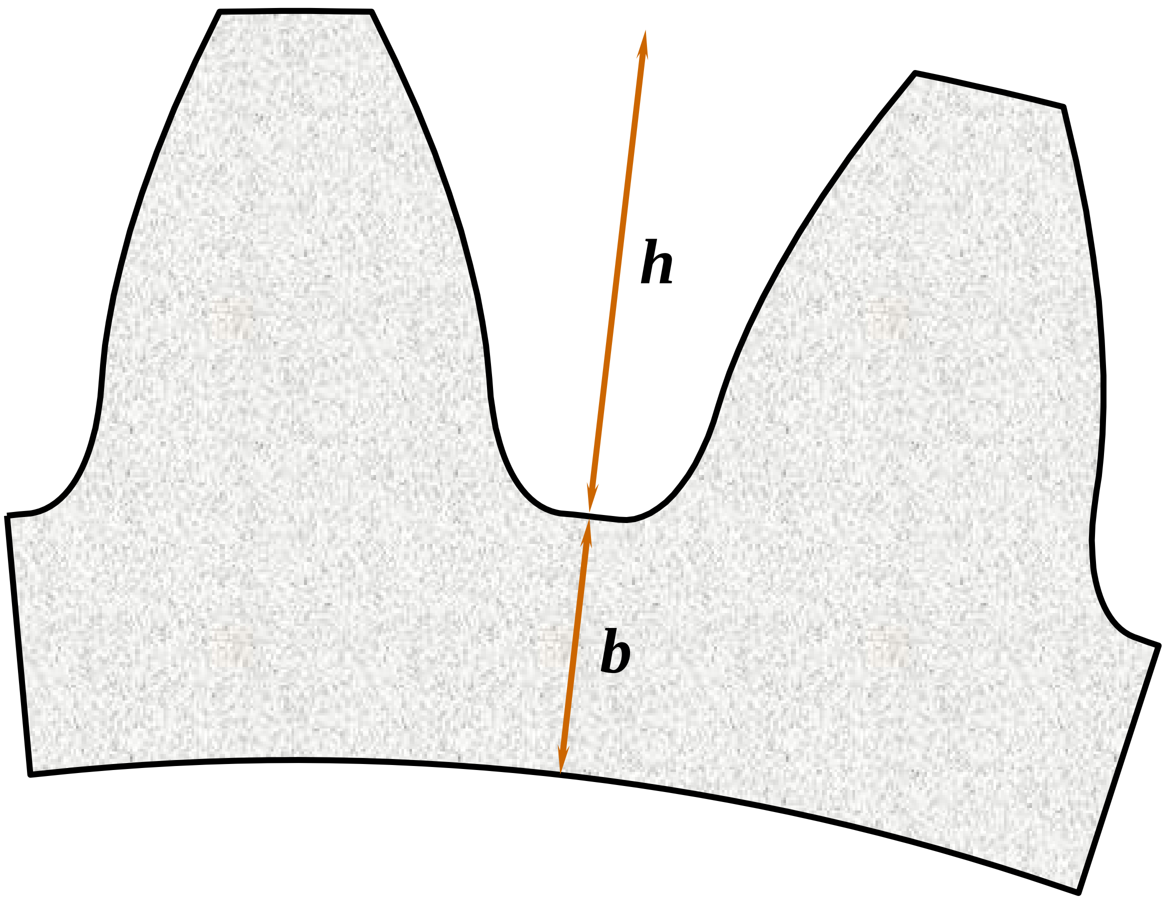

Bending stress index

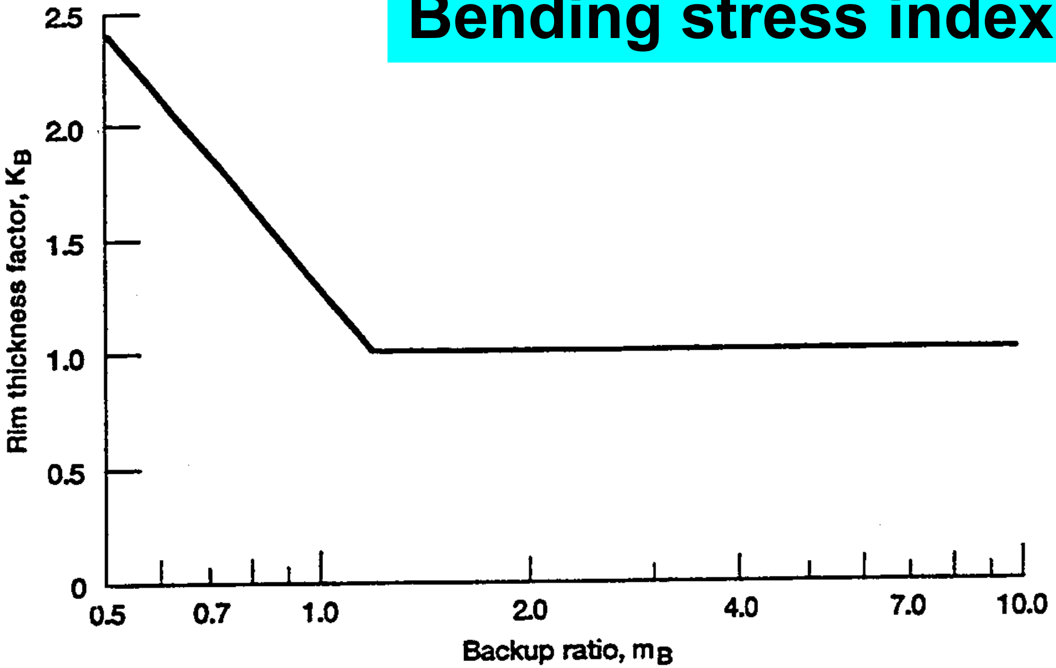

Figure 1.2.1.—Gear tooth bending stress index rim thickness correction factor (AGMA, 1990).

Crack Modeling Using Finite Element Method

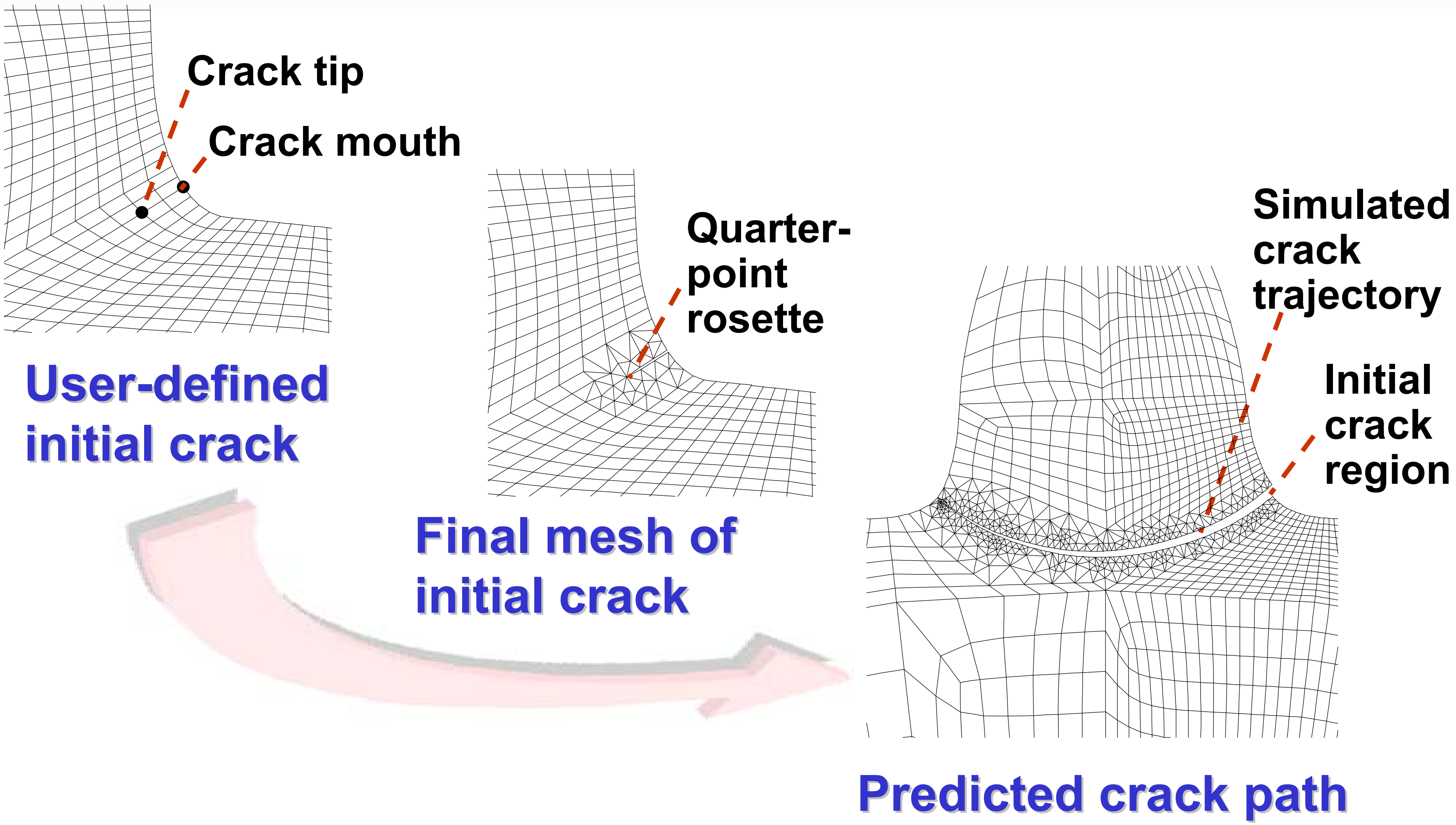

Definition of Initial Crack Location (θ_0)

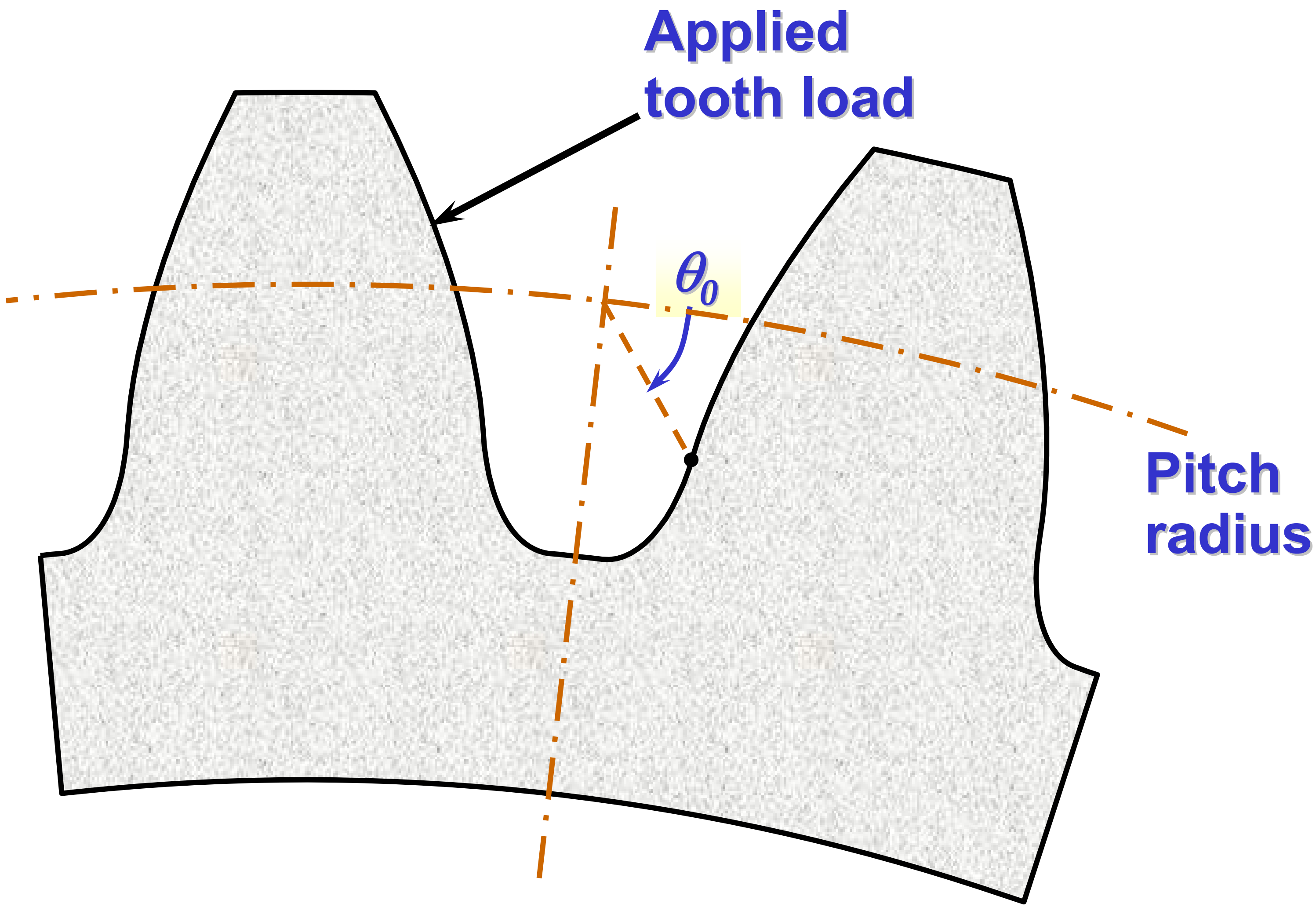

Stress Intensity Factors

K_I = mode I stress intensity factor

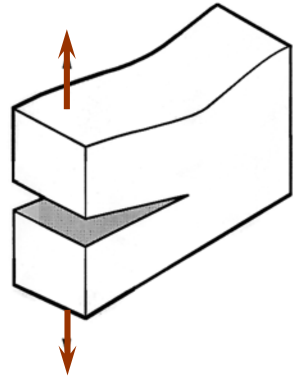

K_{II} = mode II stress intensity factor

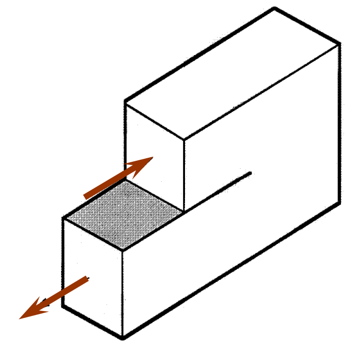

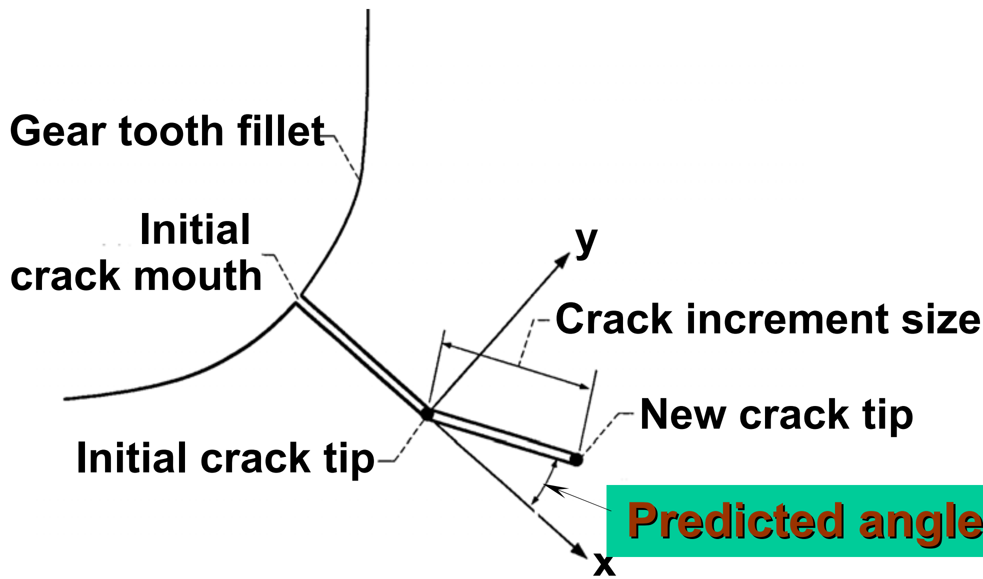

Growth rate

$$\frac{da}{dN} = C\left(\Delta K_I\right)^m$$

Predicted angle = $f\,(K_{II} / K_I)$

Crack Propagation Angle and Growth Rate

$$\theta_m = 2\tan^{-1}\left[\frac{\dfrac{K_I}{K_{II}} \pm \sqrt{\left(\dfrac{K_I}{K_{II}}\right)^2 + 8}}{4}\right]$$

3 Paris equation, $n = 2.264$, $C = 1.149\times10^{-15}$ in./cyc/(psi$\sqrt{\text{in.}}$)^n (Au and Ke, 1981)
4 Paris equation, $n = 2.954$, $C = 6.027\times10^{-19}$ in./cyc/(psi$\sqrt{\text{in.}}$)^n (Au and Ke, 1981)
5 Paris equation, $n = 2.555$, $C = 2.721\times10^{-17}$ in./cyc/(psi$\sqrt{\text{in.}}$)^n (Au and Ke, 1981)
6 Paris equation, $n = 2.420$, $C = 1.084\times10^{-16}$ in./cyc/(psi$\sqrt{\text{in.}}$)^n (Au and Ke, 1981)
10 Collipriest equation, $n = 1.63$, $C = 8.36\times10^{-9}$ in./cyc/(ksi$\sqrt{\text{in.}}$)^n, $\Delta K_{th} = 3.5$ ksi$\sqrt{\text{in.}}$, $K_{IC} = 200$ ksi$\sqrt{\text{in.}}$, $R = 0$ (Forman and Hu, 1984)

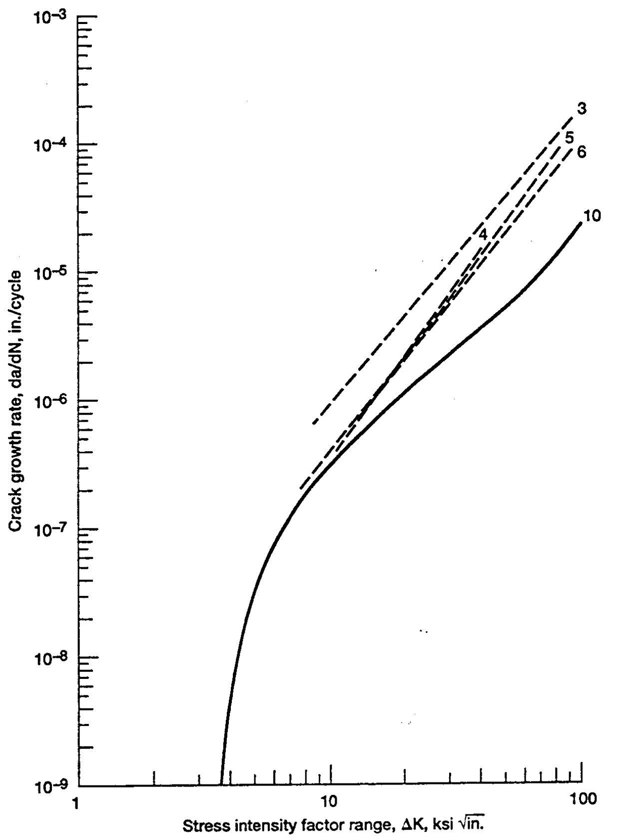

Figure 3.7.3.—Comparison of fatigue crack growth rates using Paris equation and Collipriest equation for AISI 9310 steel.

Typical Finite Element Gear Model

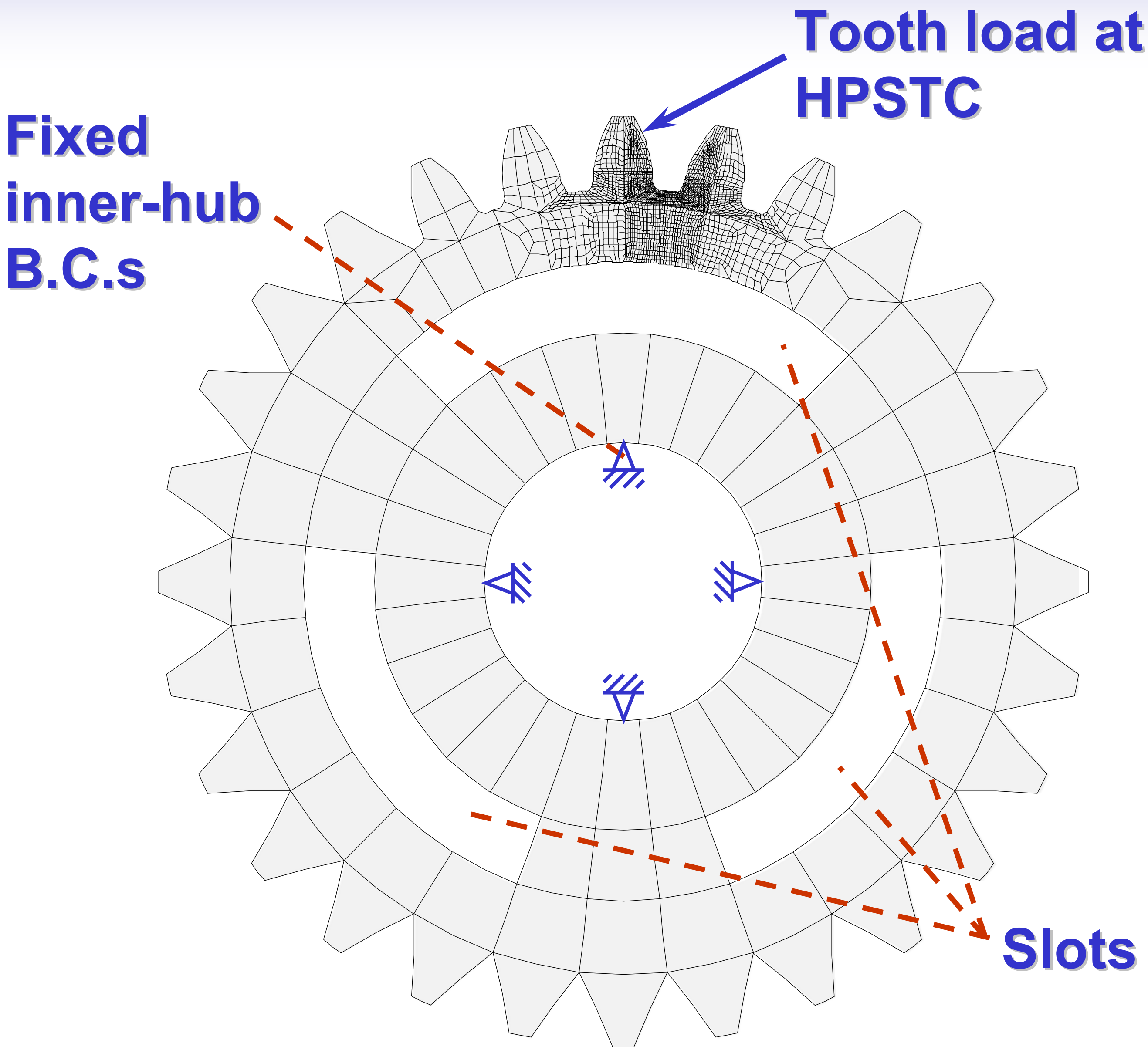

Load Case Locations for FEM

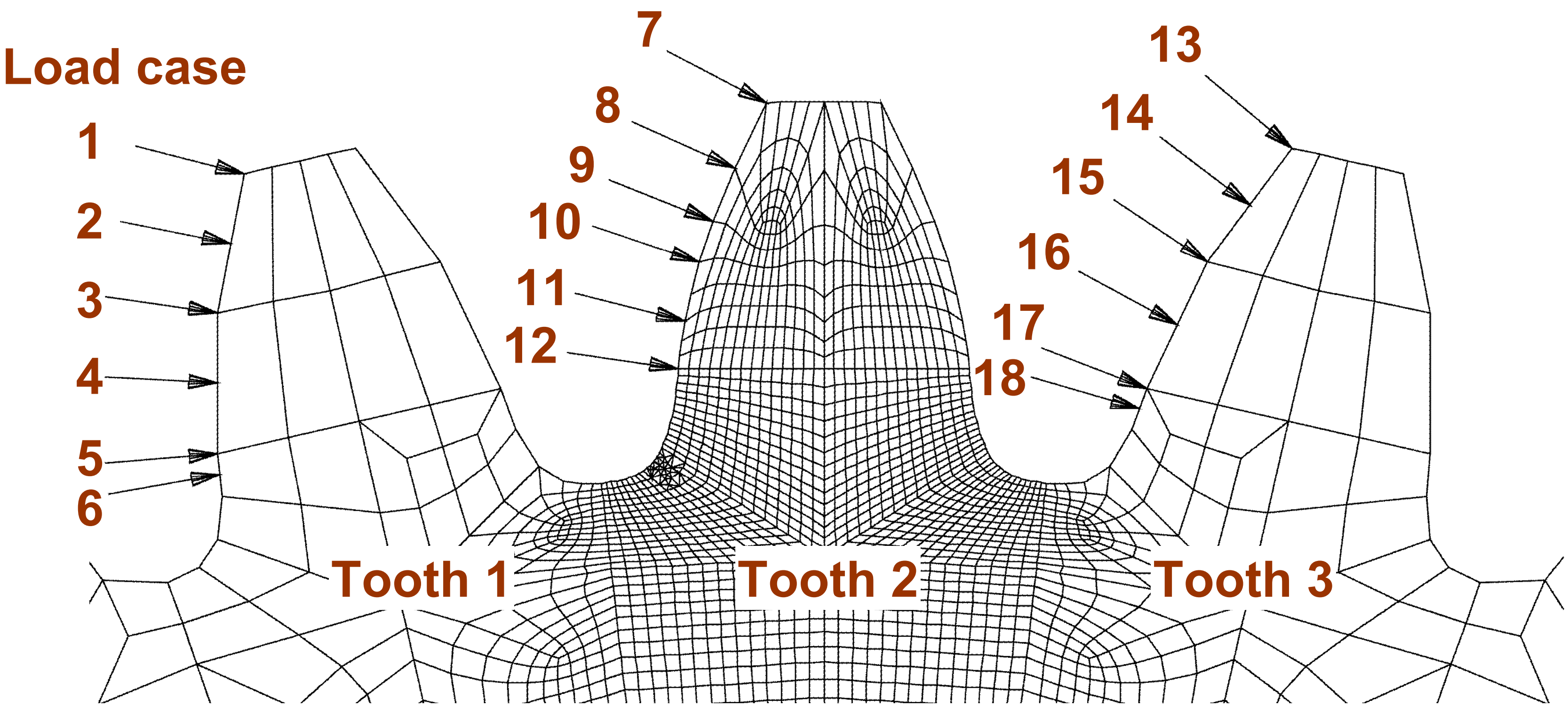

0.26-mm crack size, 68 N-m driver gear torque.

Effect of Initial Crack Location on Crack Path

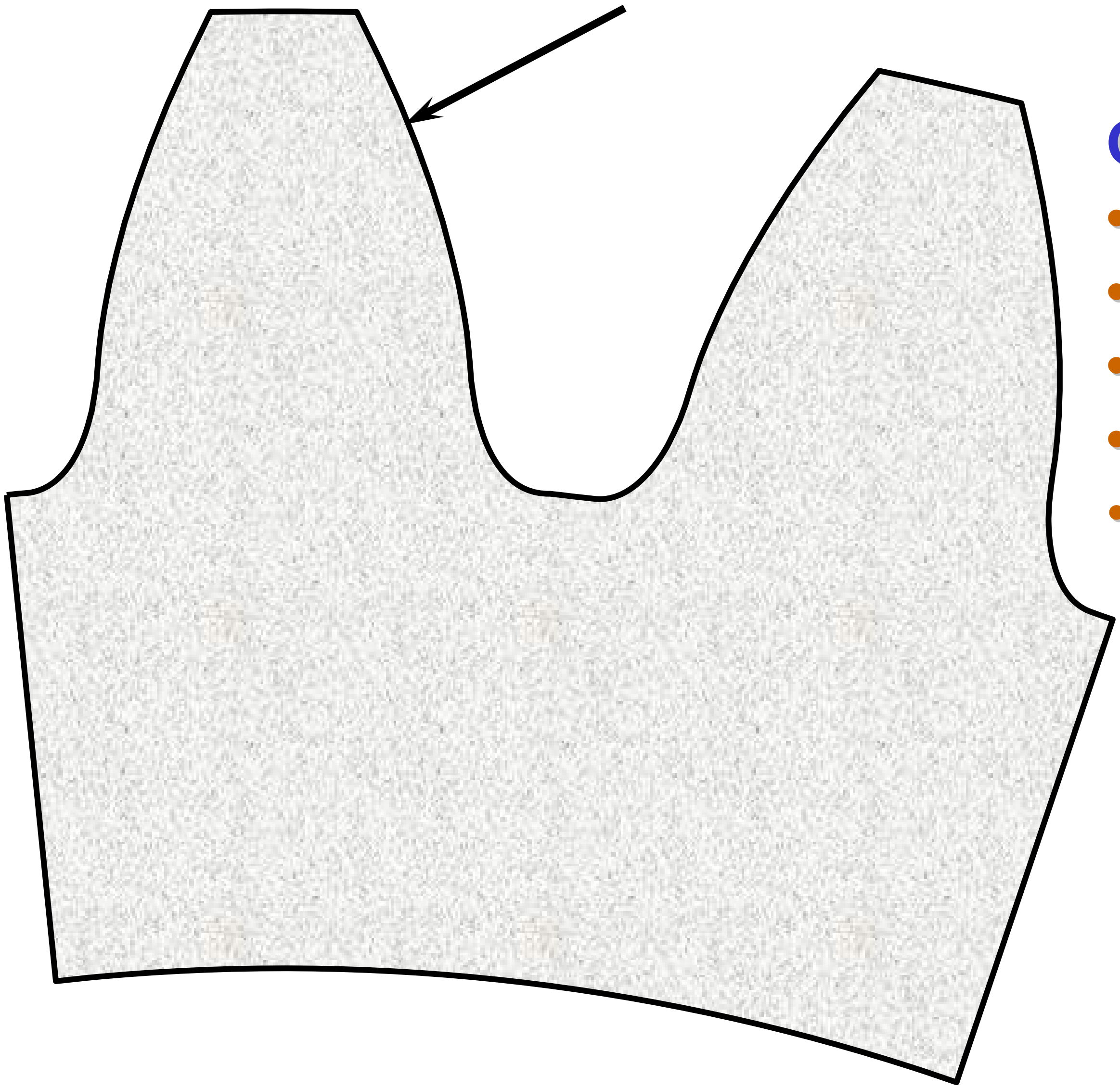

Gear Parameters:

- 28 teeth
- 8 pitch
- 1.75" pitch rad
- 20° pressure angle
- m_B = 1.0

Effect of Initial Crack Location on Crack Path

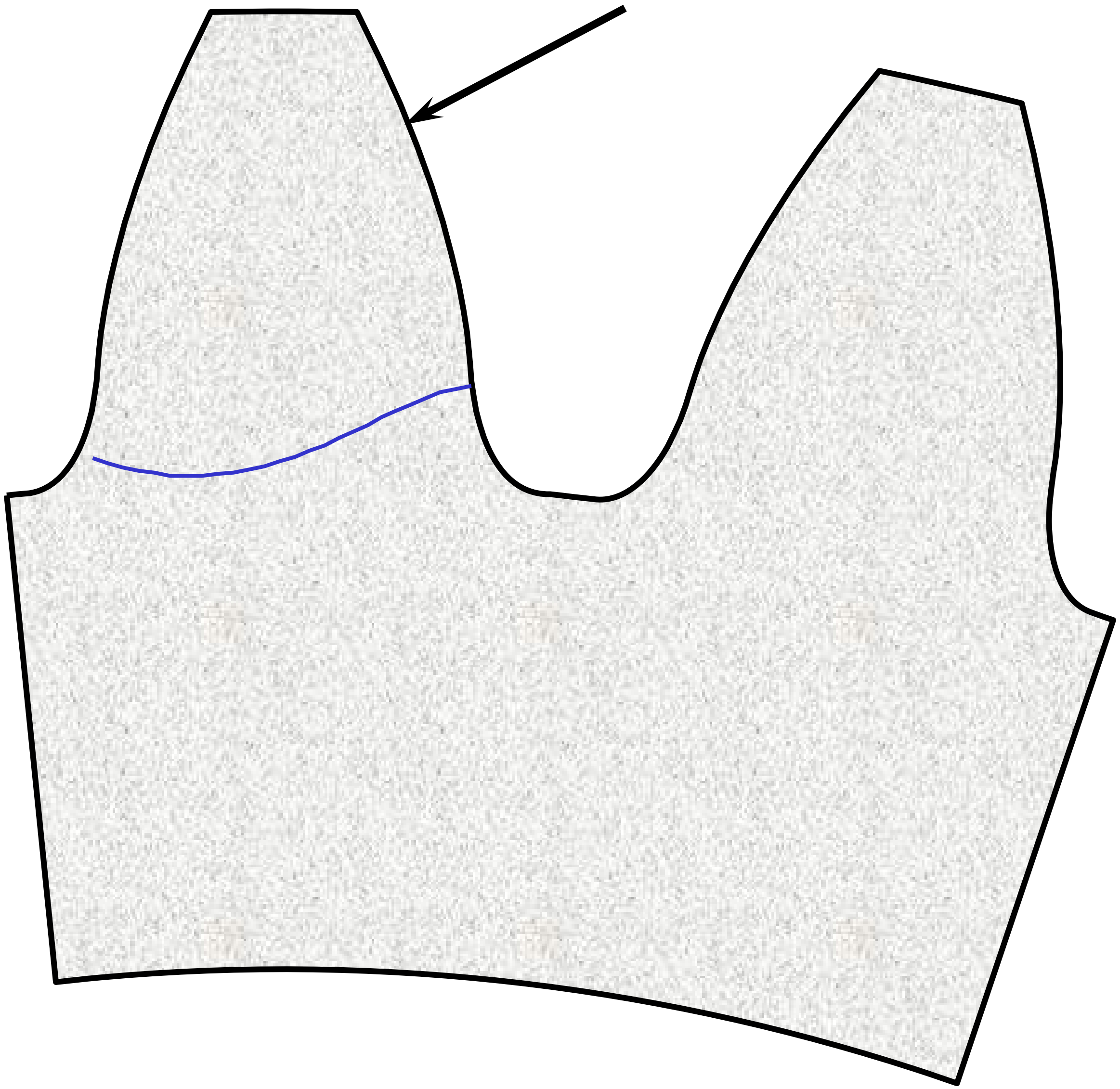

Initial crack location:
θ_0 = 120°

Failure mode:
Tooth fracture

Effect of Initial Crack Location on Crack Path

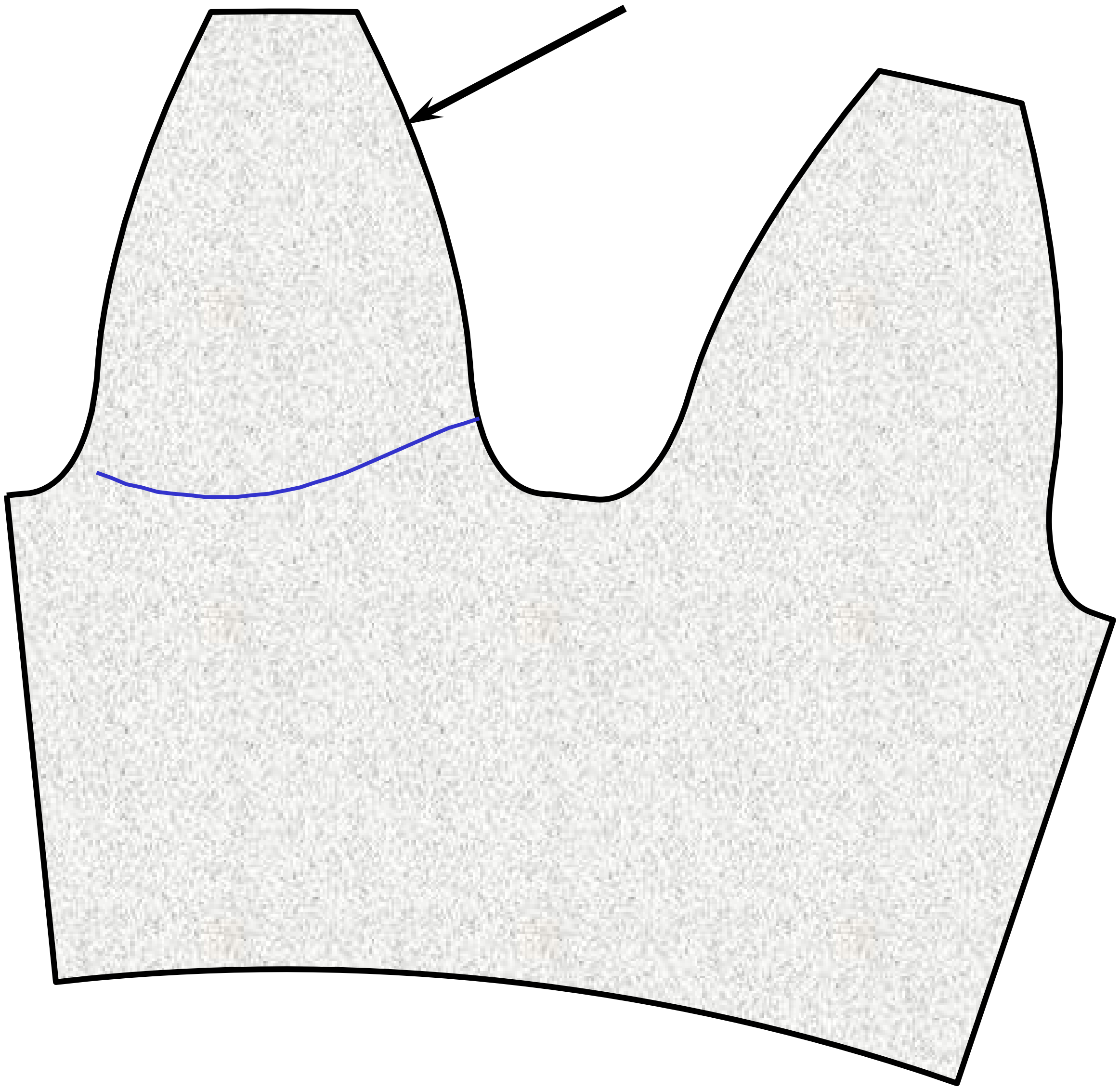

Initial crack location:
θ_0 = 114°

Failure mode:
Tooth fracture

Effect of Initial Crack Location on Crack Path

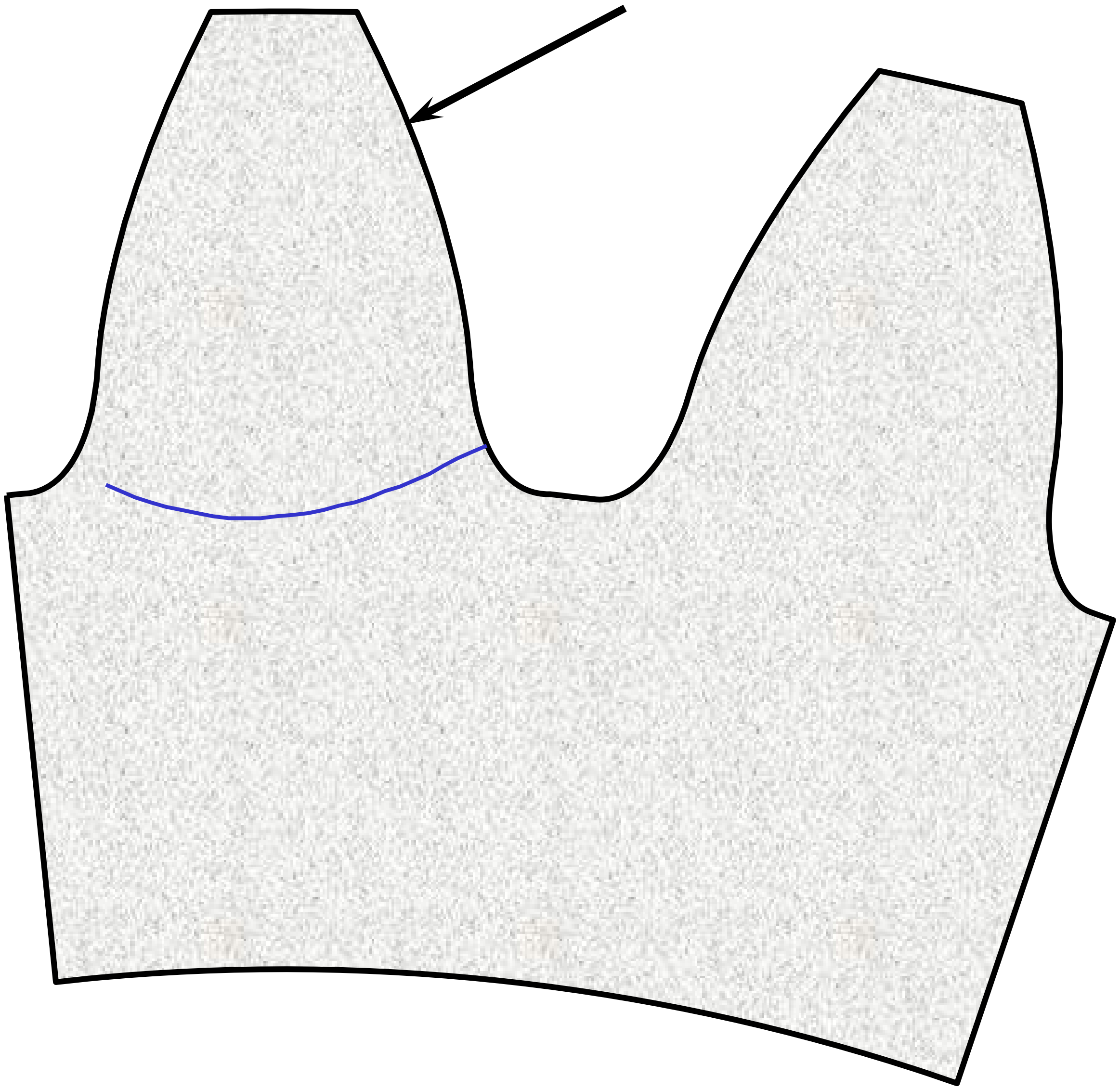

Initial crack location:
θ_0 = 109°

Failure mode:
Tooth fracture

Effect of Initial Crack Location on Crack Path

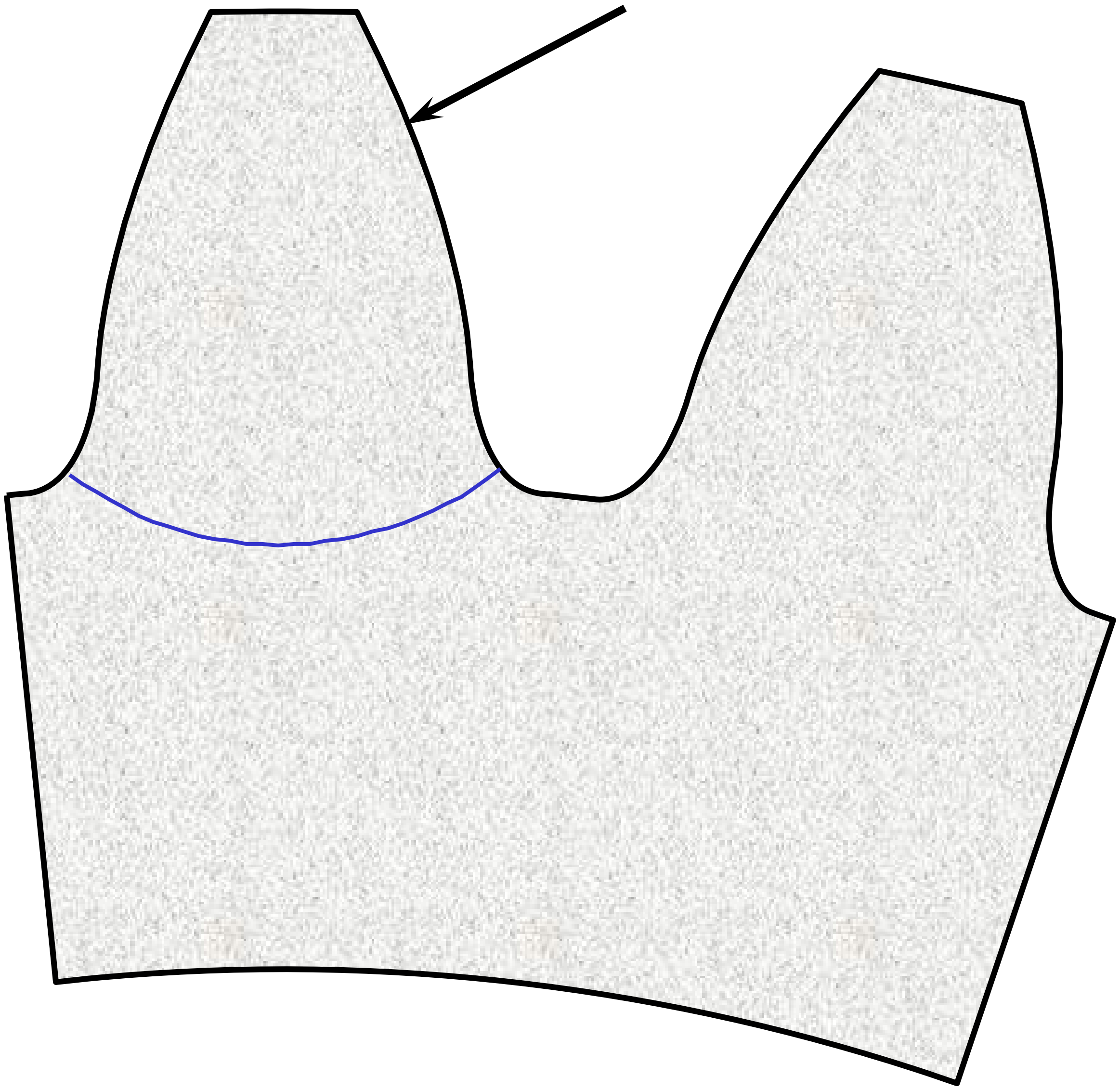

Initial crack location:
θ_0 = 104°
(max tensile)

Failure mode:
Tooth fracture

Effect of Initial Crack Location on Crack Path

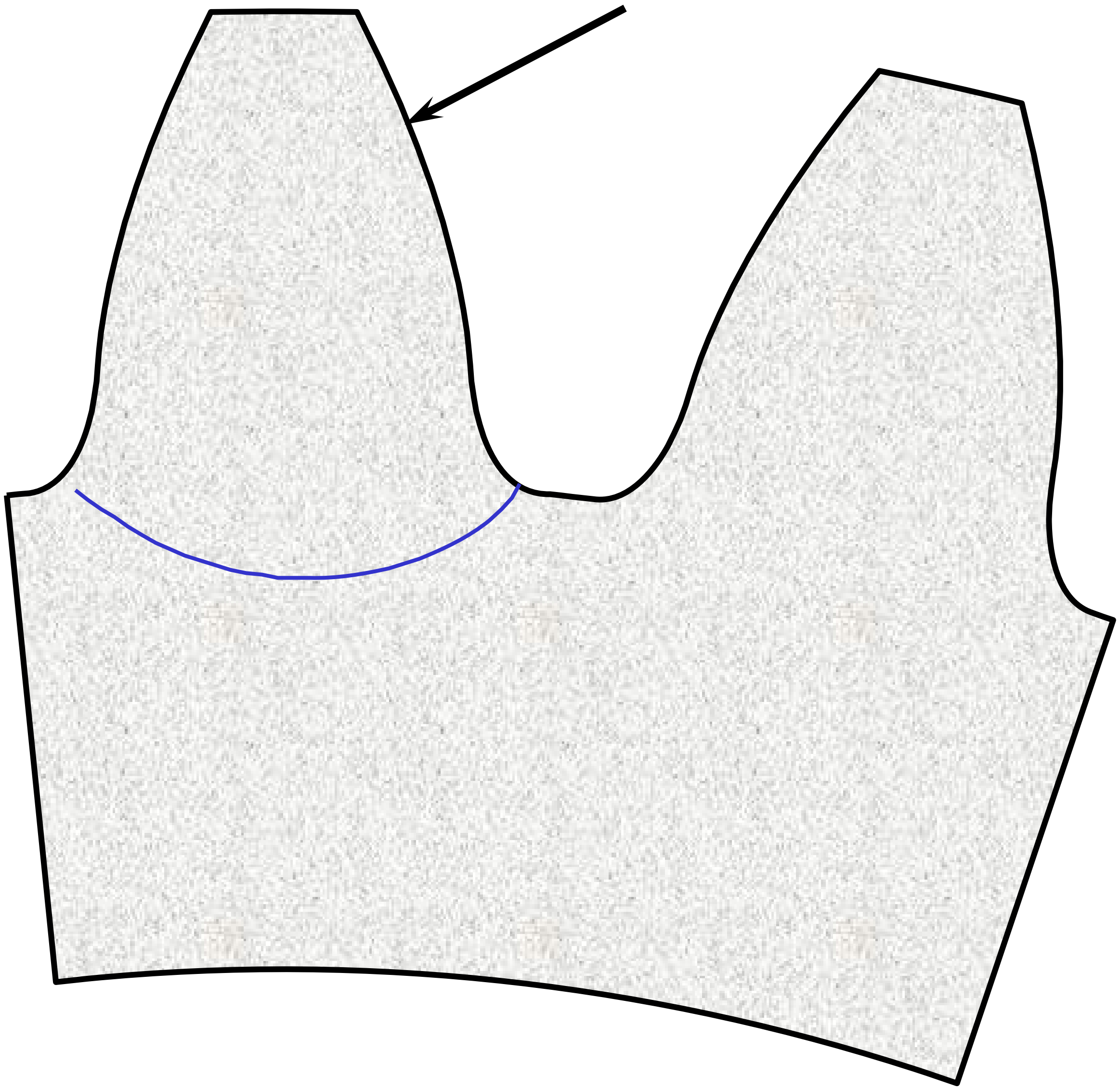

Initial crack location:
θ_0 = **99°**

Failure mode:
Tooth fracture

Effect of Initial Crack Location on Crack Path

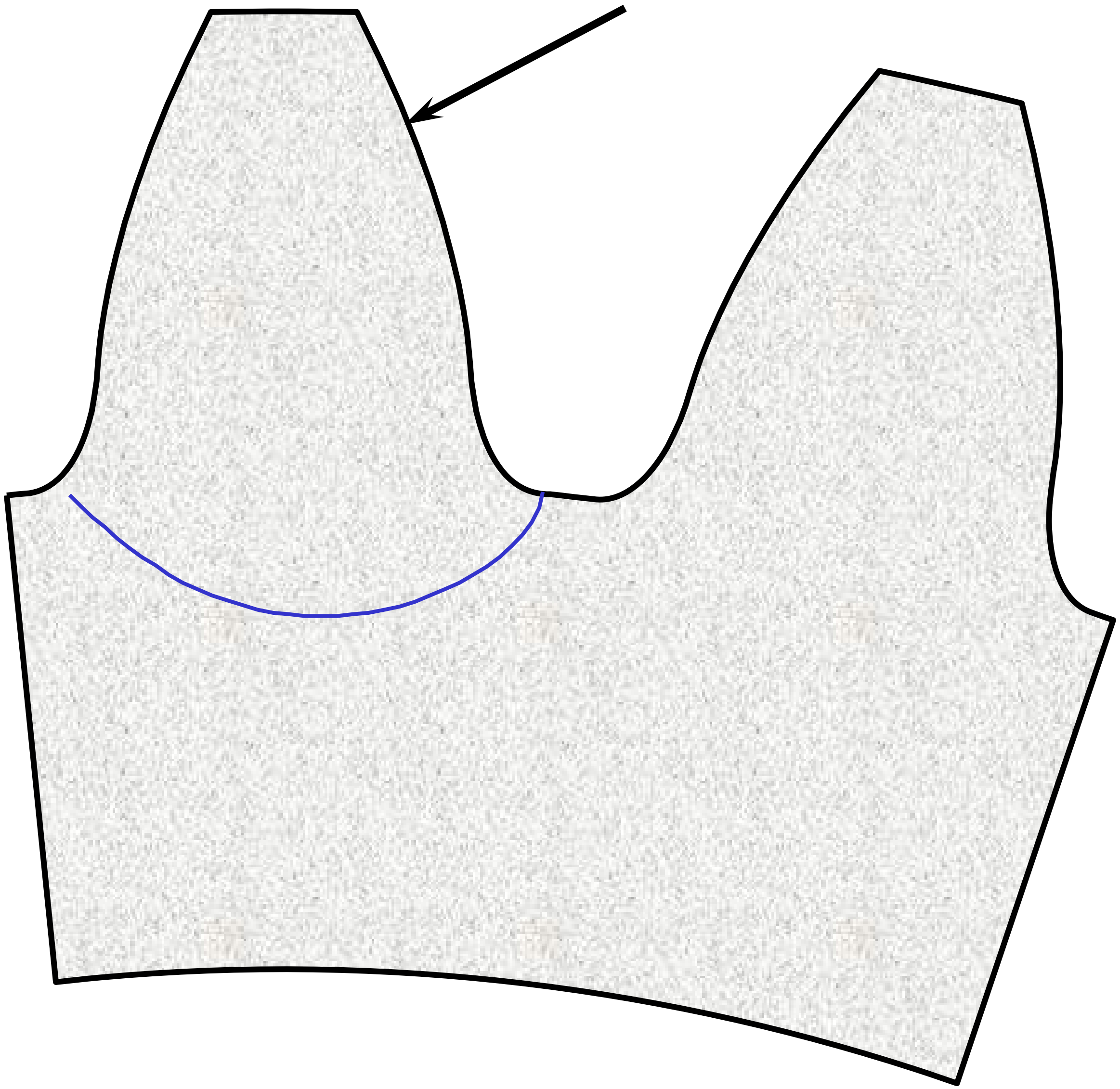

Initial crack location:
θ_0 = **94°**

Failure mode:
Tooth fracture

Effect of Initial Crack Location on Crack Path

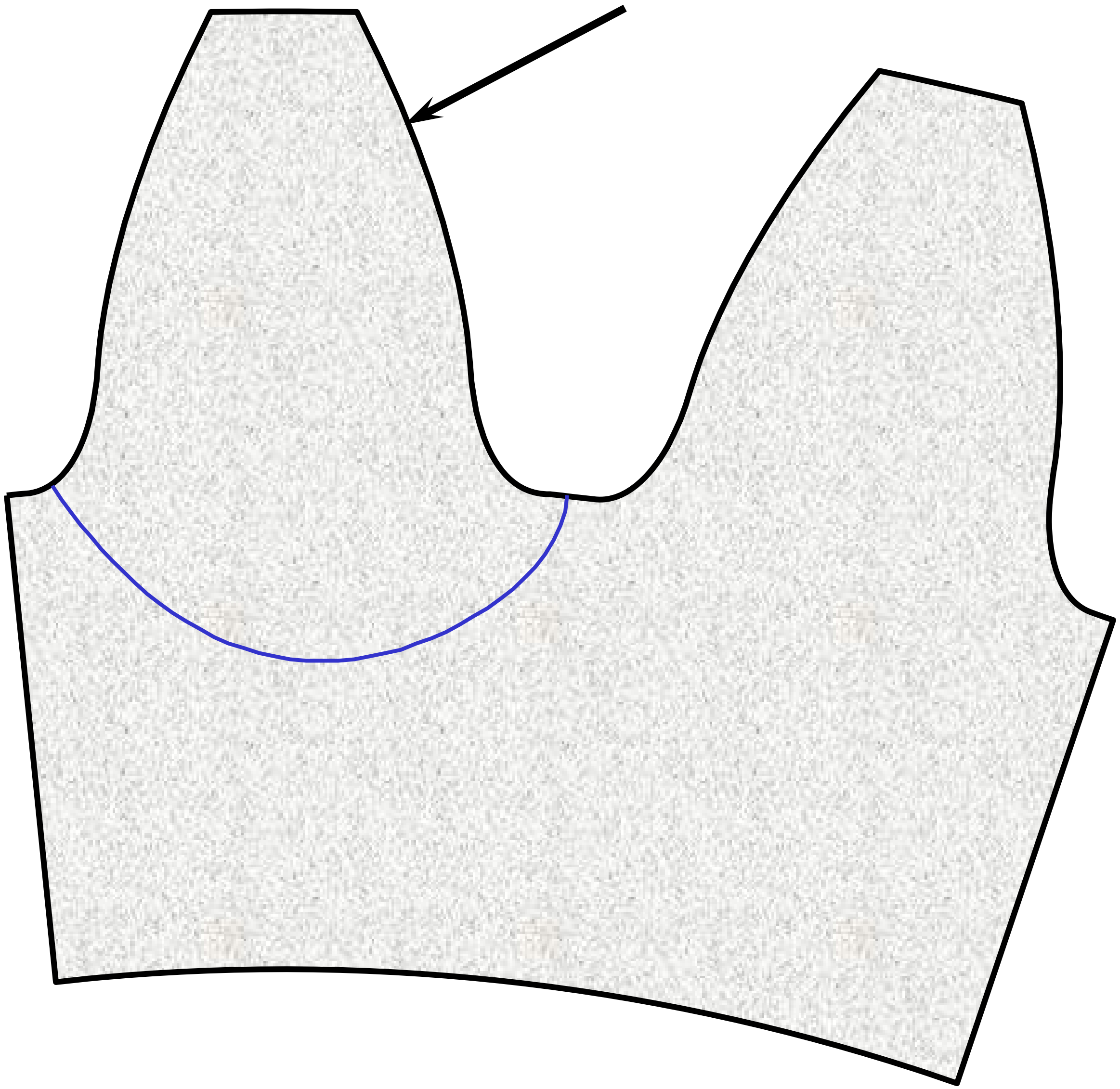

Initial crack location:
θ_0 = 88°
(root centerline)

Failure mode:
Tooth fracture

Effect of Initial Crack Location on Crack Path

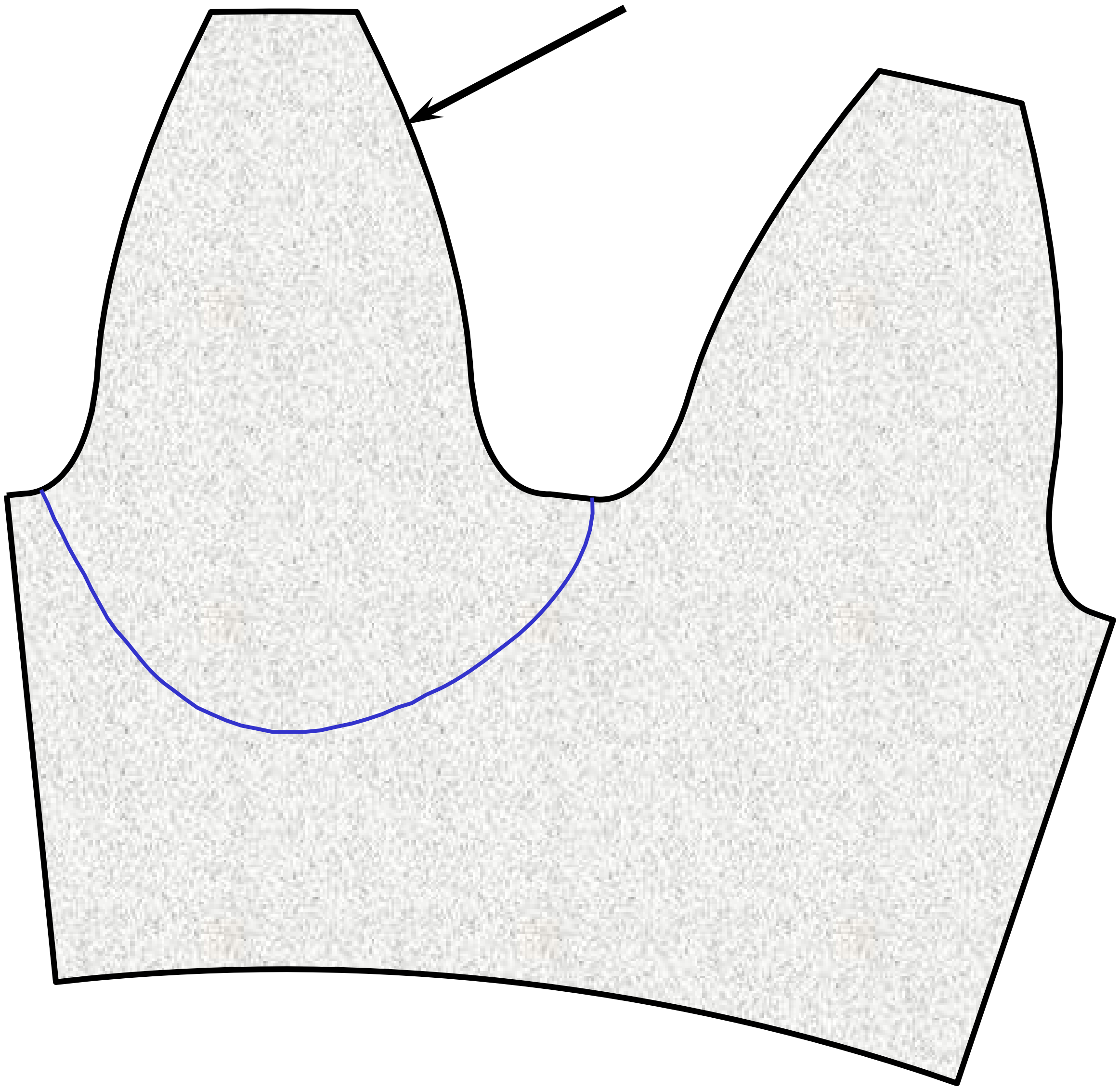

Initial crack location:
θ_0 = 83°

Failure mode:
Tooth fracture

Effect of Initial Crack Location on Crack Path

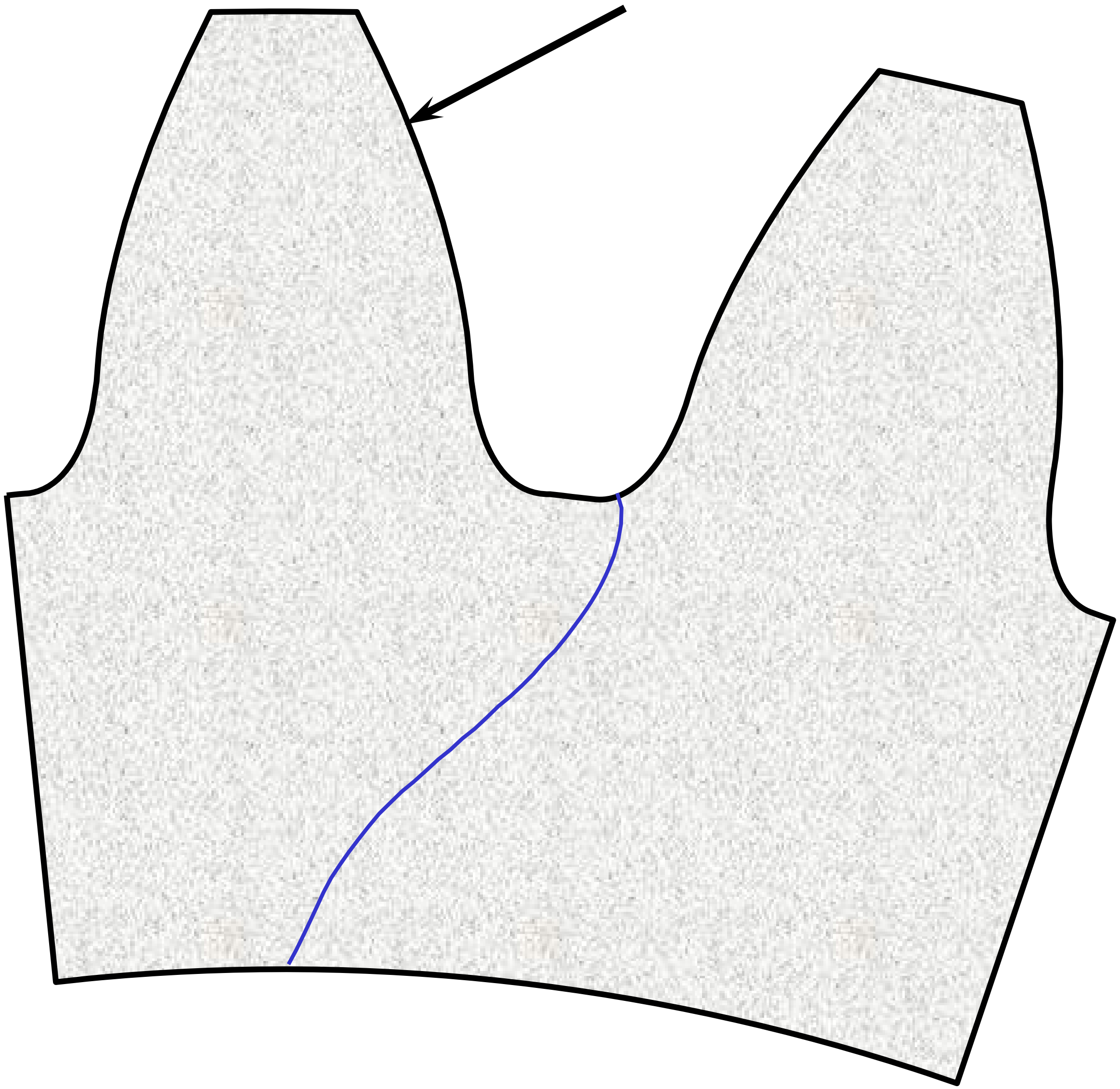

Initial crack location:
θ_0 = **78°**

Failure mode:
Rim fracture

Effect of Initial Crack Location on Crack Path

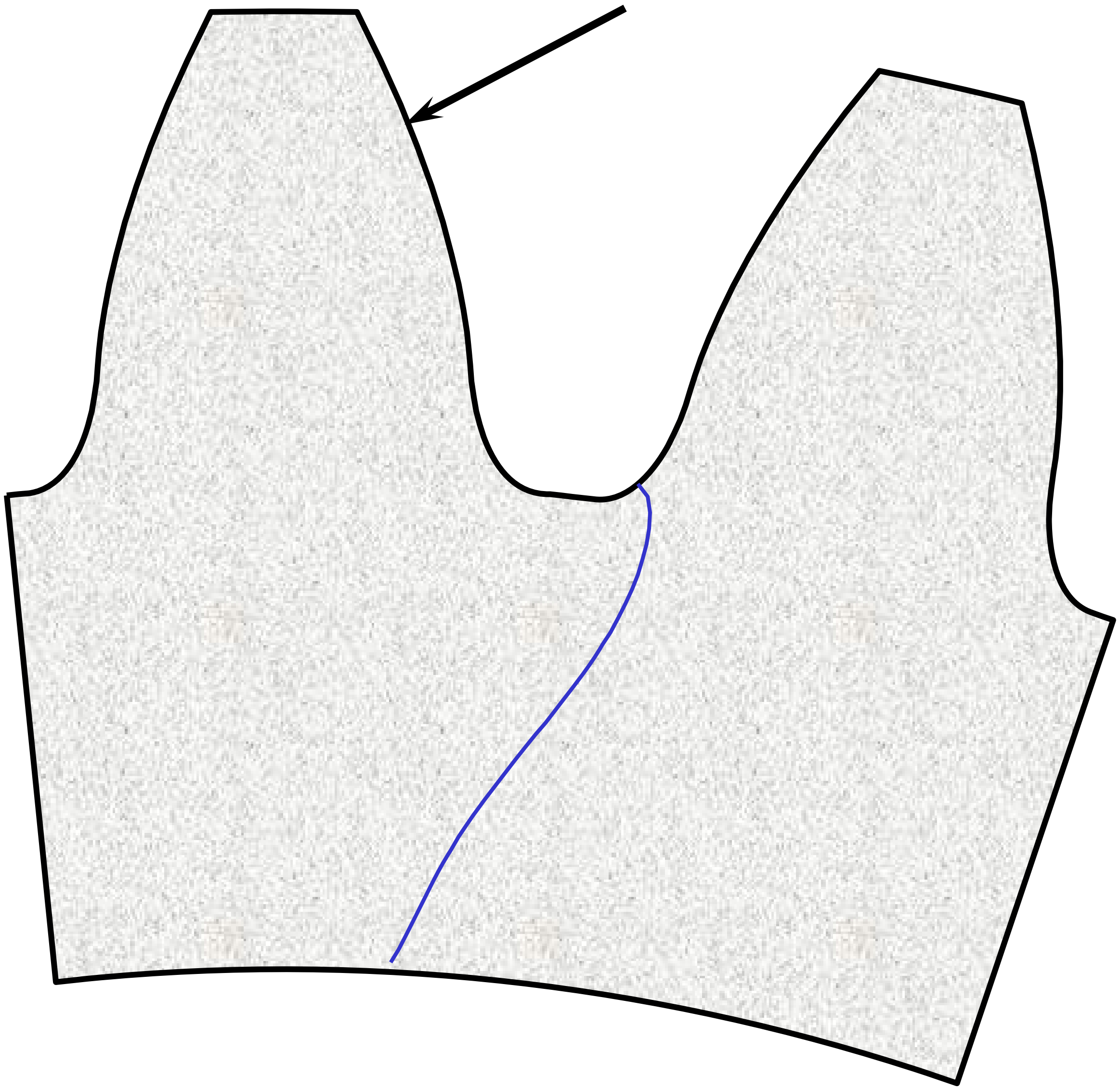

Initial crack location:
θ_0 = **73°**

Failure mode:
Rim fracture

Effect of Initial Crack Location on Crack Path

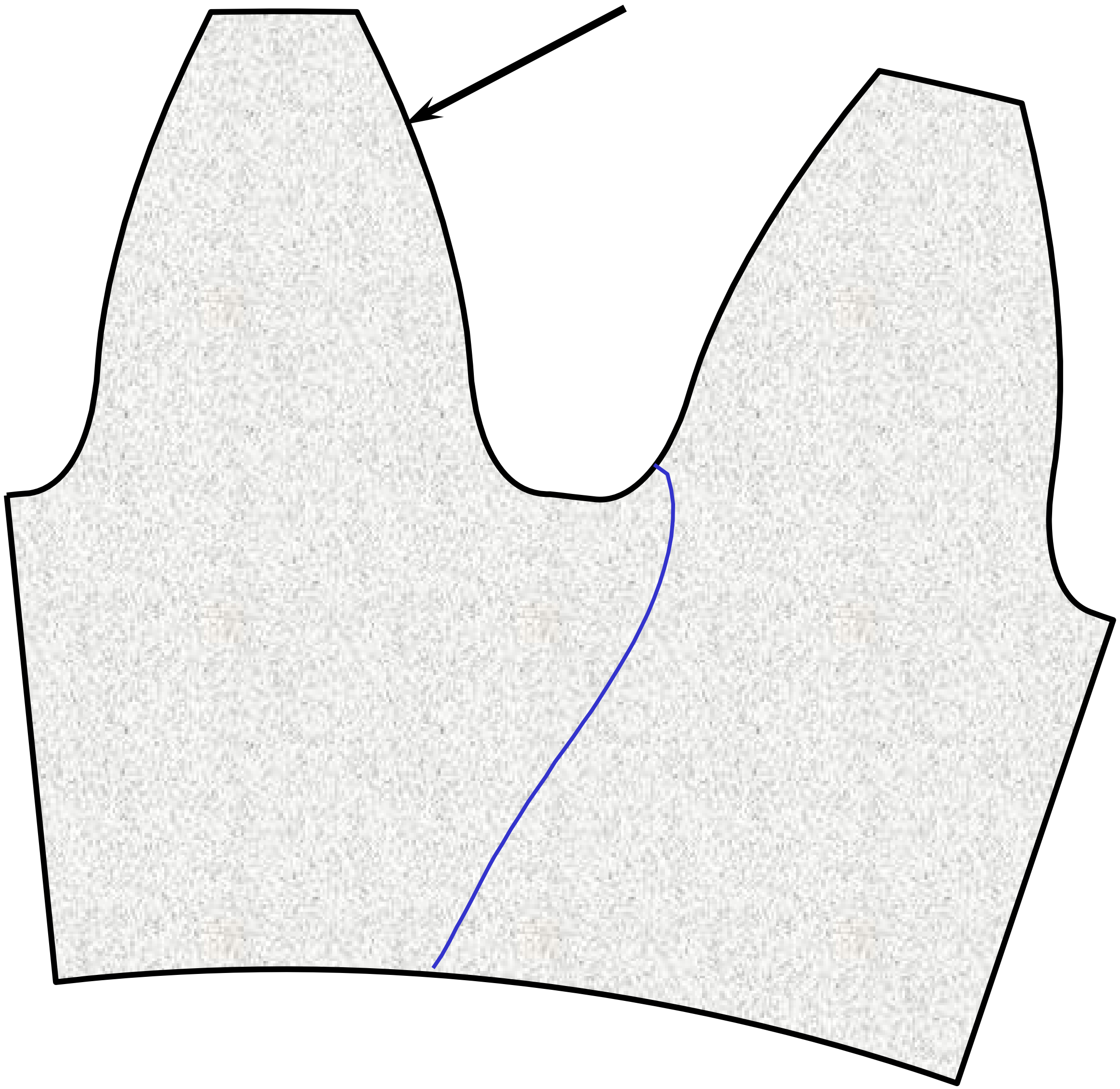

Initial crack location:
θ_0 = 68°

Failure mode:
Rim fracture

Effect of Initial Crack Location on Crack Path

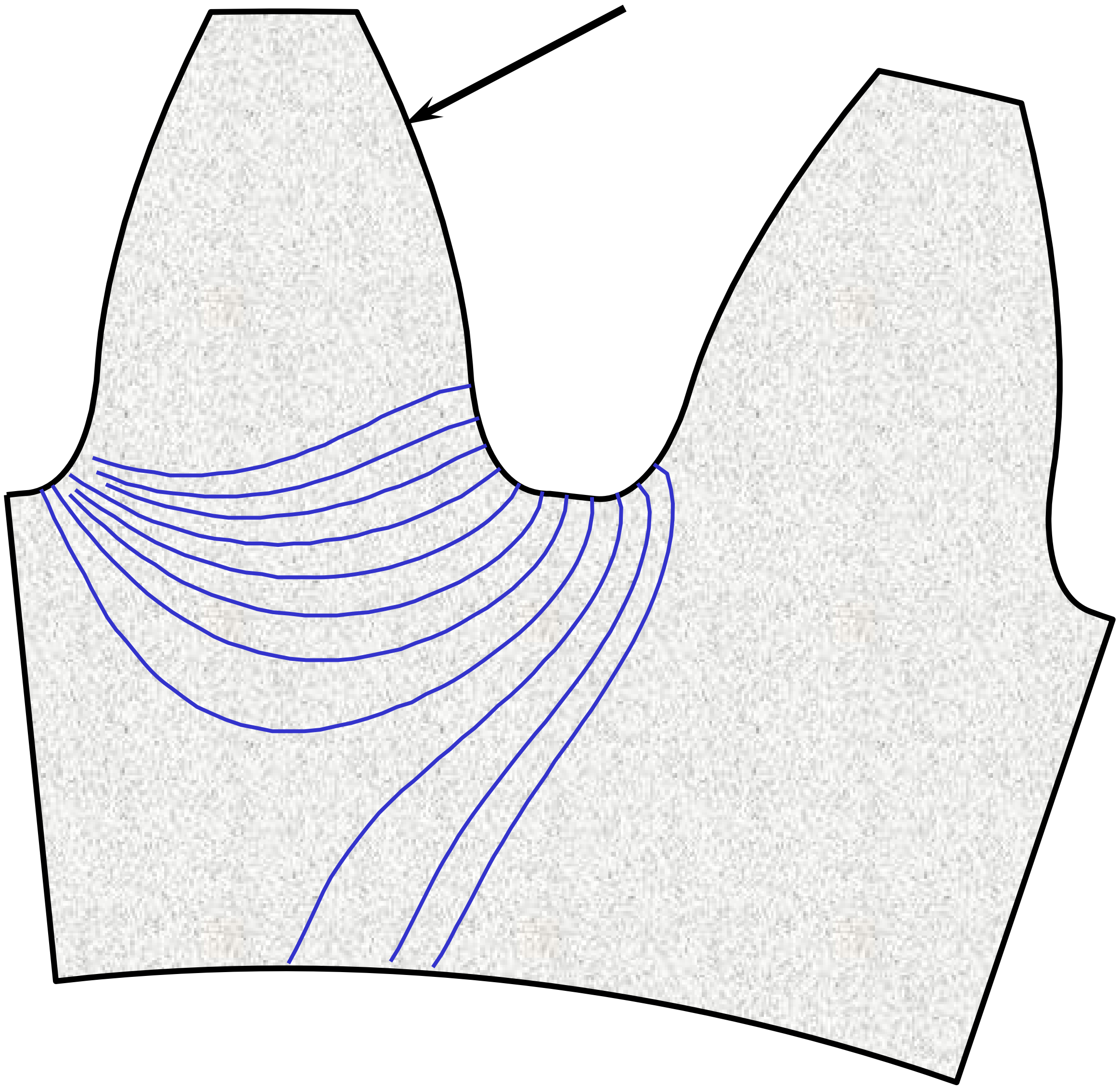

Stress Intensity Factors

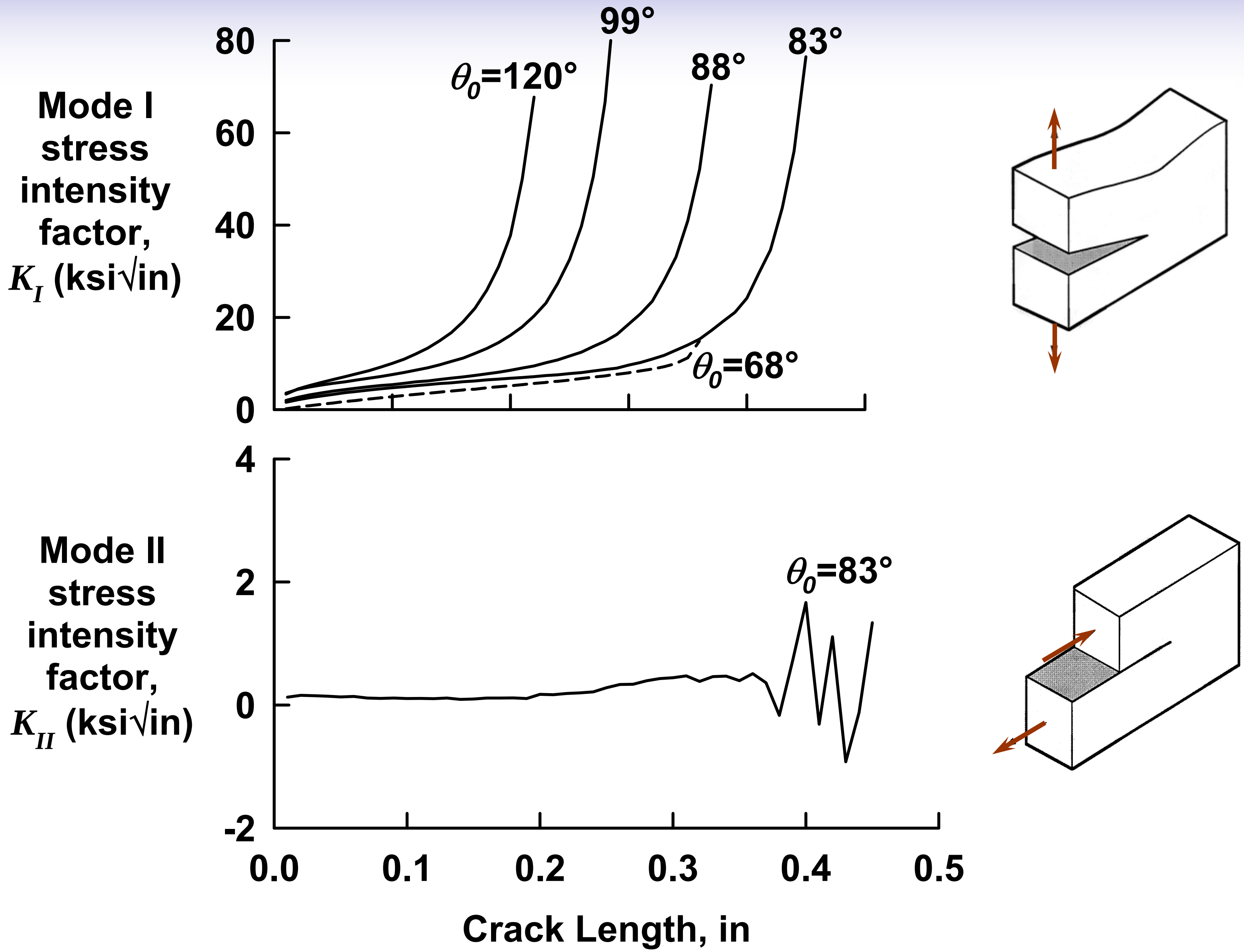

Effect of Backup Ratio on Crack Path

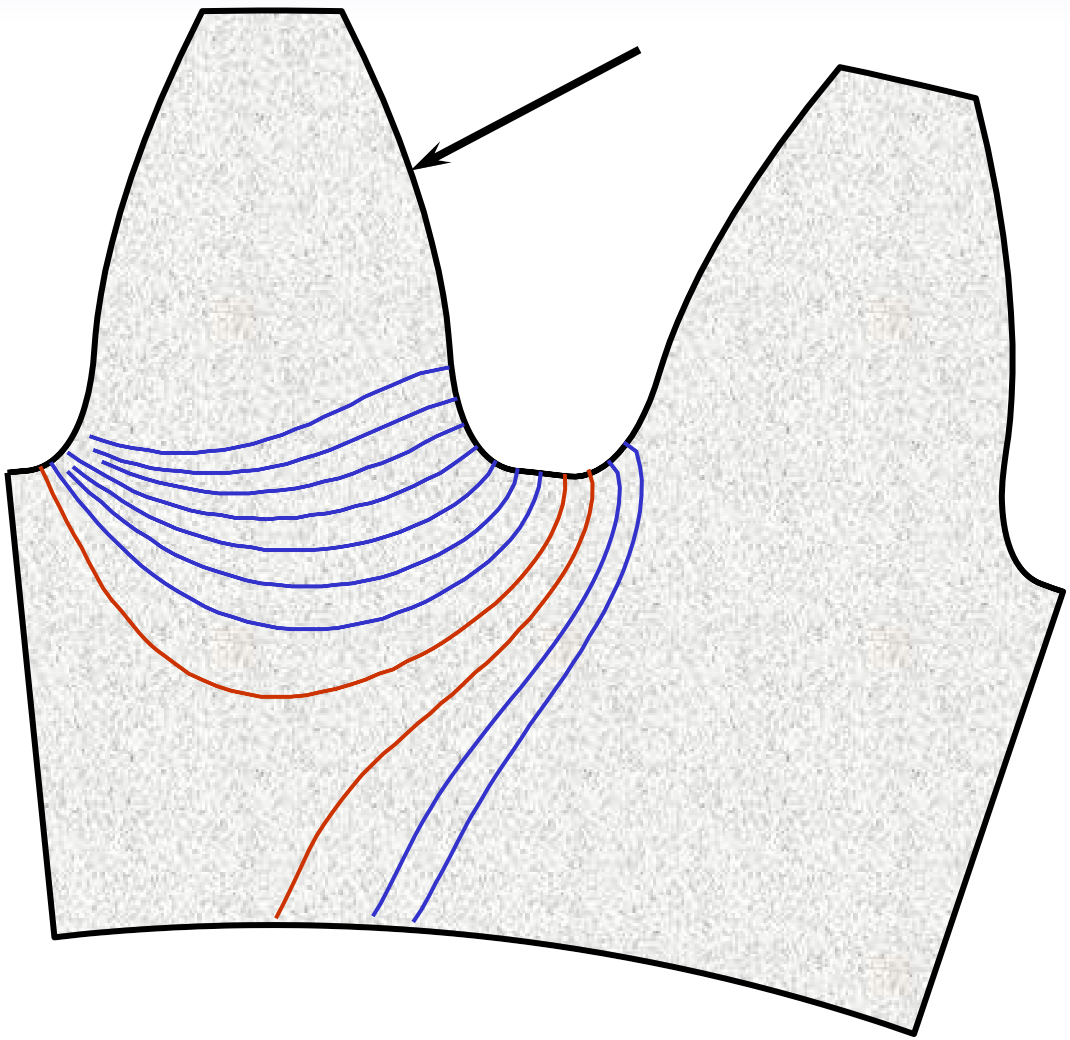

Backup ratio:
m_B = **1.0**

Tooth/rim fracture transition:
θ_0 = **81°**

Effect of Backup Ratio on Crack Path

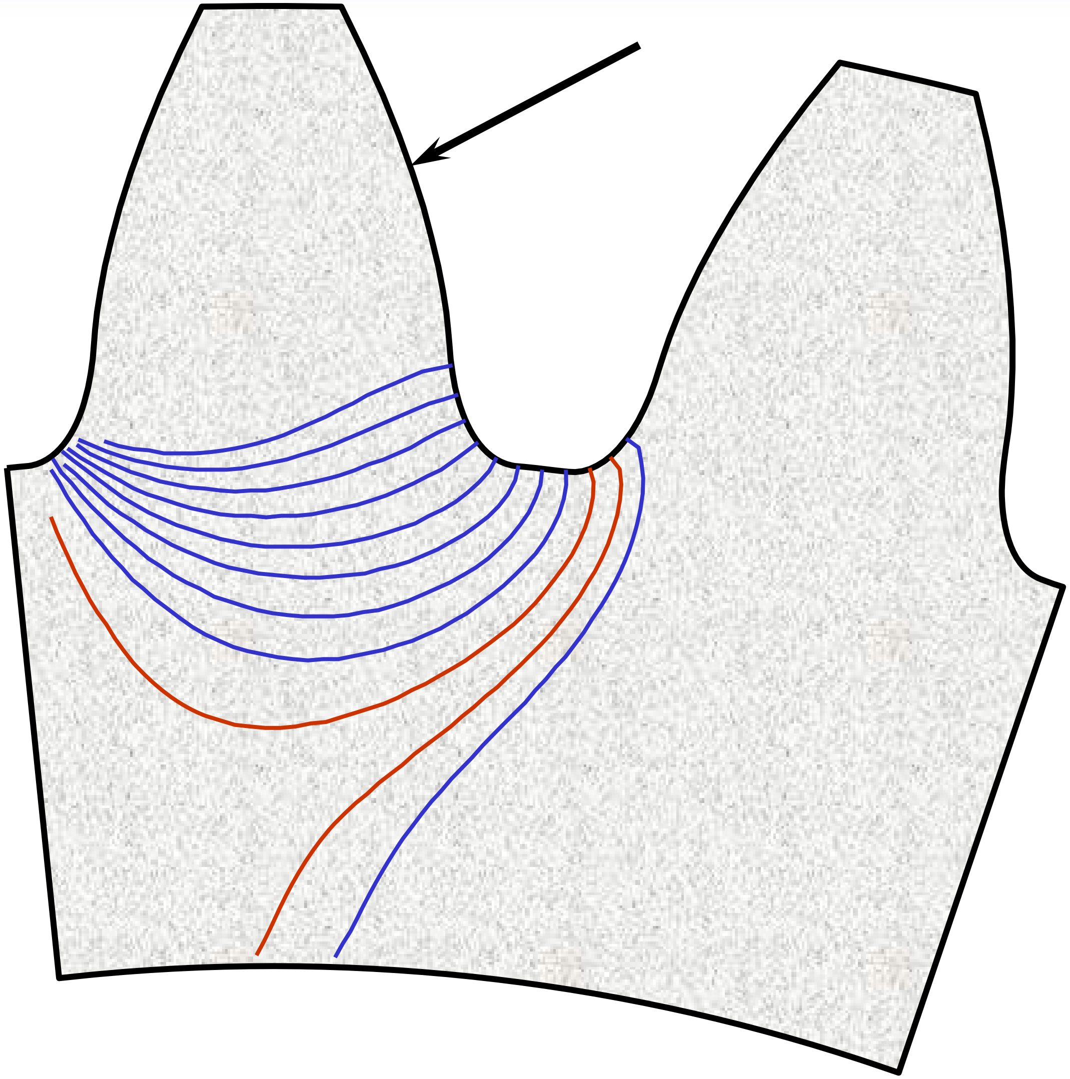

Backup ratio:
m_B = **1.1**

Tooth/rim fracture transition:
θ_0 = **76°**

Effect of Backup Ratio on Crack Path

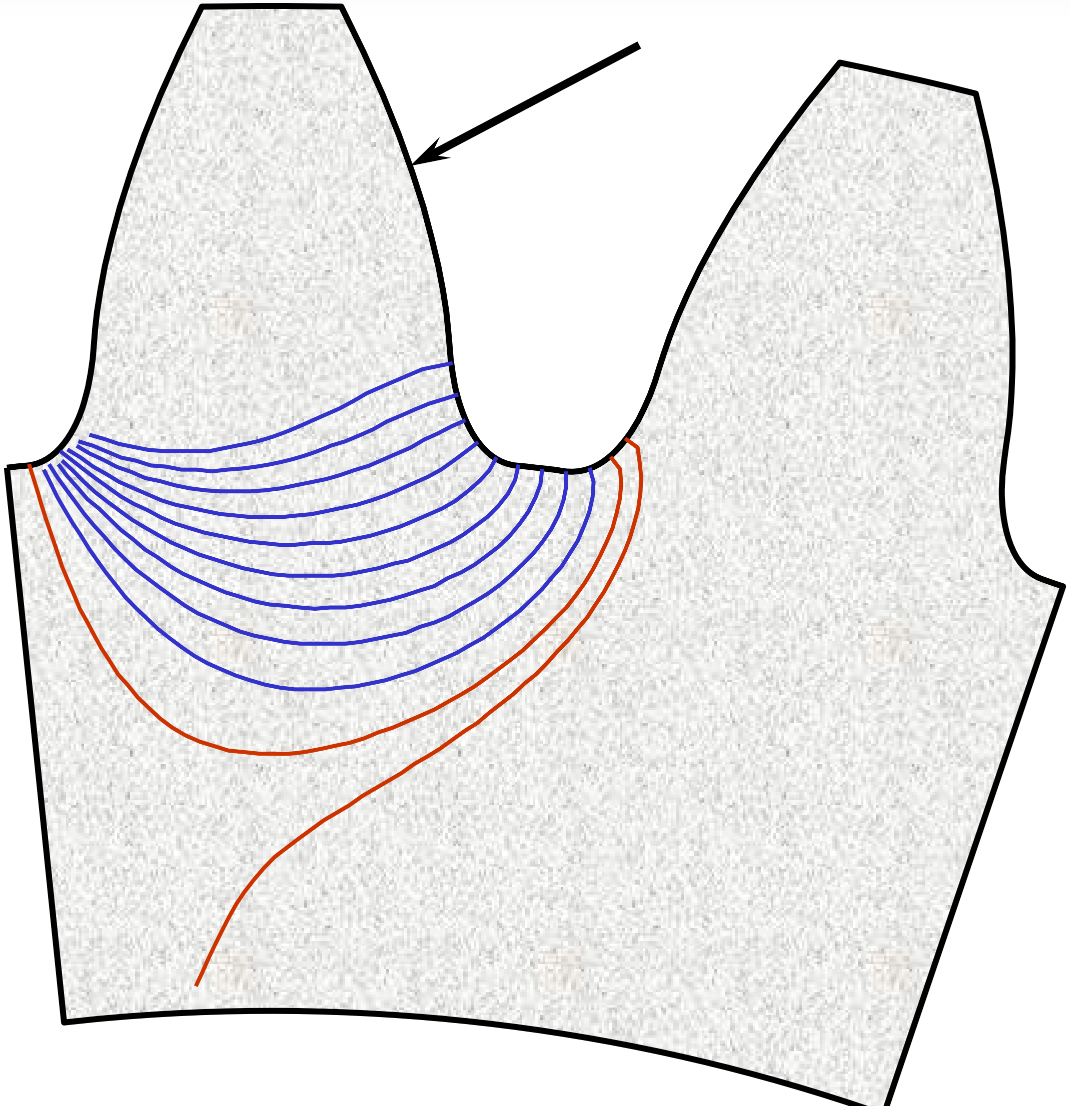

Backup ratio:

m_B = **1.2**

Tooth/rim fracture transition:

θ_0 = **71°**

Effect of Backup Ratio on Crack Path

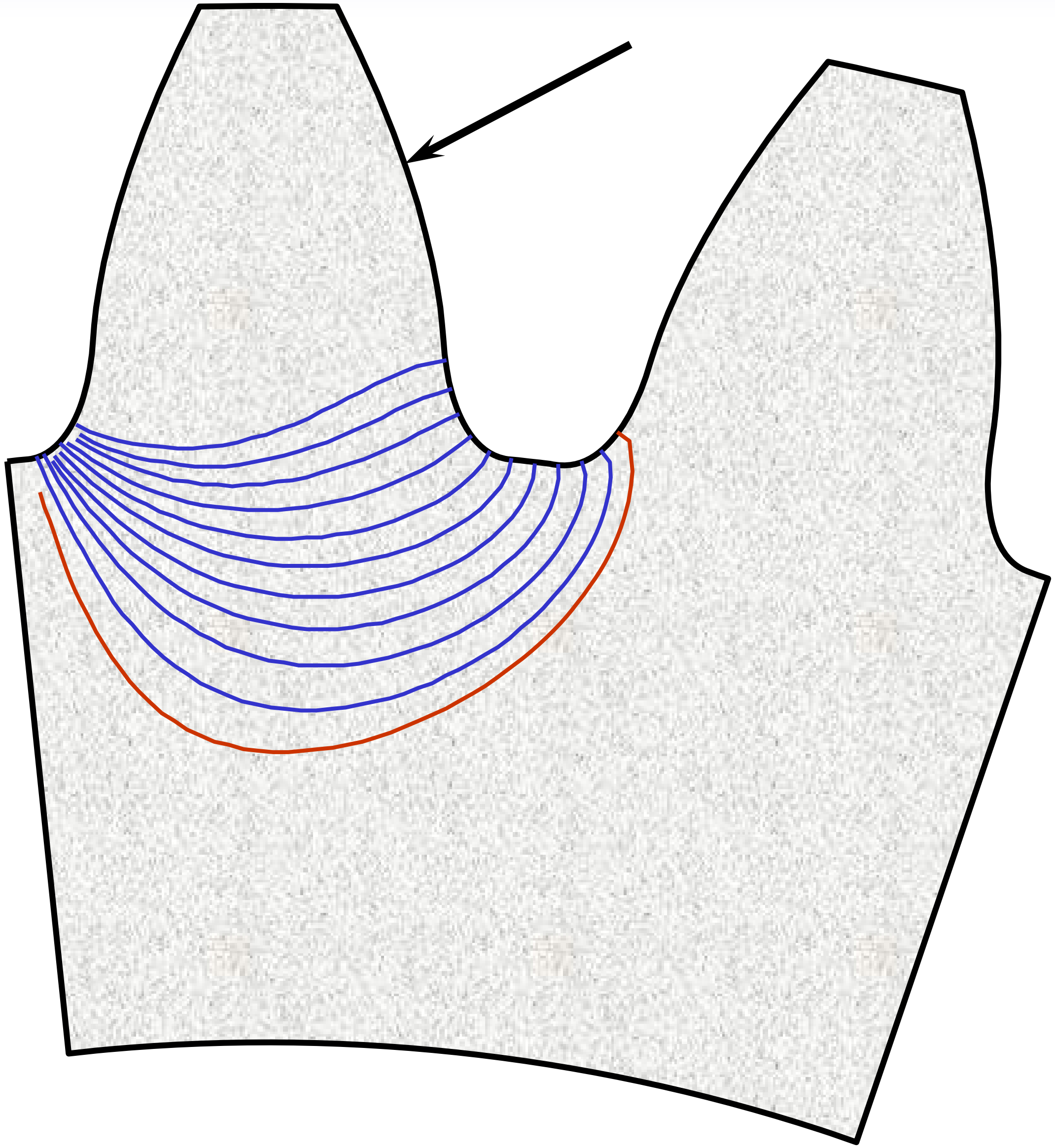

Backup ratio:
m_B = 1.3

Tooth/rim fracture transition:
All tooth fractures

Effect of Backup Ratio on Crack Path

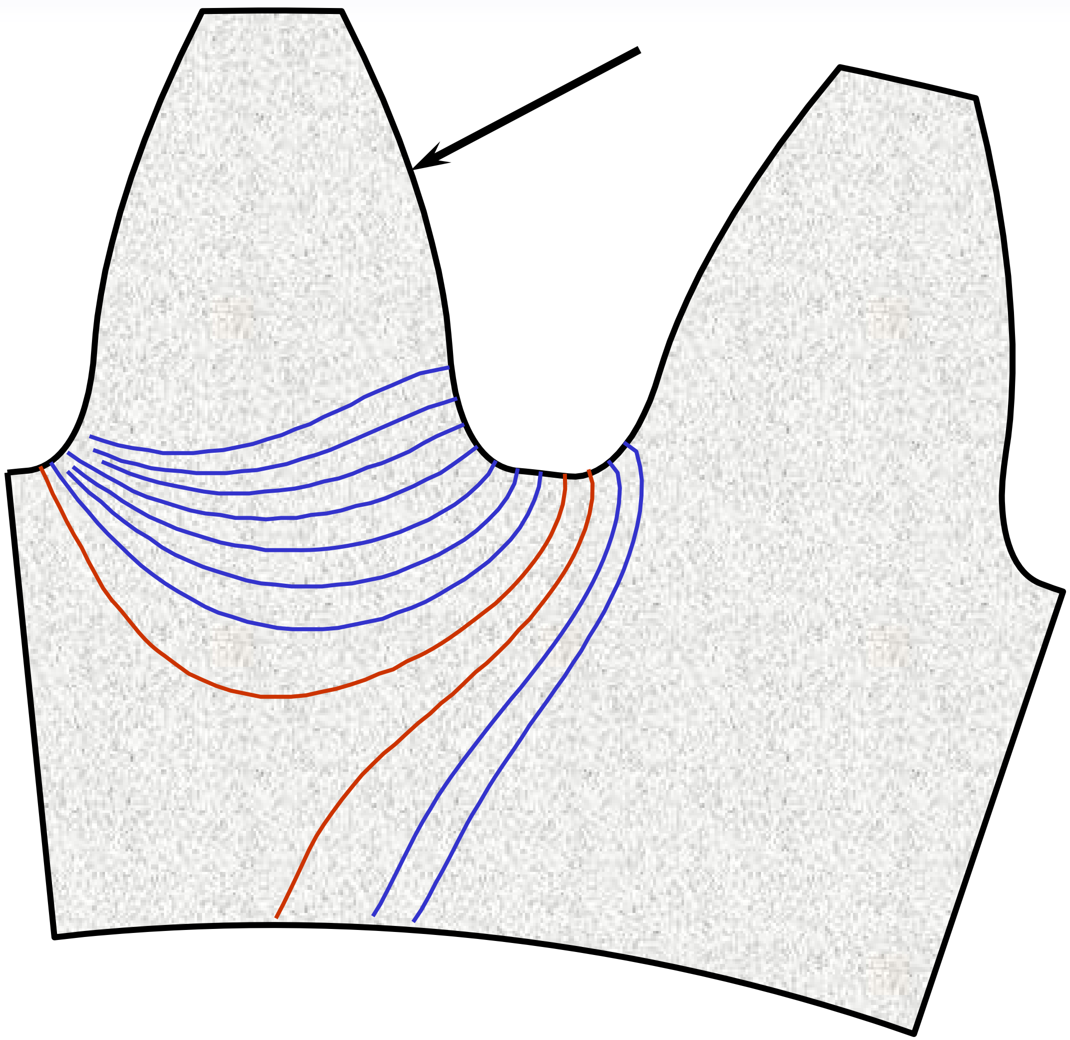

Backup ratio:

m_B = **1.0**

Tooth/rim fracture transition:

θ_0 = **81°**

Effect of Backup Ratio on Crack Path

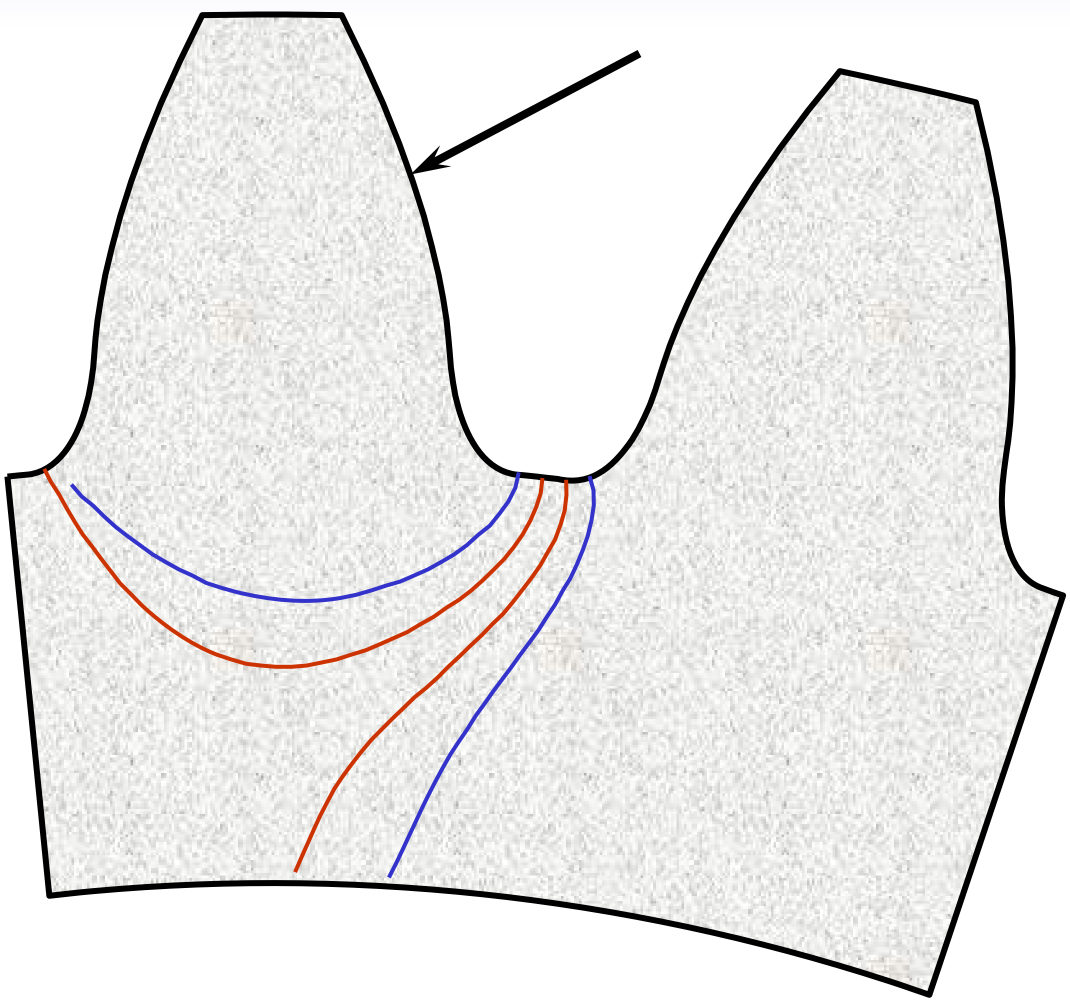

Backup ratio:

m_B = **0.9**

Tooth/rim fracture transition:

θ_0 = **86°**

Effect of Backup Ratio on Crack Path

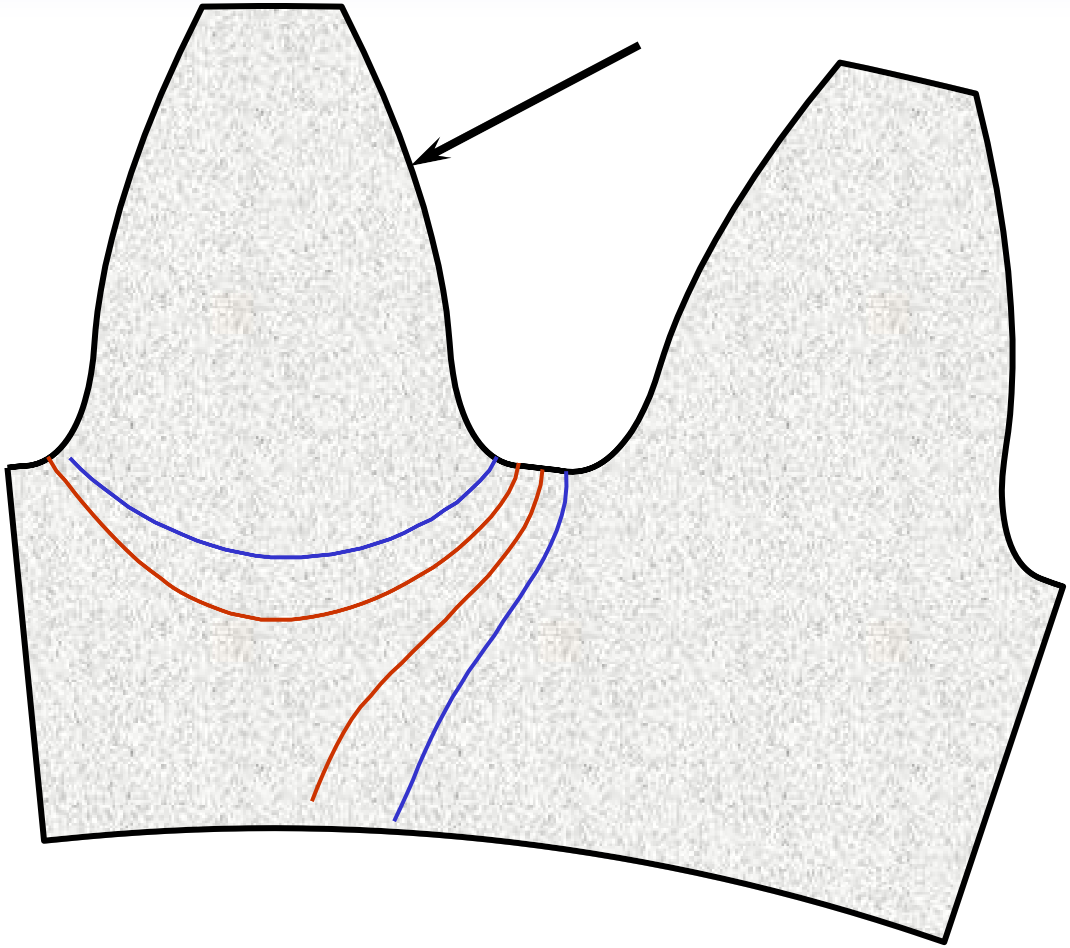

Backup ratio:
m_B = **0.8**

Tooth/rim fracture transition:
θ_0 = **91°**

Effect of Backup Ratio on Crack Path

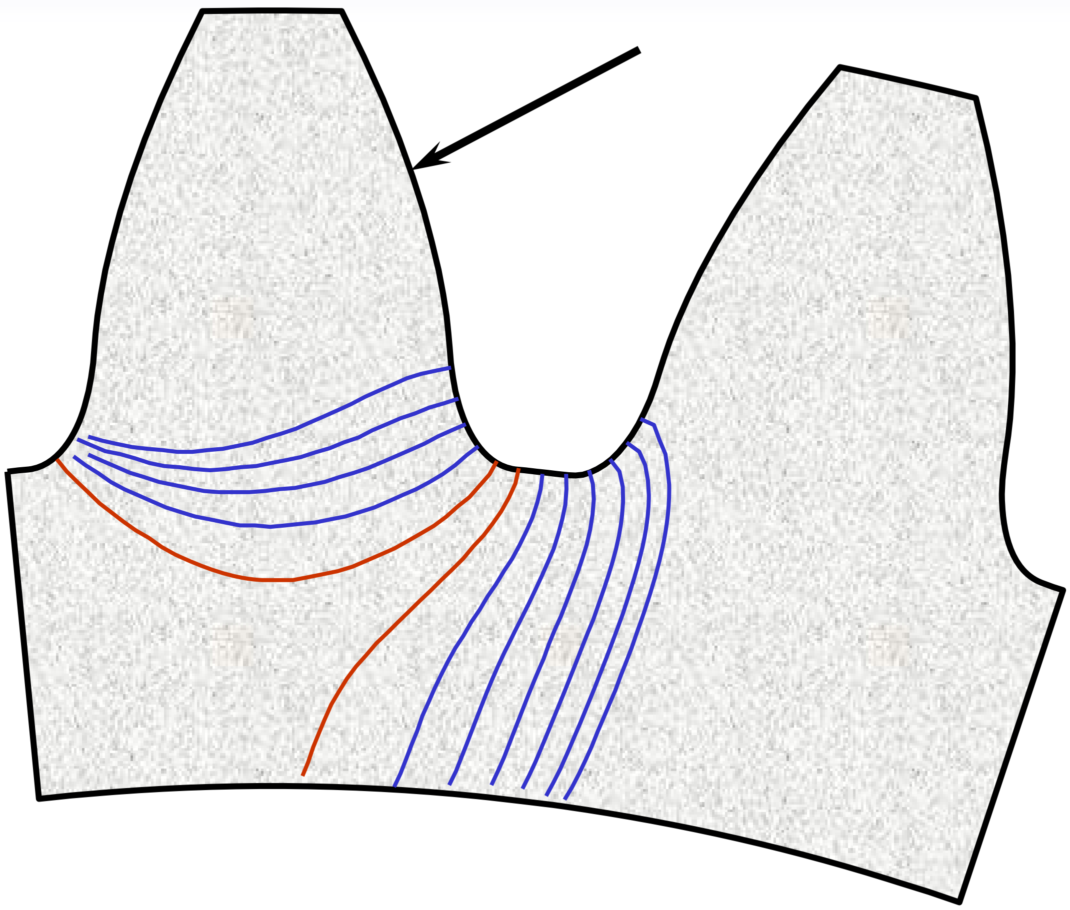

Backup ratio:

m_B = **0.7**

Tooth/rim fracture transition:

θ_0 = **97°**

Effect of Backup Ratio on Crack Path

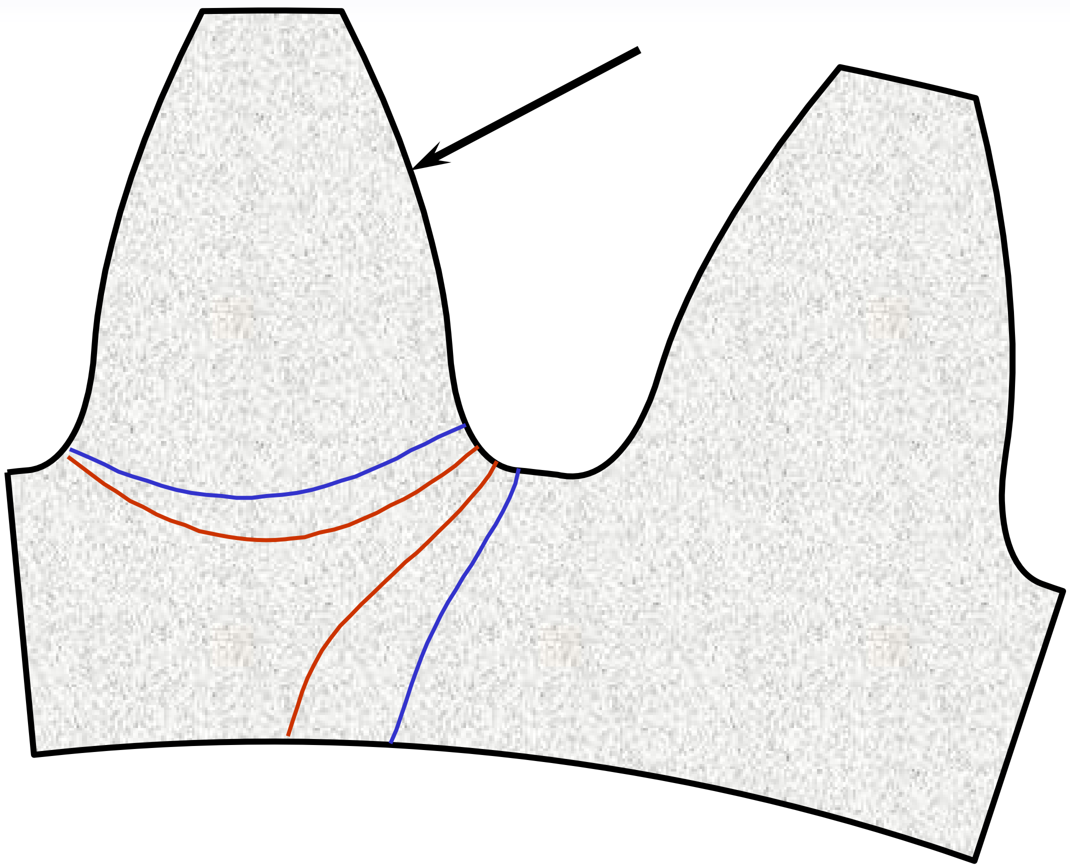

Backup ratio:

m_B = **0.6**

Tooth/rim fracture transition:

θ_0 = **102°**

Effect of Backup Ratio on Crack Path

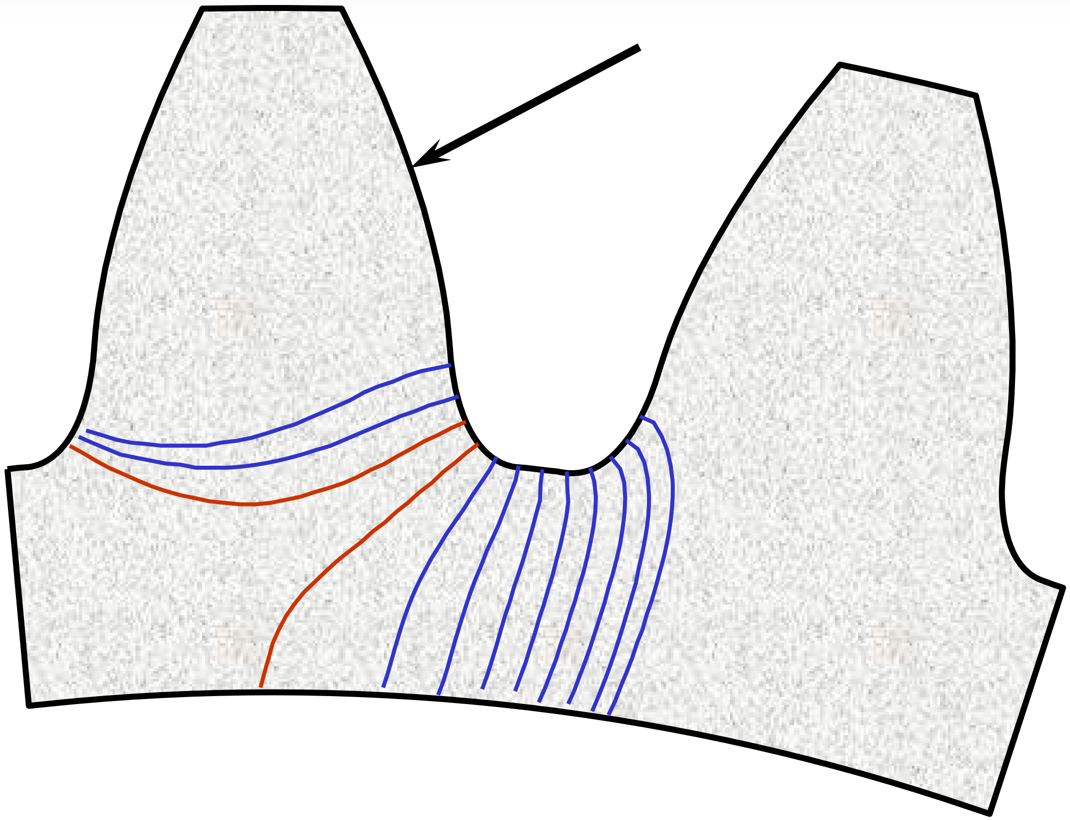

Backup ratio:
m_B = **0.5**

Tooth/rim fracture transition:
θ_0 = **107°**

Design Map

T = tooth fractures
R = rim fractures
C = compression

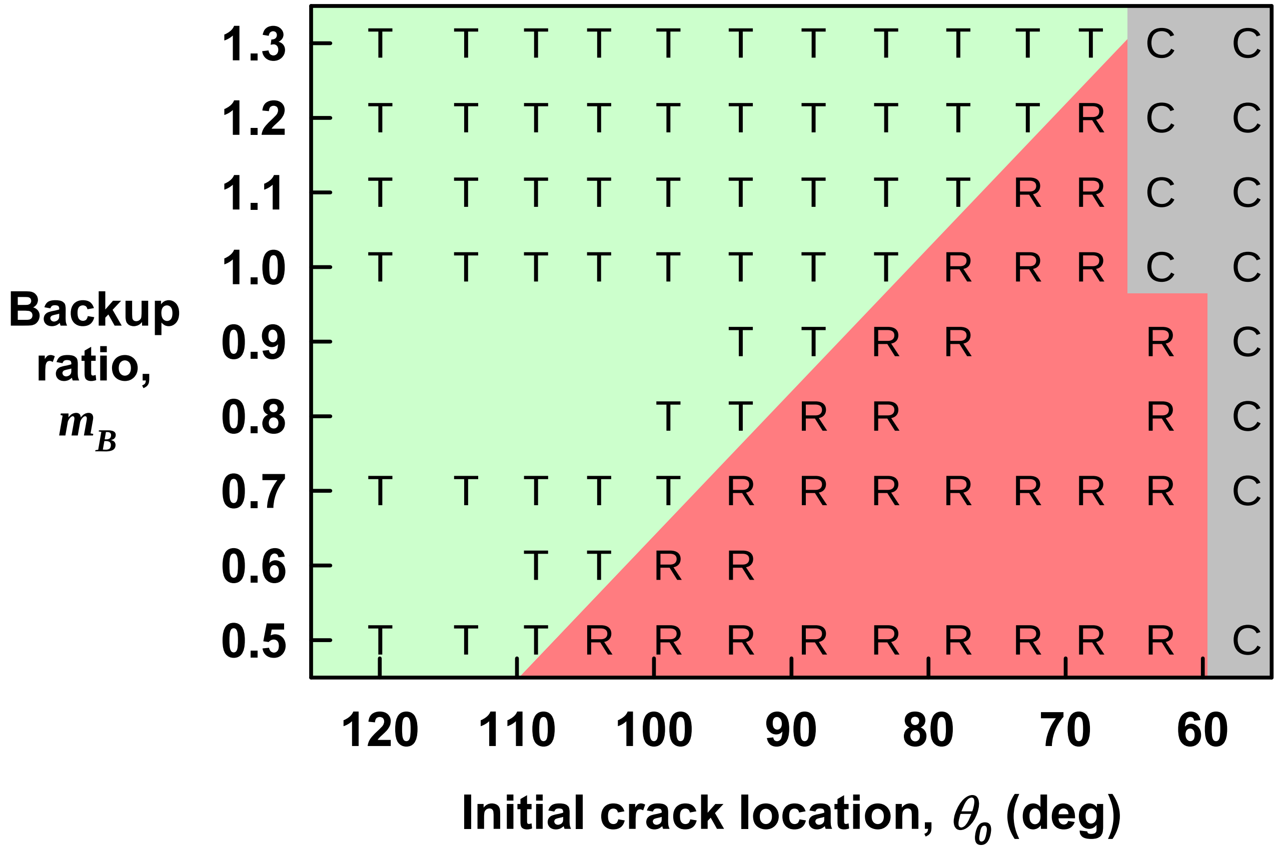

Mode I Stress Intensity Factors

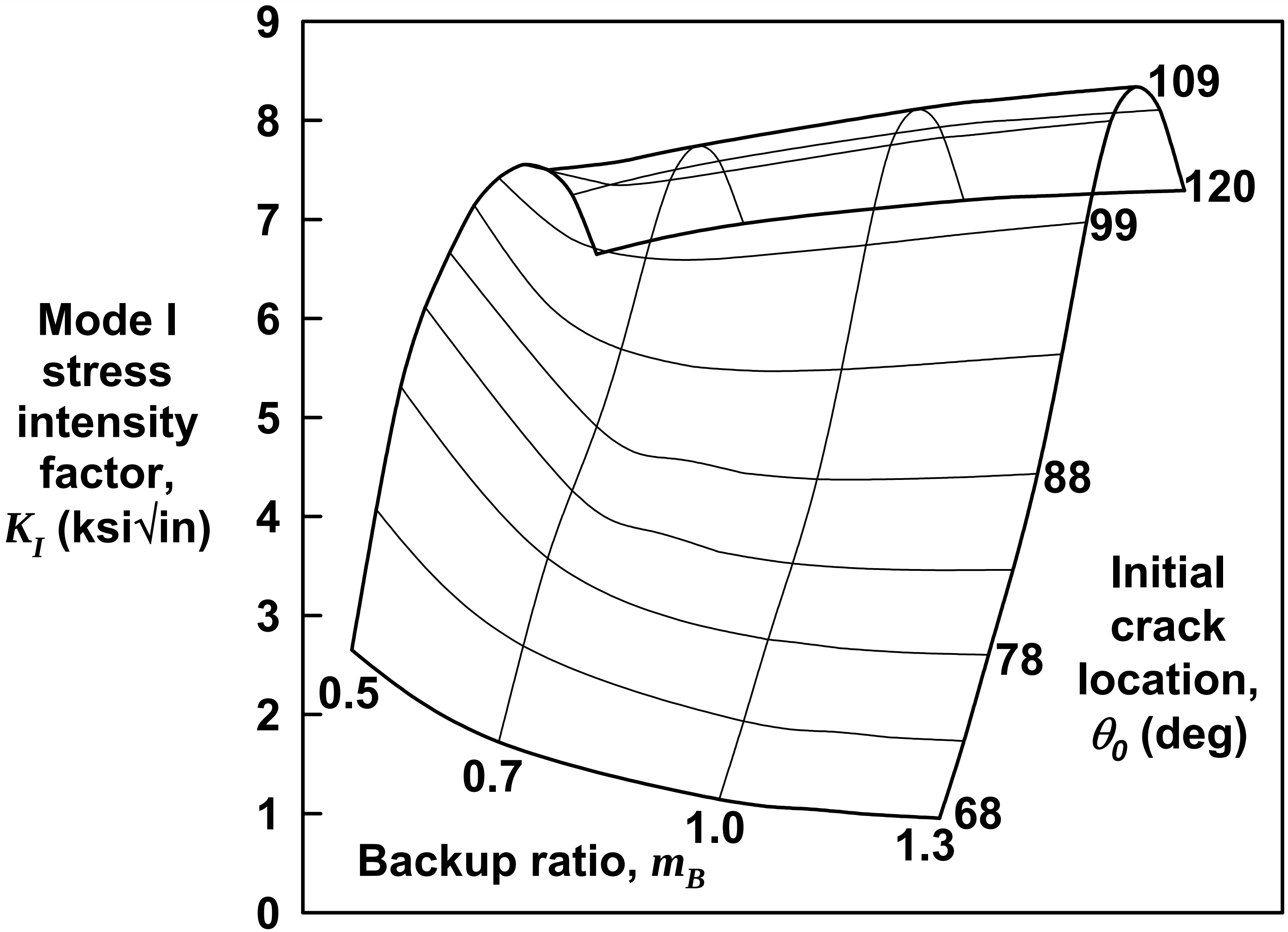

Gear Parameters:

- 28 teeth
- 8 pitch
- 1.75" pitch rad
- 20° press angle

- 500 lb tooth load
- 0.030" crack size

Mode I Stress Intensity Factors

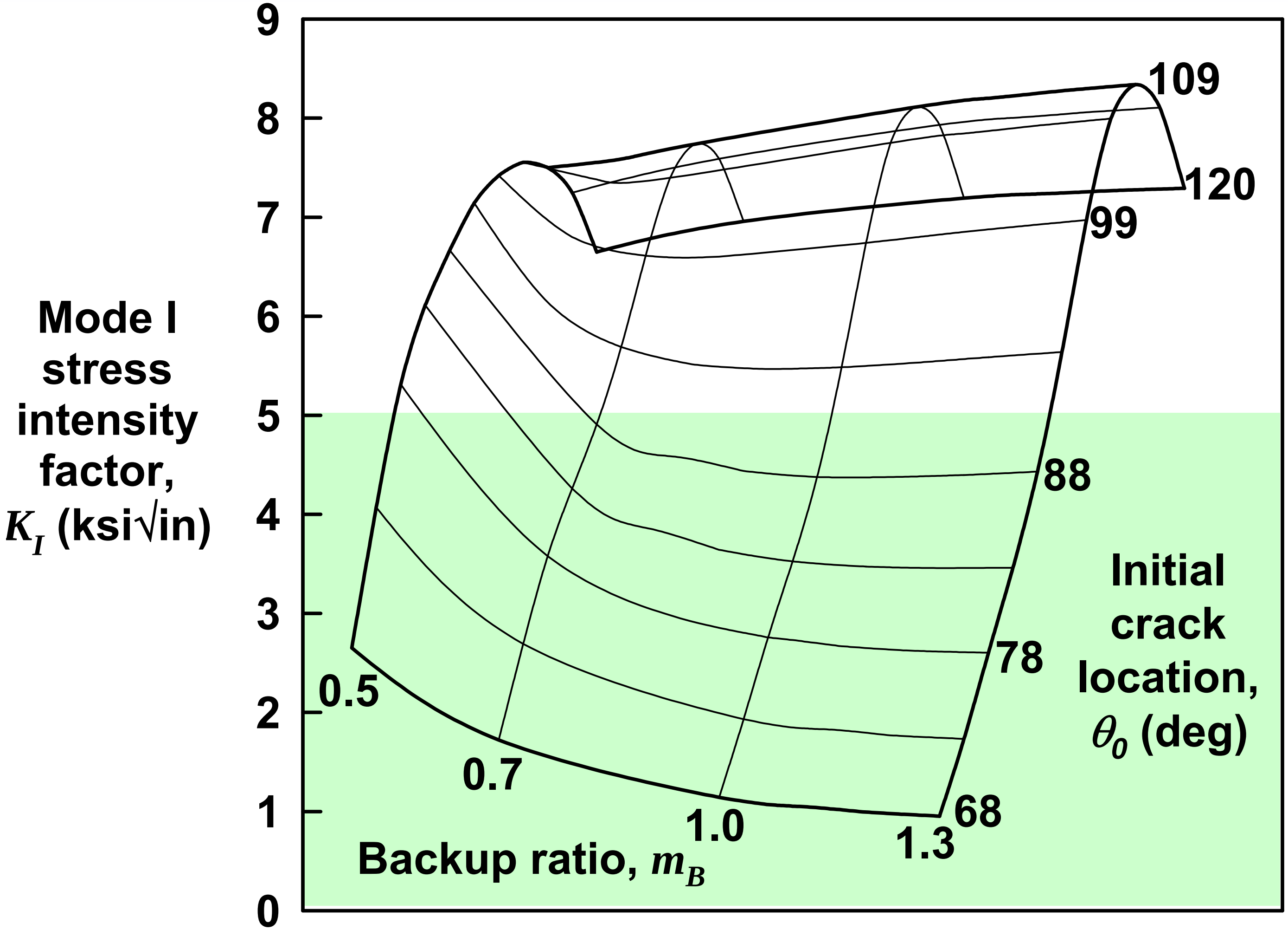

Gear Parameters:

- 28 teeth
- 8 pitch
- 1.75" pitch rad
- 20° press angle

- 500 lb tooth load
- 0.030" crack size

- AISI 9310 steel
- ΔK_{th} = 5 ksi√in

Design Map

T = tooth fractures
R = rim fractures
N = no fracture

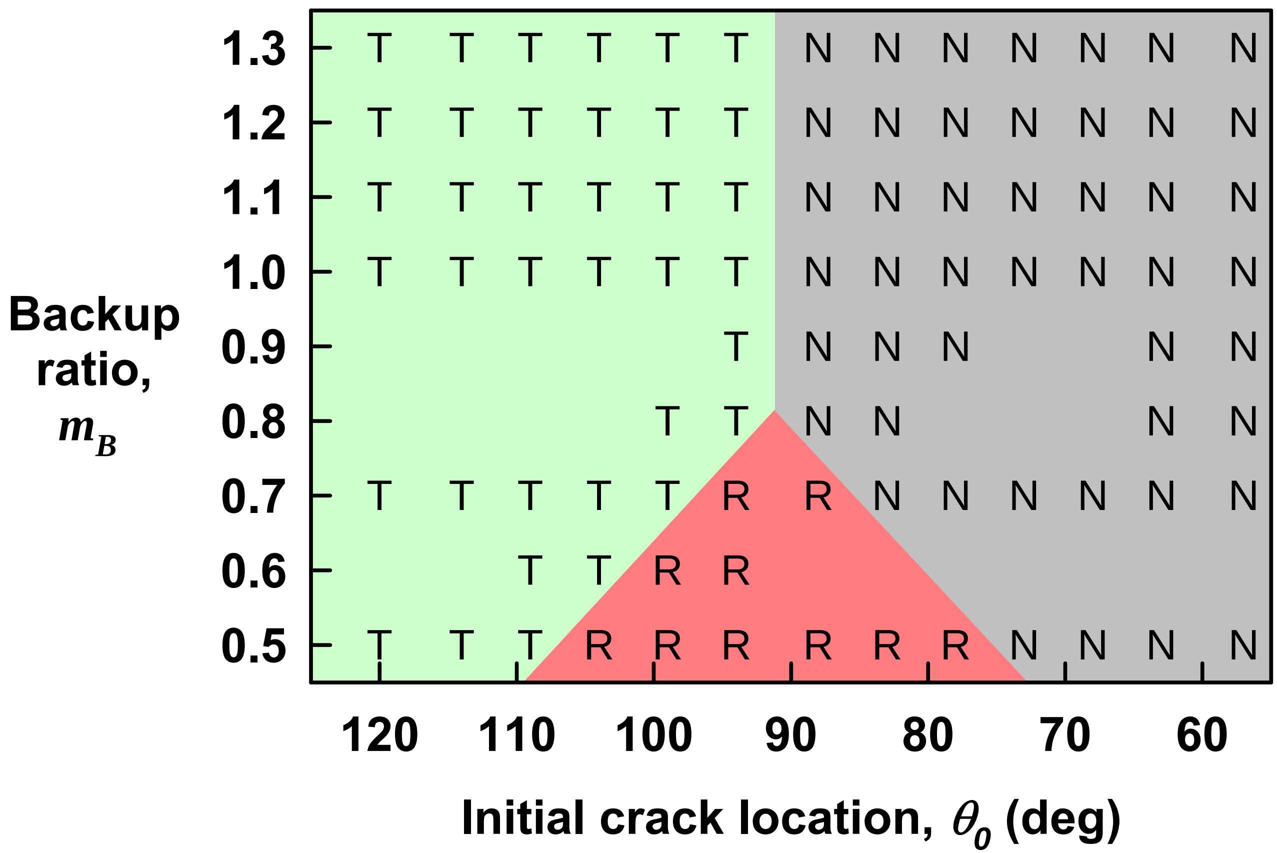

Test Gears

AISI 9310 Steel
Case carburized and ground
Effective Case Depth 0.032 in.

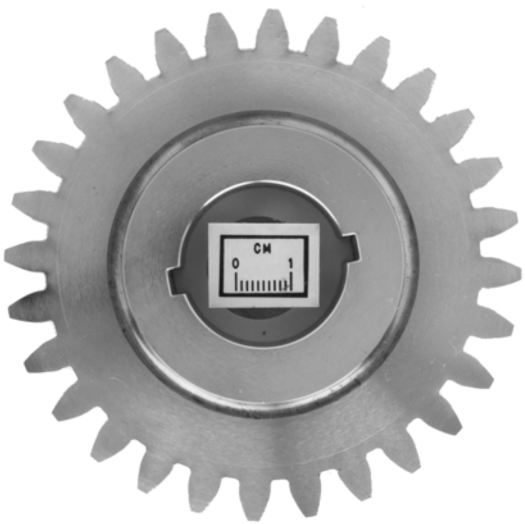

Backup ratio = 3.3

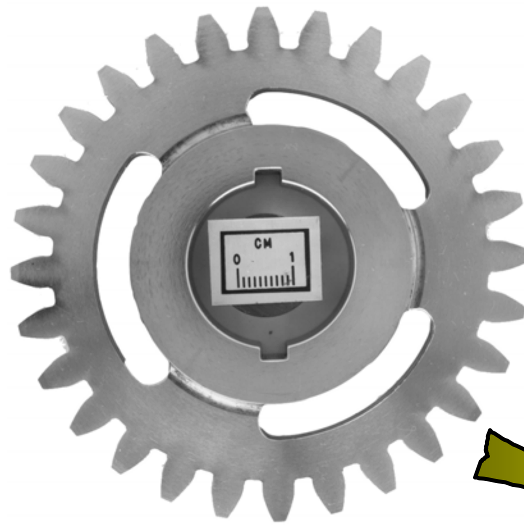

Backup ratio = 1.0

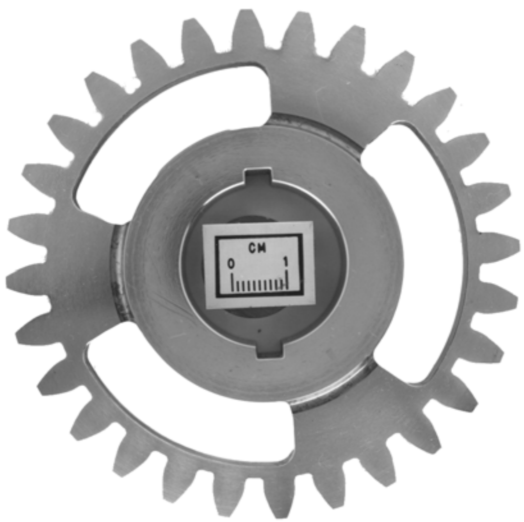

Backup ratio = 0.3

Notch inserted in tooth fillet

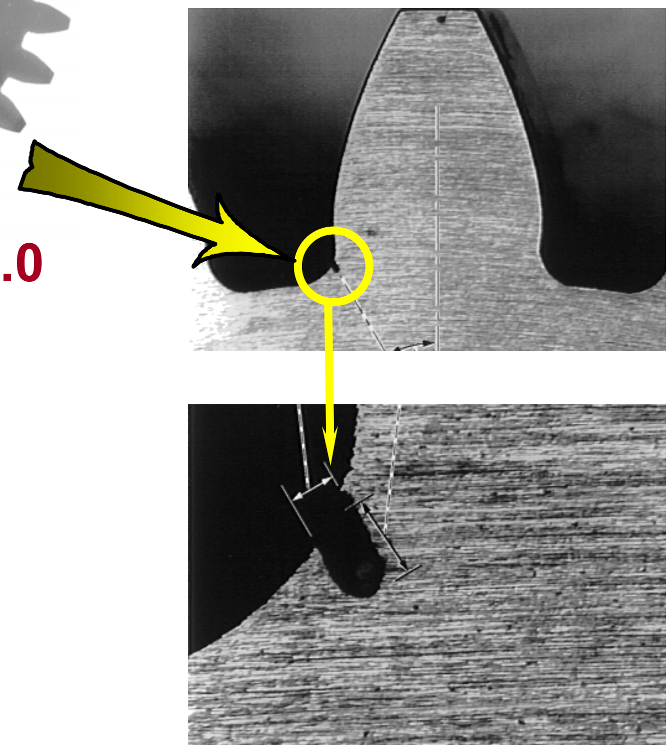

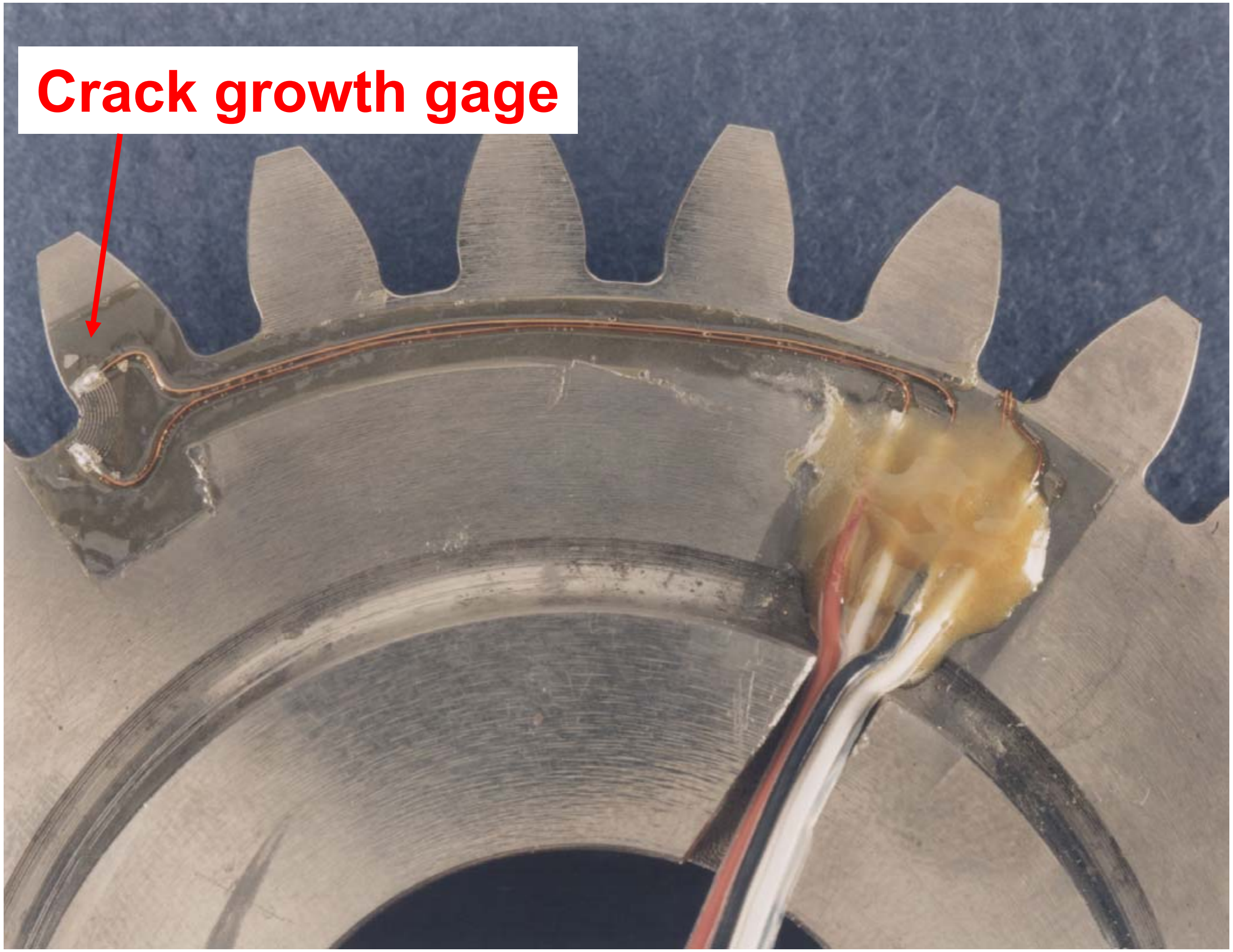
Crack growth gage

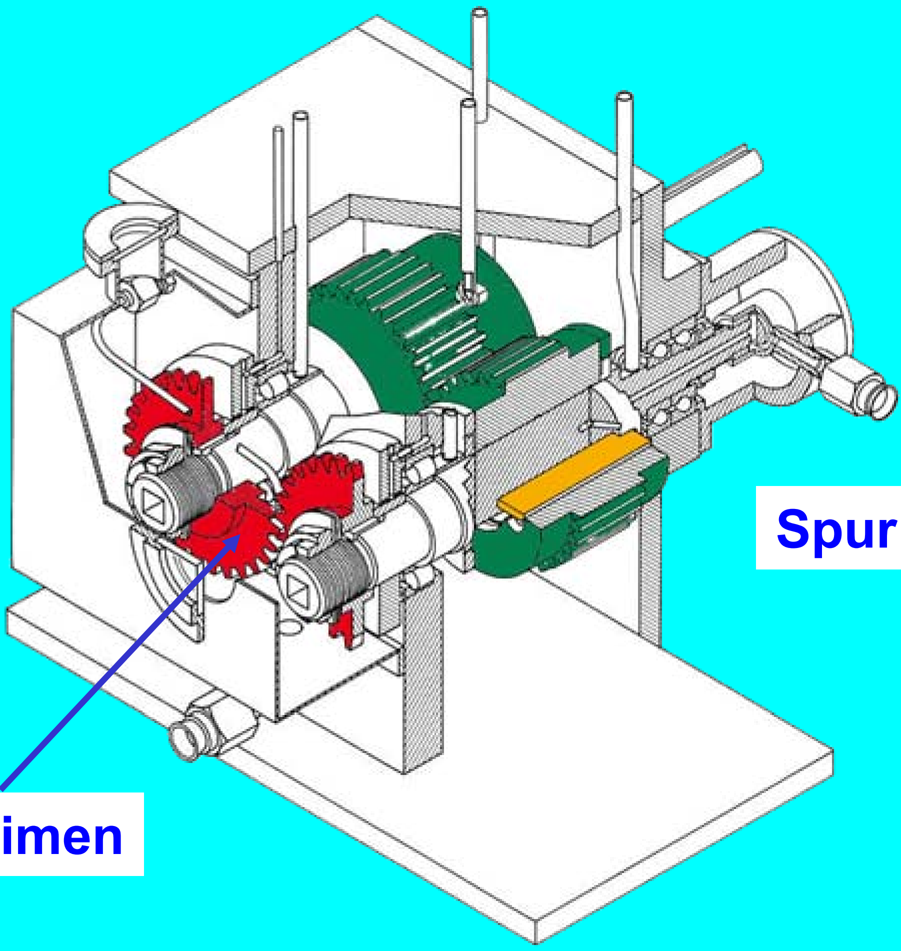

Spur gear rig at NASA Glenn

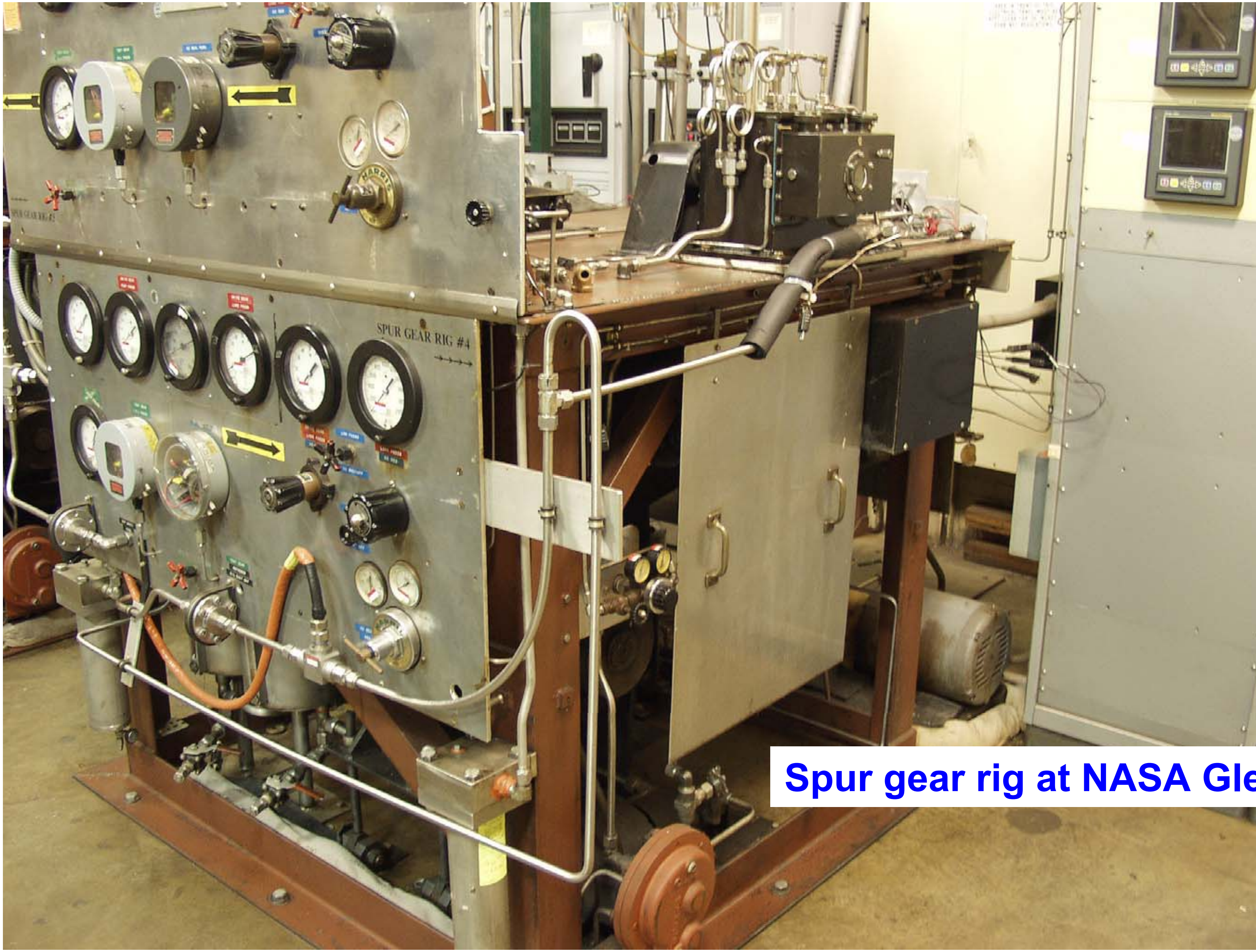

Spur gear rig at NASA Glenn

Validation of Finite Element Modeling

Backup ratio = 3.3

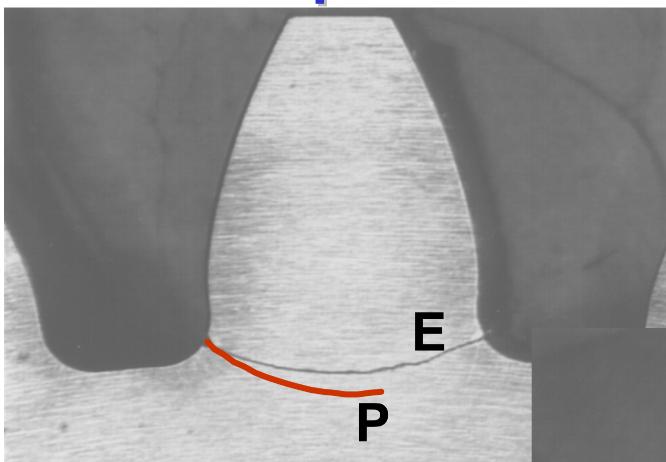

E = Experiment
P = Predicted

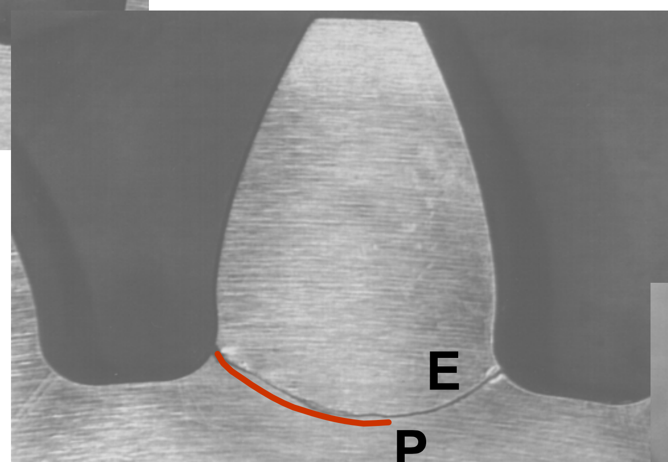

Backup ratio = 1.0

Backup ratio = 0.5

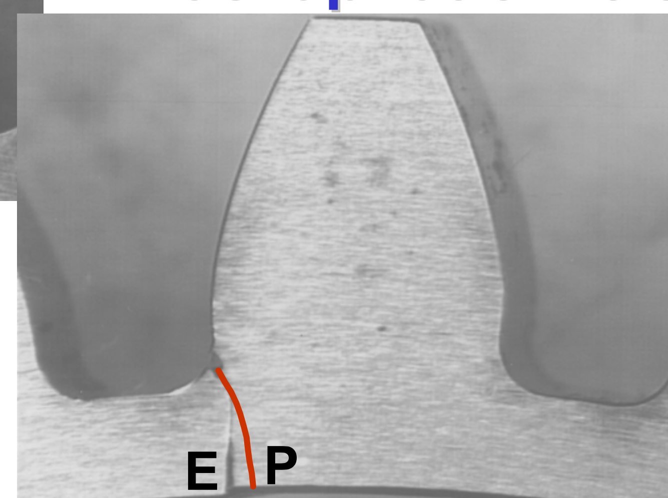

Fracture and Fatigue of MEMS Polysilicon and Silicon Carbide

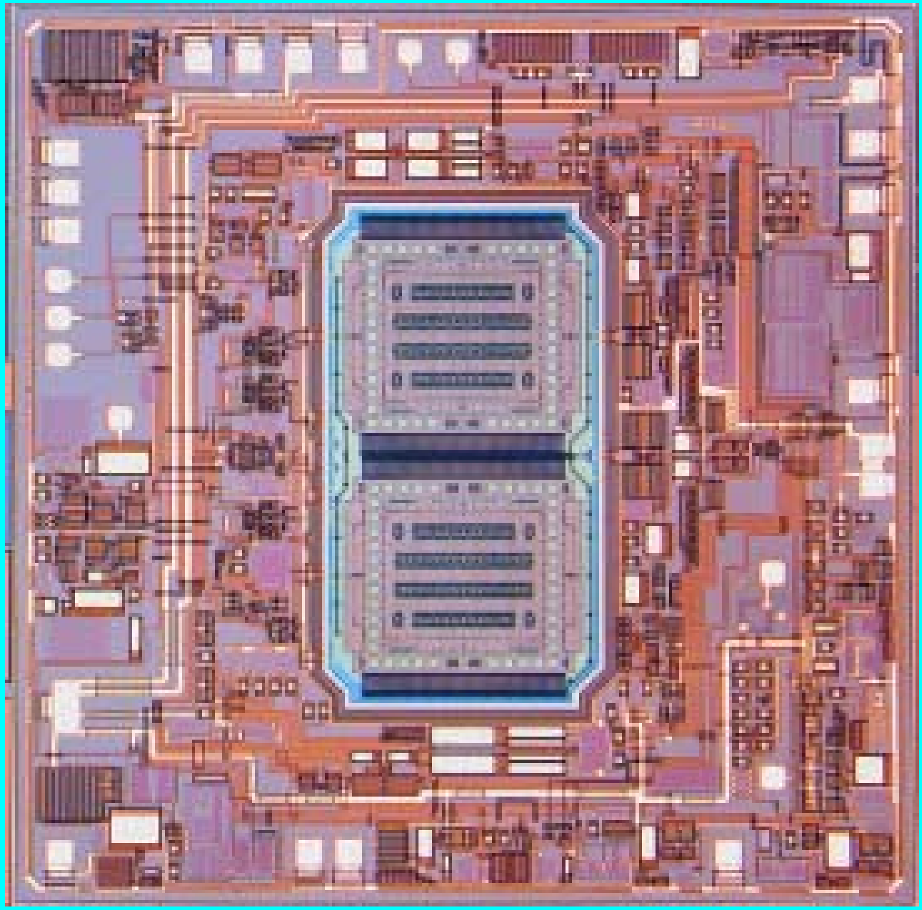

Analog Devices Gyroscope

iMEMS Gyro Die Showing the Rate Sensor and Integrated Electronics

http://www.analog.com/technology/mems/gyroscopes/index.html

MEMS Device-Fuel Atomizer

Motivation

- Reduce cost through batch fabrication
- Achieve desired tolerances using a precise silicon micromachining technology

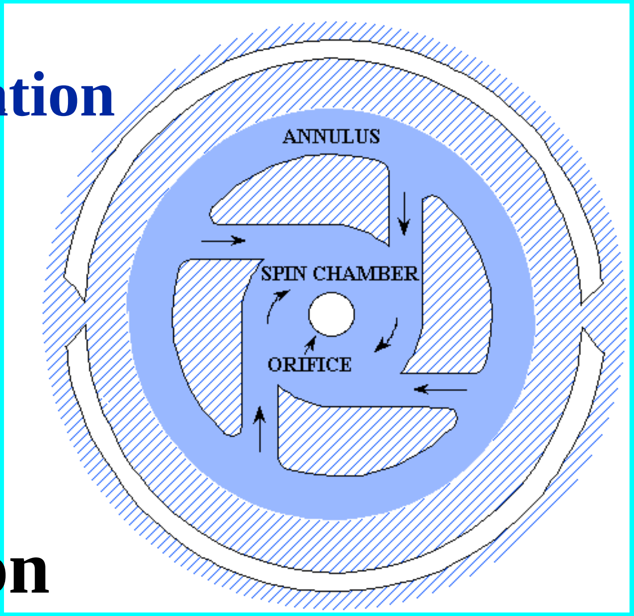

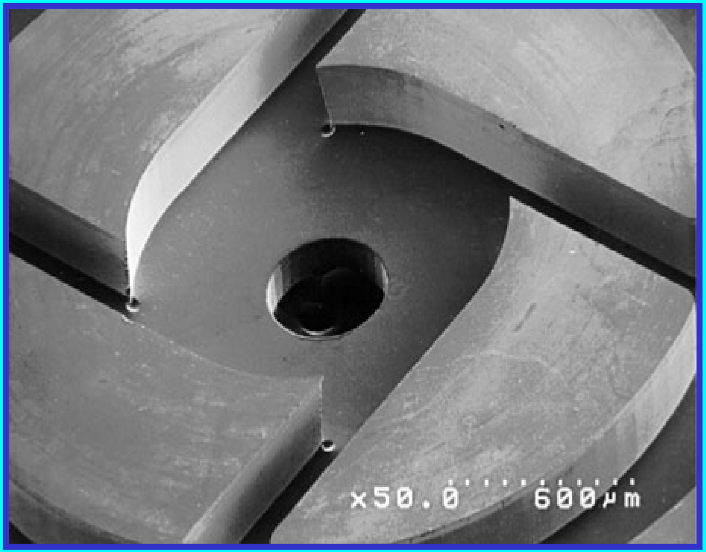

Operation

- Fuel enters the spin chamber through tangential slots
- Fuel swirls in the spin chamber and exits through the orifice in a hollow conical spray
- Swirling produces sprays with wider spray angles as compared to plain orifice atomizers

Ant Carrying a (1000 μm)^2 Microchip

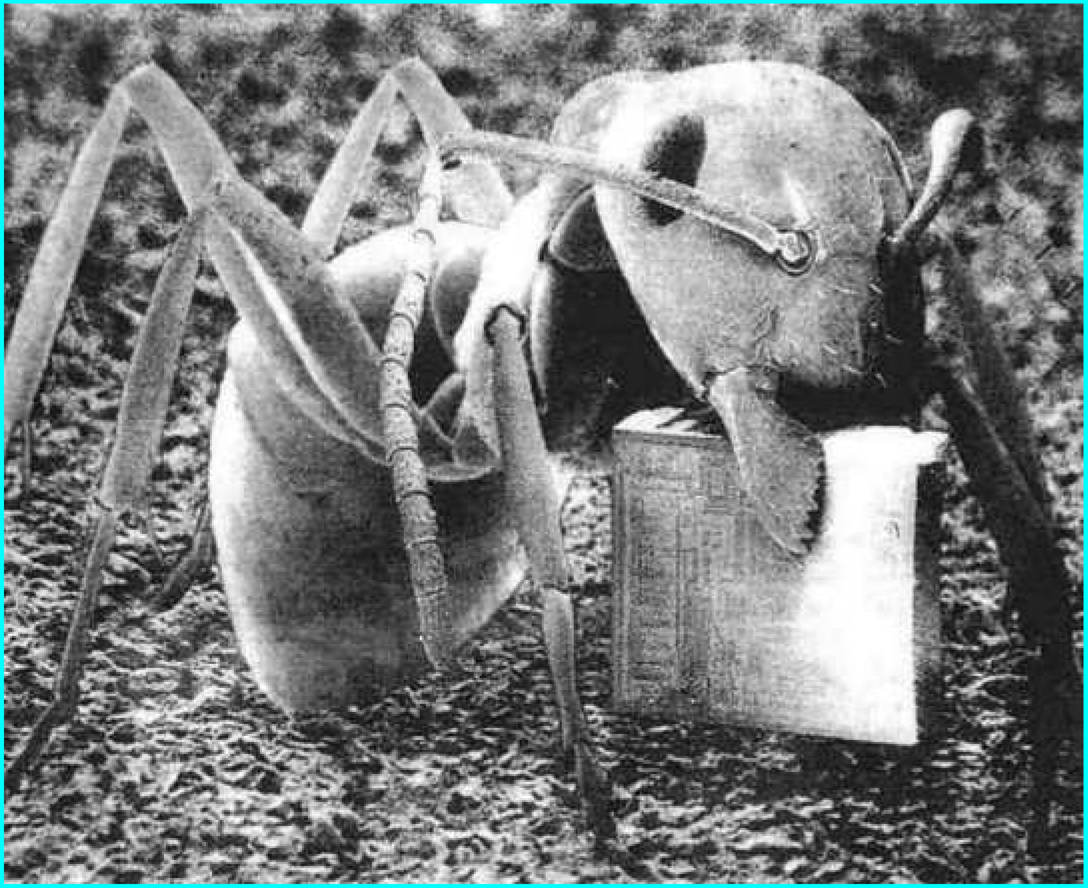

Or is it a Palm Pilot?

INDENTATION CRACKING

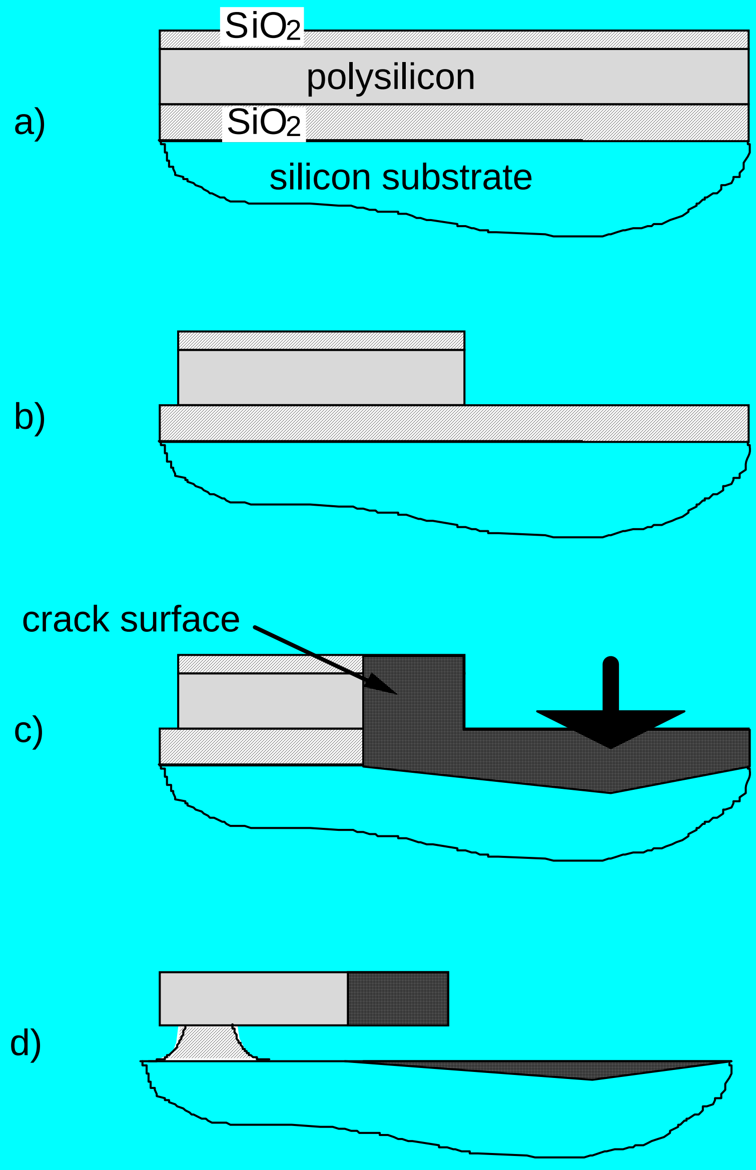

ORIGINAL OBJECTIVES

Characterize strength, fracture toughness, high cycle fatigue and environmentally assisted crack growth in poly-Si, poly-SiC, and SiC at scales relevant to MEMS devices.

•Develop (micron size) *on-chip* specimens.
•Generate data.
•Study mechanisms.
•Formulate predictive models.

CHALLENGES

•Experiments are difficult to design, execute and interpret.

CRACK GROWTH MECHANISMS

Fast fracture

$$K_I = F(a/b)\sigma\sqrt{\pi a} = K_I^{cr}$$

High cycle fatigue

$$\frac{da}{dN} = C\left(\Delta K_I\right)^m \qquad ???$$

Stress corrosion

$$\frac{da}{dt} = DK_I^n \qquad ???$$

If applicable, how sensitive are the parameters to processing procedures?

Two types of on-chip specimens have been developed:

- **Loading through electrostatic actuation**
- **Loading through fabrication-induced residual stress**

Why subcritical crack initiation and growth should be studied in MEMS

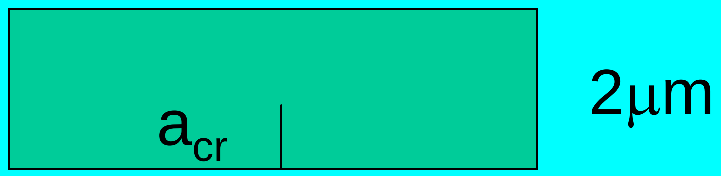

Say a_{cr}=1μm

Say t_{life}=10yrs

Then $v_{cr}<10^{-15}$ m/s !!!

CVD Polysilicon - Effects of Deposition Temperature

550°C

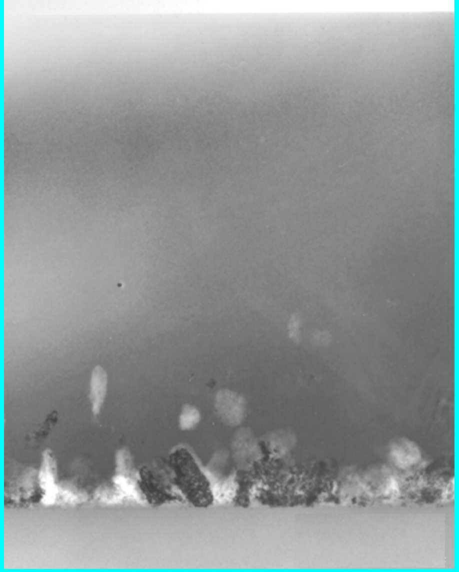

580°C

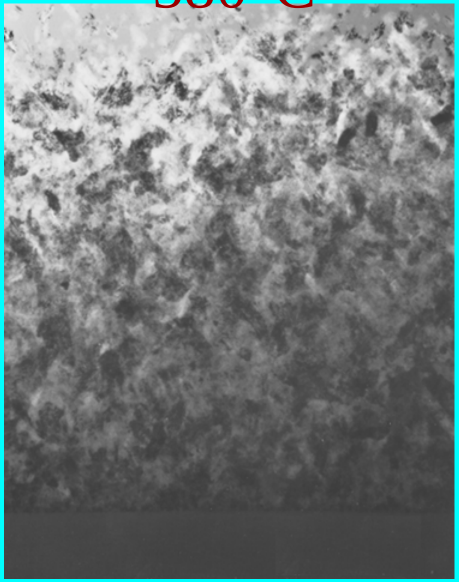

615°C

1100°C

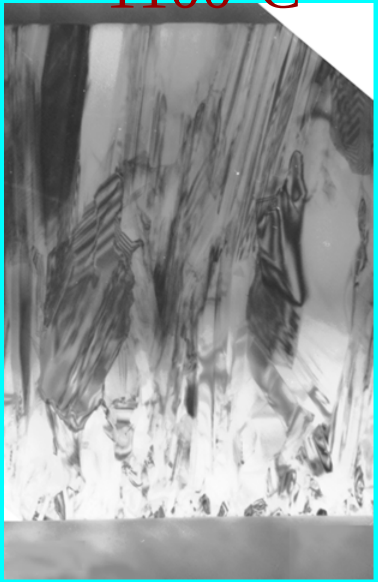

570/615°C

all films are ~2-6 μm thick, and deposited on SiO_2

MEMS Fracture Mechanics Specimen
integrated with
MEMS Loading Device Actuator

(*Proc. Royal Soc.* A, 455, 3807-3823, 1999)

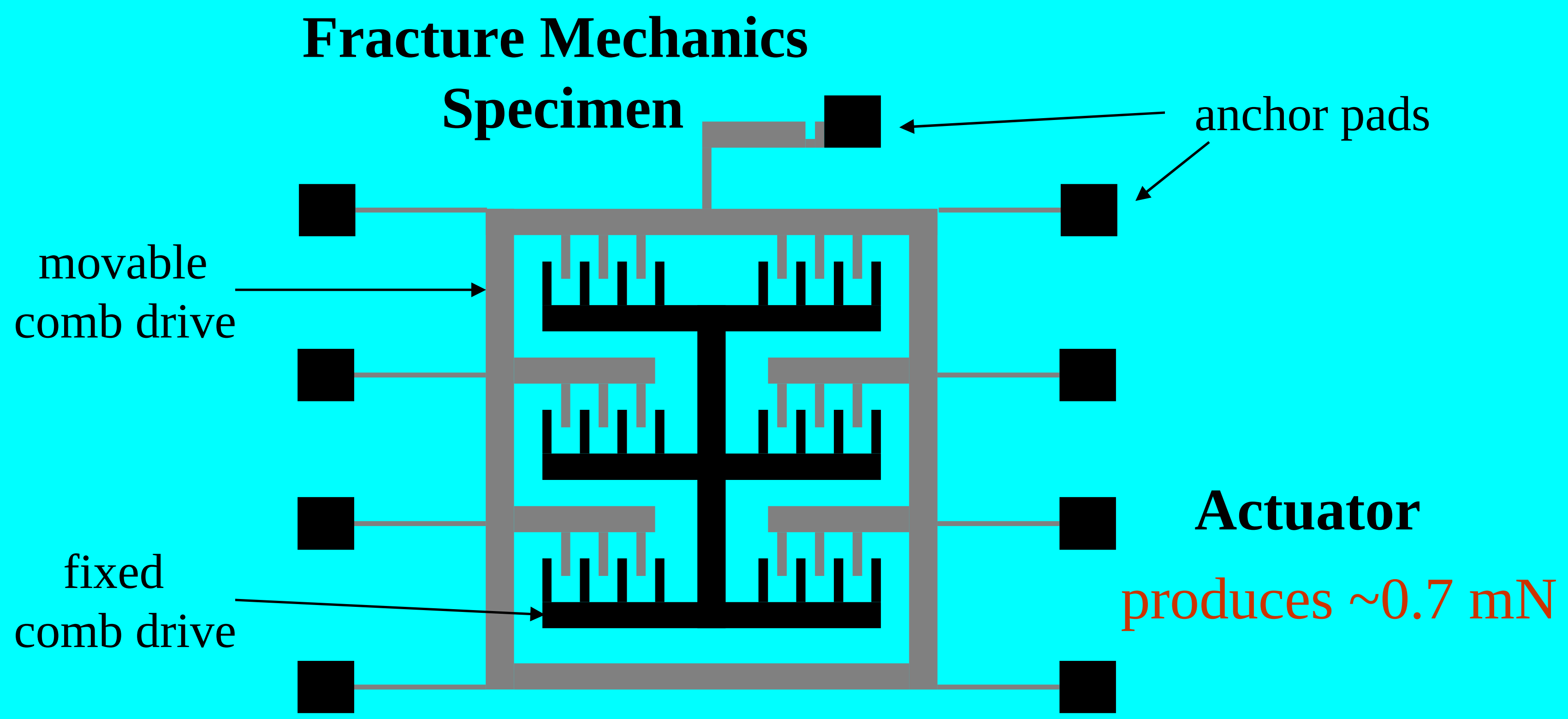

Fracture Device (notched specimen)

specimen

actuator

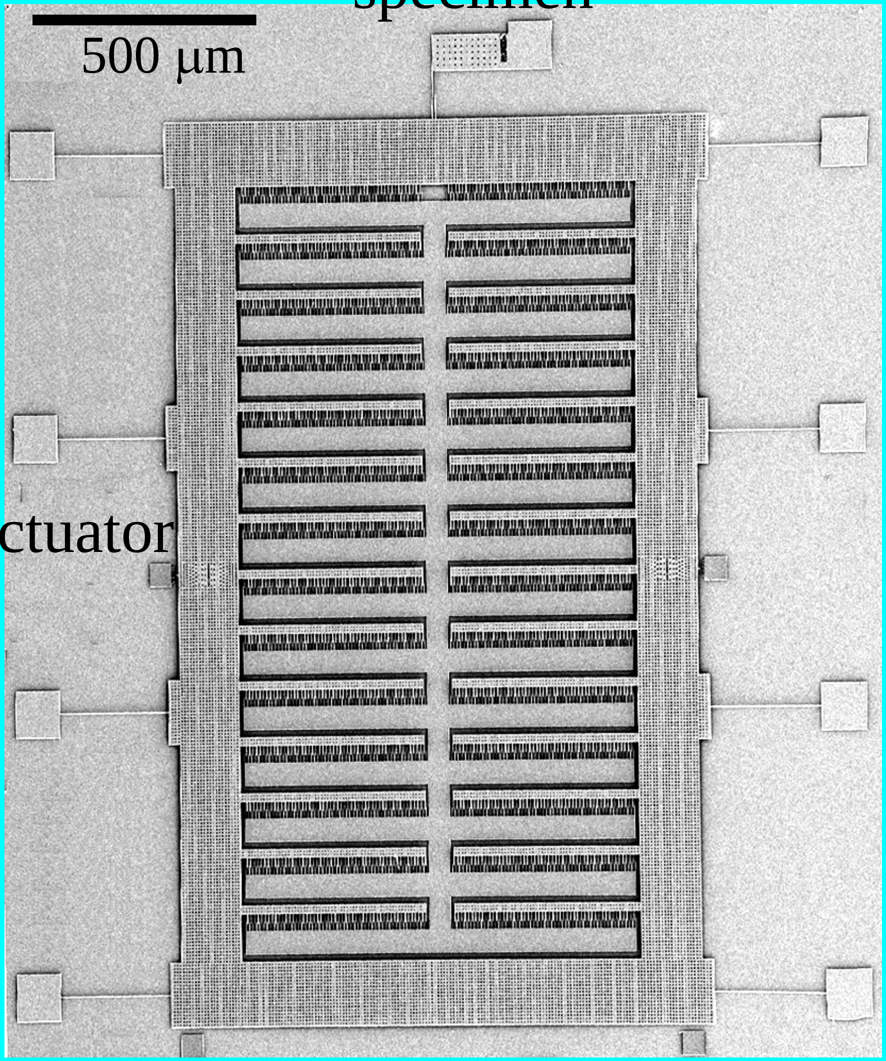

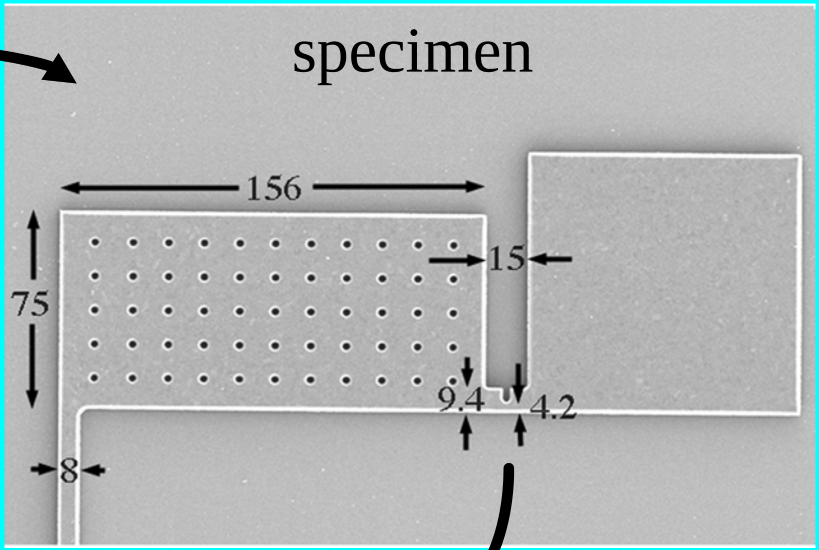

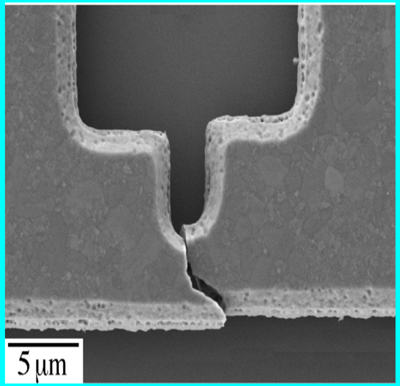

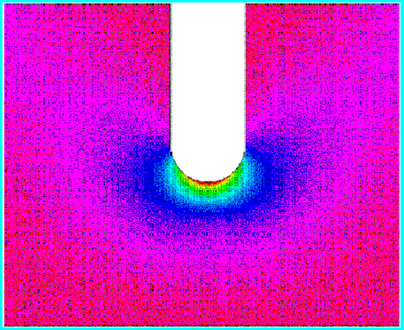

ADVANTAGES OF THIS “ON-CHIP” SPECIMEN

•No need for external loading device.
•Resonance loading can be used to study *very* high cycle fatigue.
•Uncracked ligament size of the same order as dimensions of typical MEMS components.

CURRENT LIMITATIONS

•Low “yield”, but improving

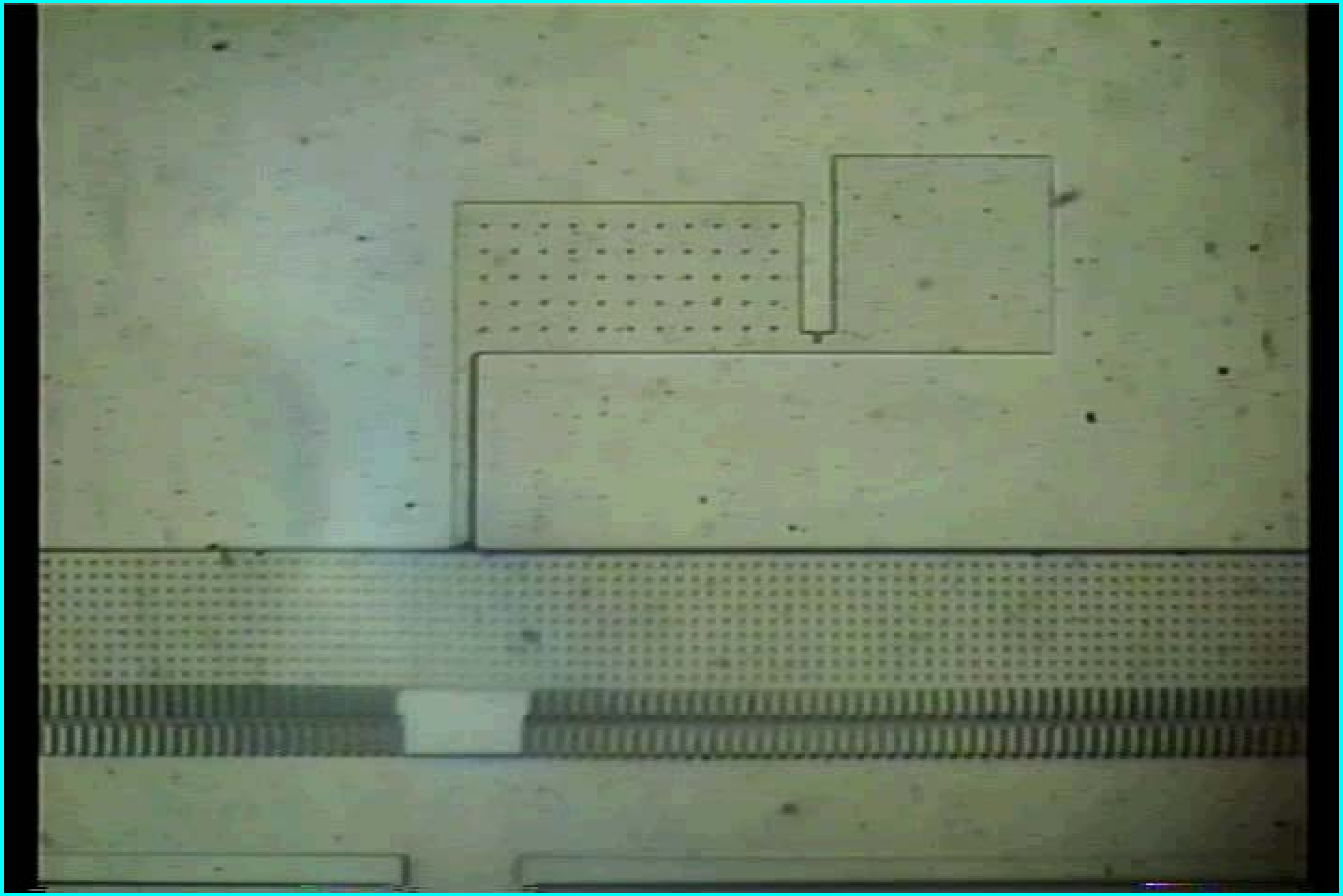

Fatigue of Notched Polysilicon

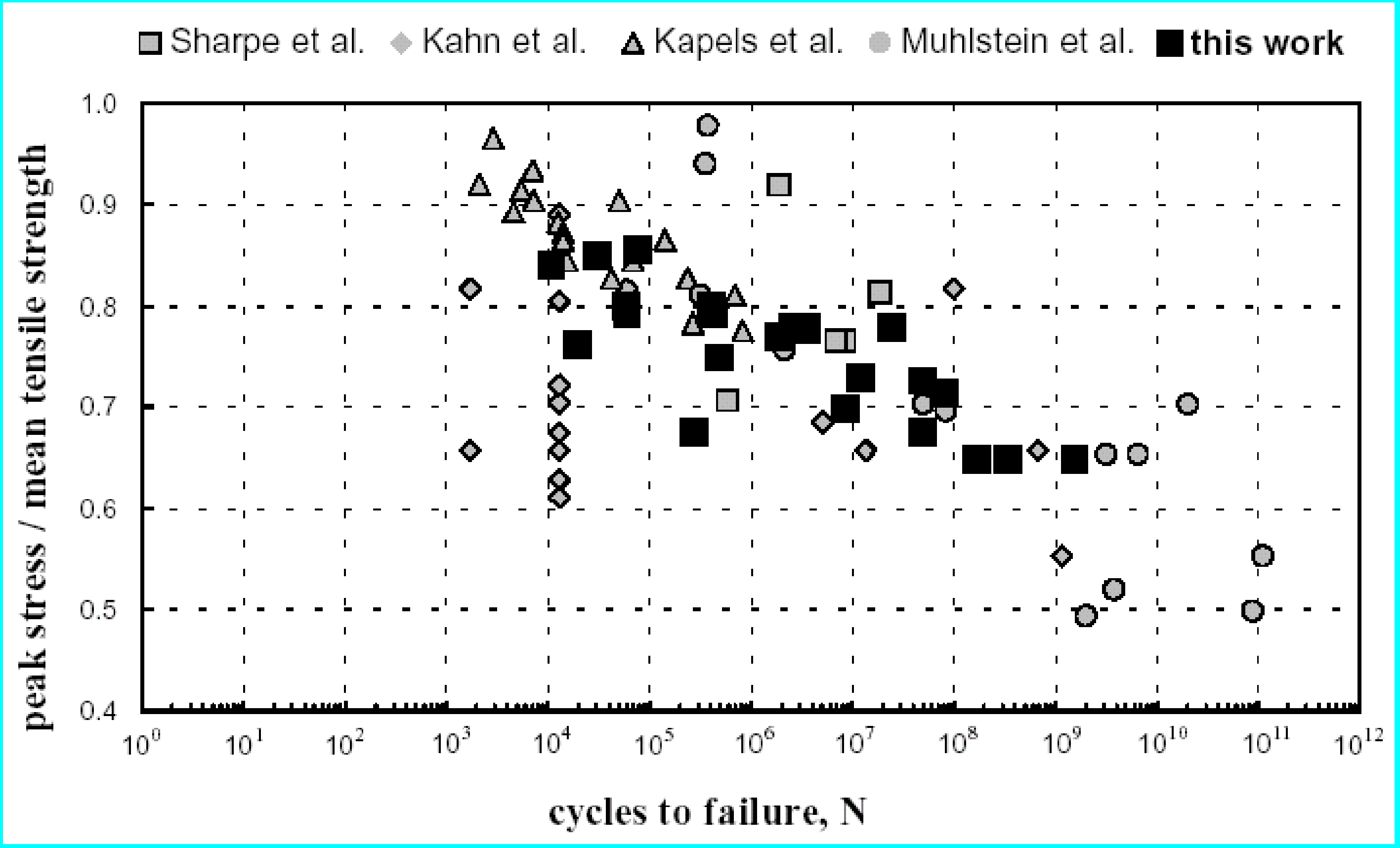

Sharpe and Bagdahn, Proc. Fatigue 2002

DIFFICULTIES IN DETERMINING ENVIRONMENTAL EFFECTS USING THESE TESTS

- Tests involve cyclic loading, not constant load.

- Tests involve tension and compression.

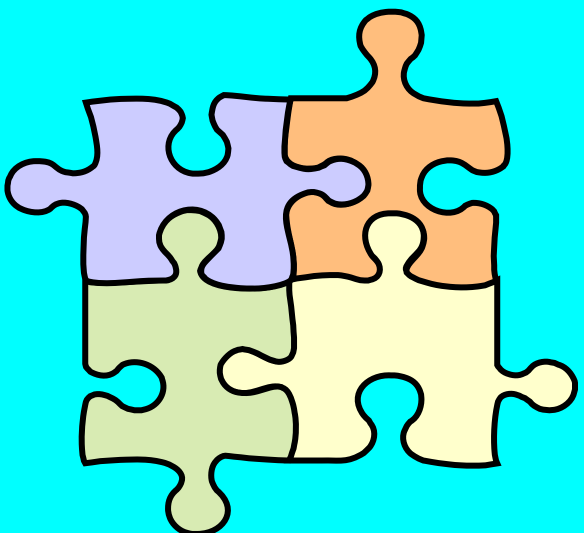

VARIATIONS ON A THEME

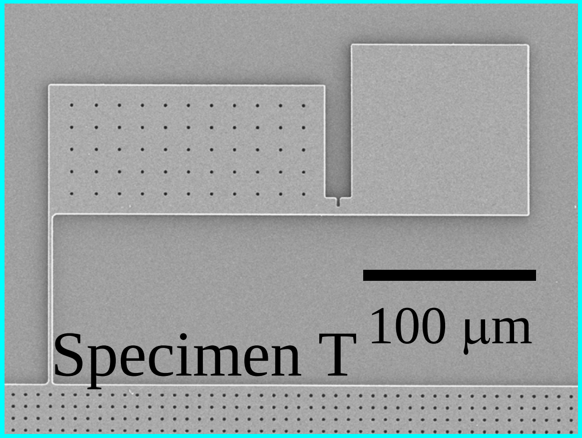

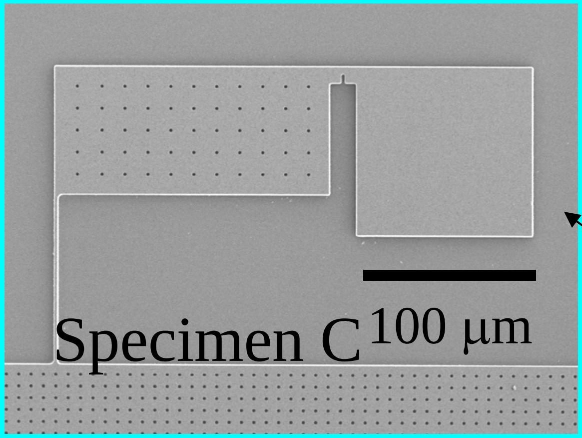

R-ratio and mean stress effects

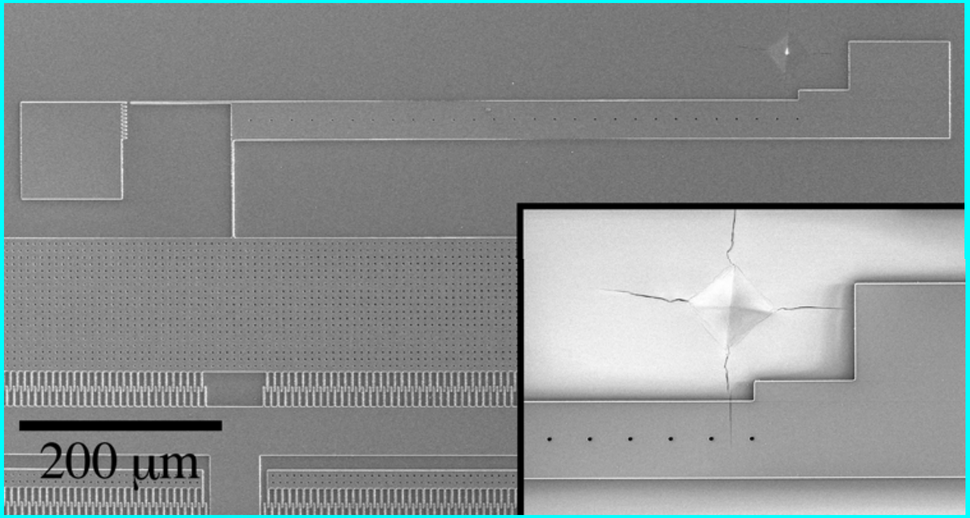

Dynamic Fatigue Results

low-cycle fatigue

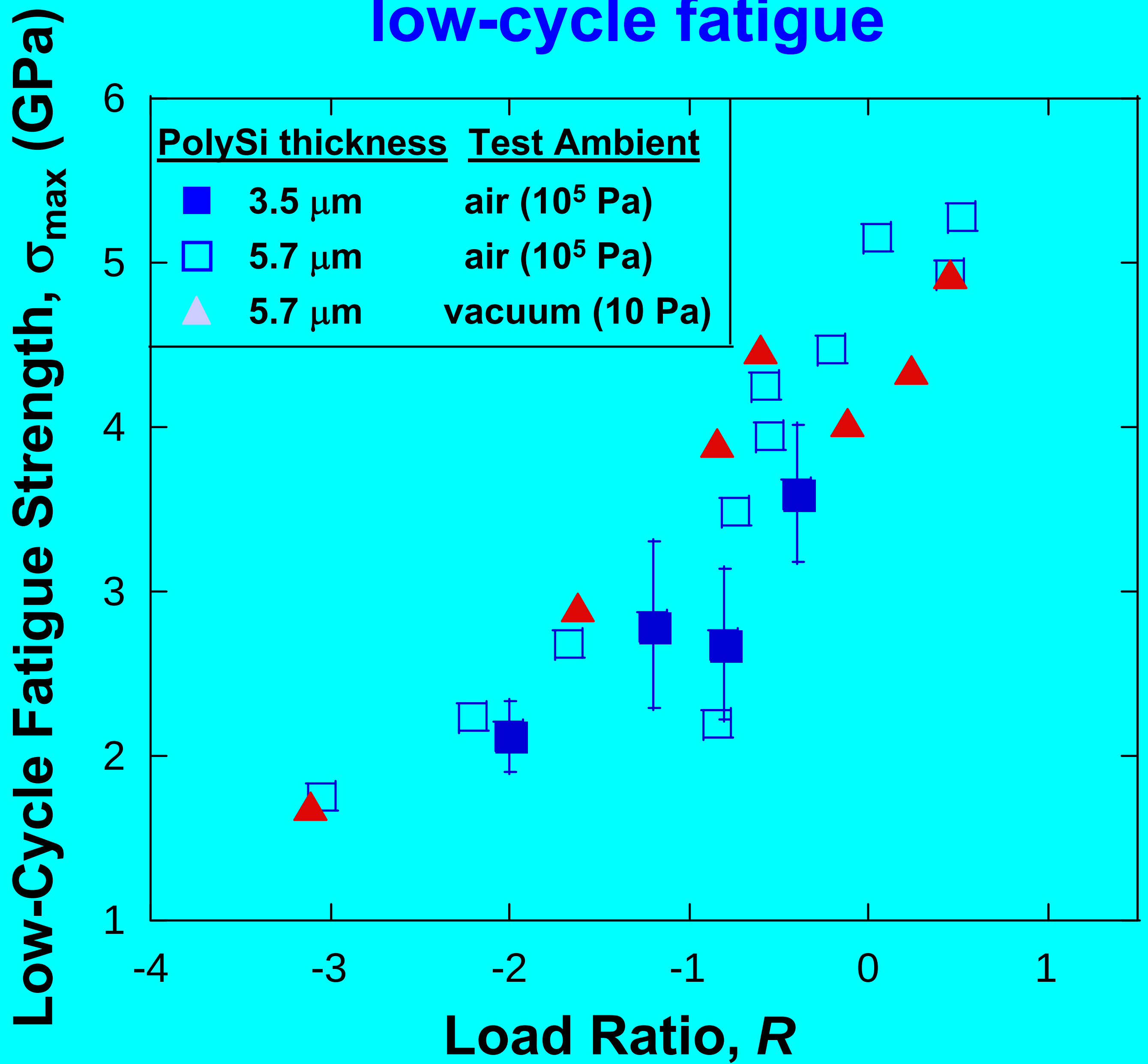

PASSIVE DEVICE ASSOCIATED WITH CONSTANT TENSION

(*Science*, 2002)

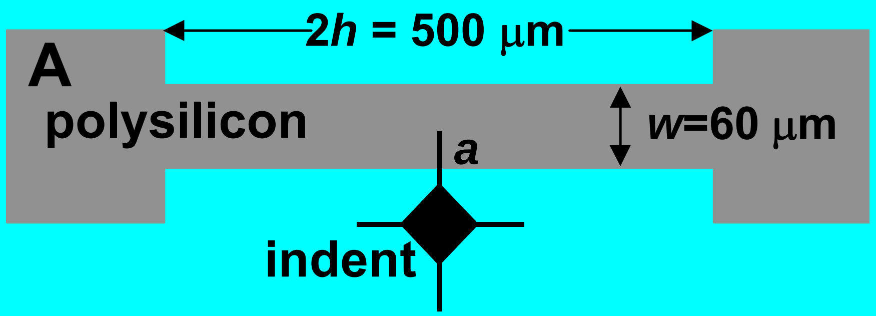

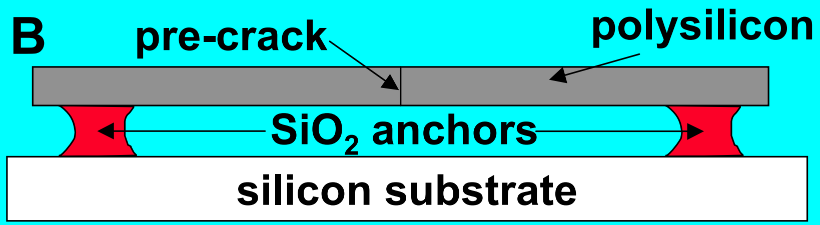

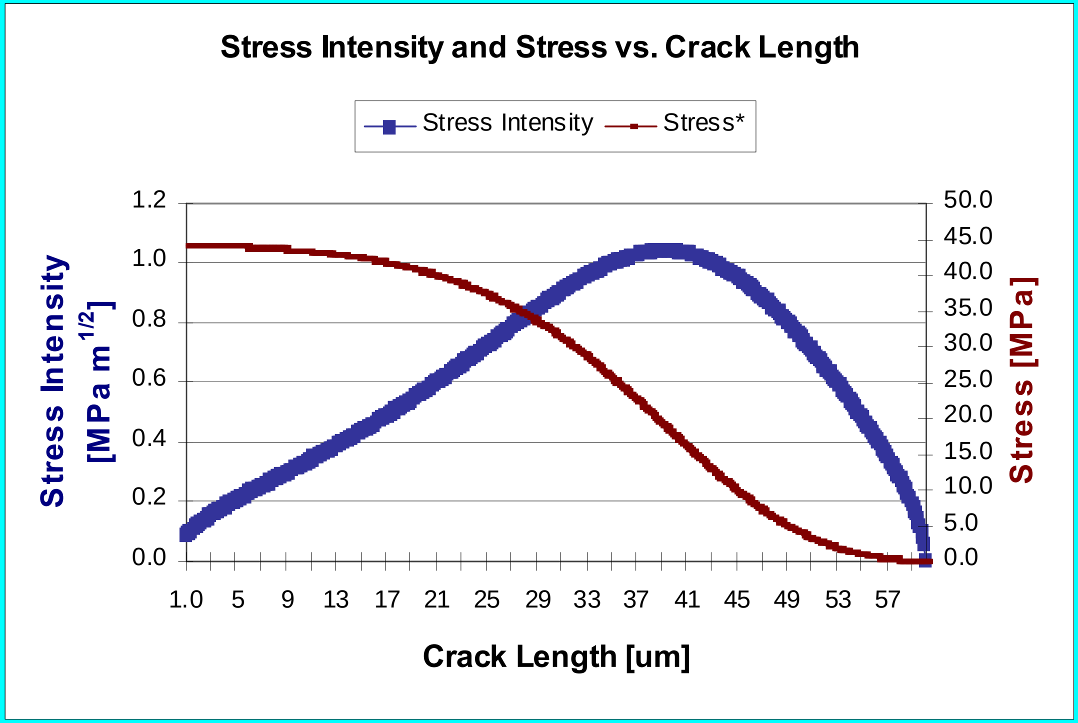

$$K = \sigma^* \sqrt{\pi a} F(\alpha)$$

$$\sigma^* = \sigma_{residual} / (1 + 4aV(\alpha)/2h)$$

INDENTATION CRACK

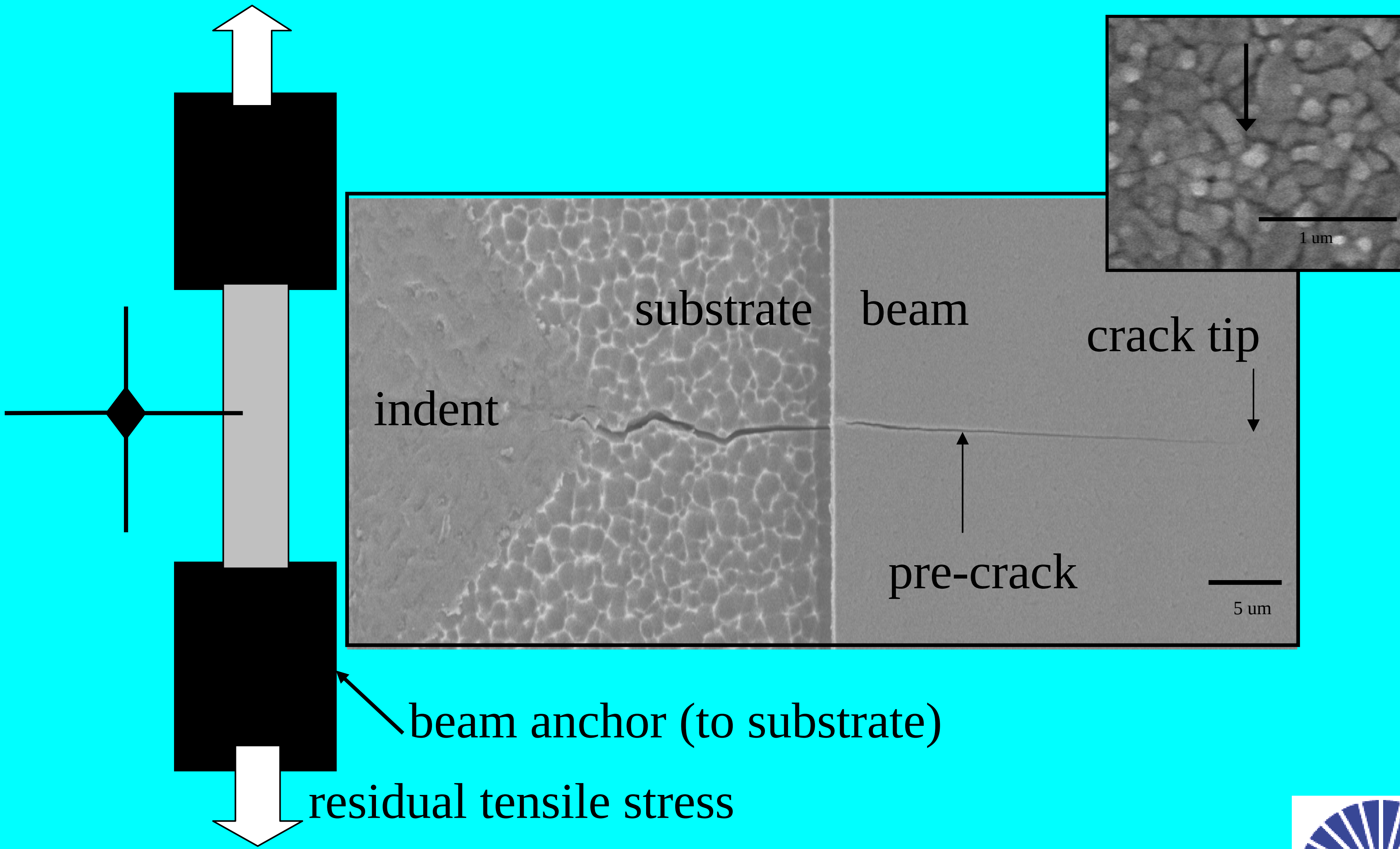

CWRU

FINE-GRAINED POLYSILICON FRACTURE TOUGHNESS

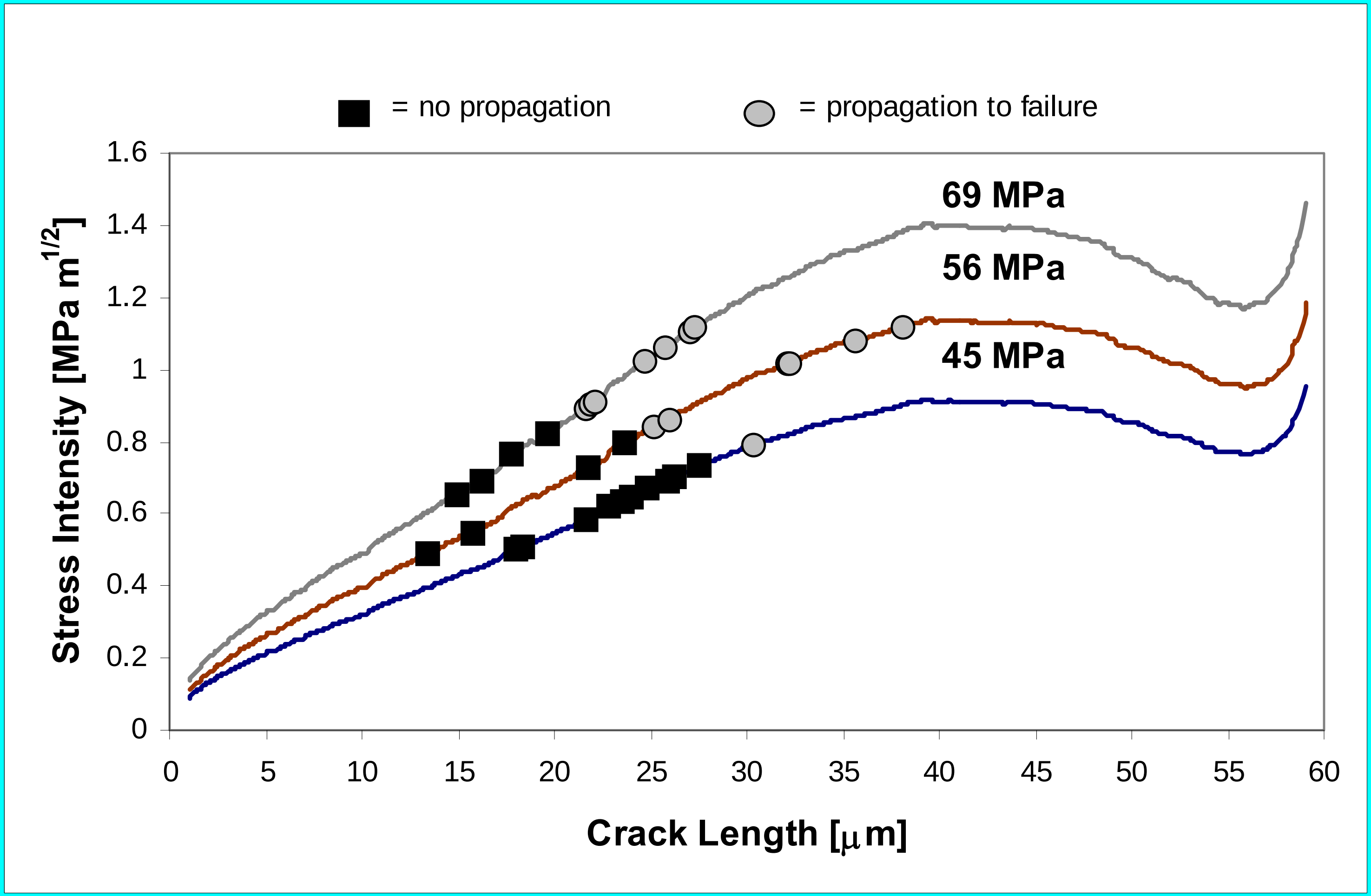

FRACTURE TOUGHNESS DATA
($MPa\text{-}m^{1/2}$)

Multilayered silicon	$0.79 < K_{Ic} < 0.84$
Fine-grained silicon	$0.76 < K_{Ic} < 0.86$
SiC	$2.80 < K_{Ic} < 3.41$

FINE-GRAINED SILICON
STATIC FATIGUE STUDY
90% RH

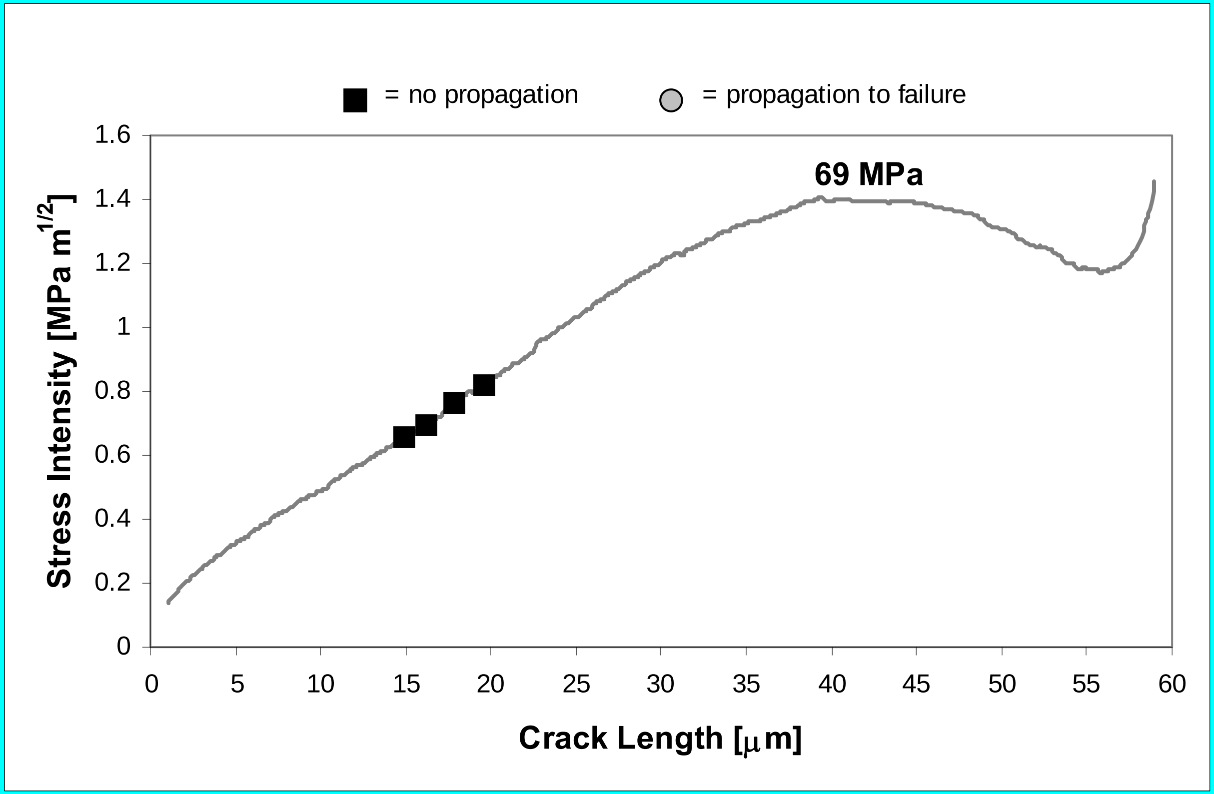

K between 0.62- 0.86 MPa-m$^{1/2}$

No growth in 30 days

V< 3.9 x10^{-14} m/s

Same results for eight multipoly specimens

Schematic Bend Strength Tests

Monotonic

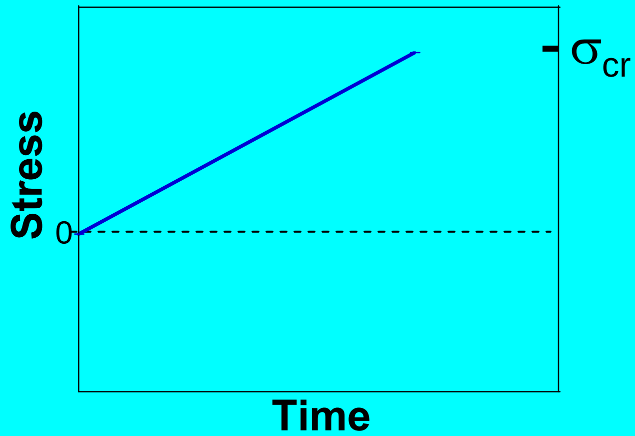

Increasing Amplitude Fatigue

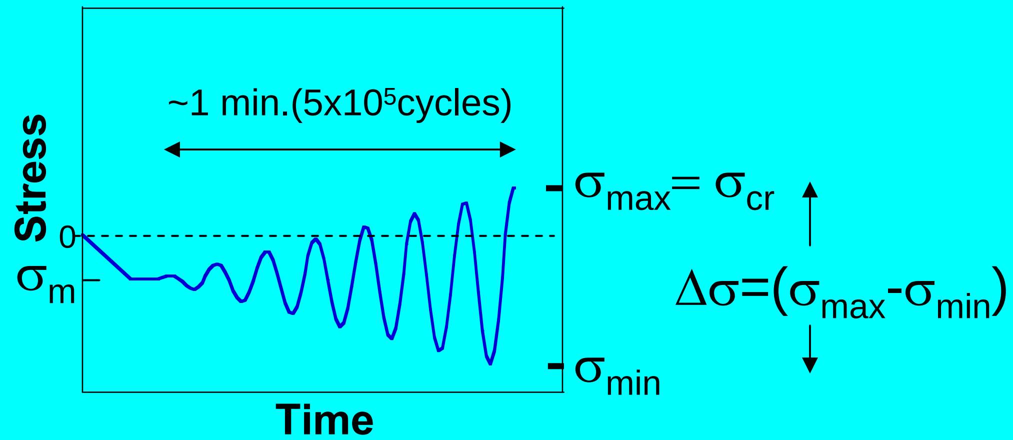

1 Comp/Mono

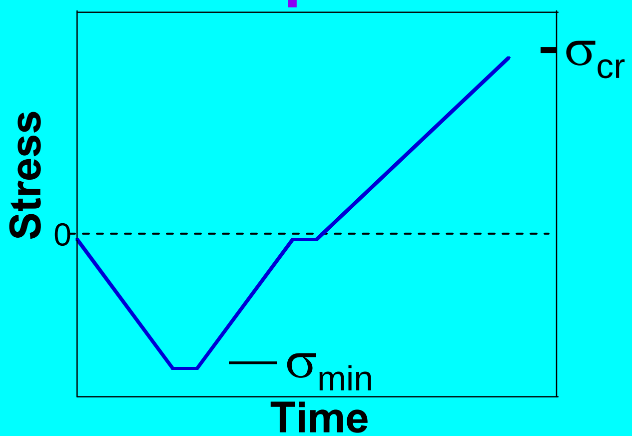

Fixed Δσ Fatigue/Mono

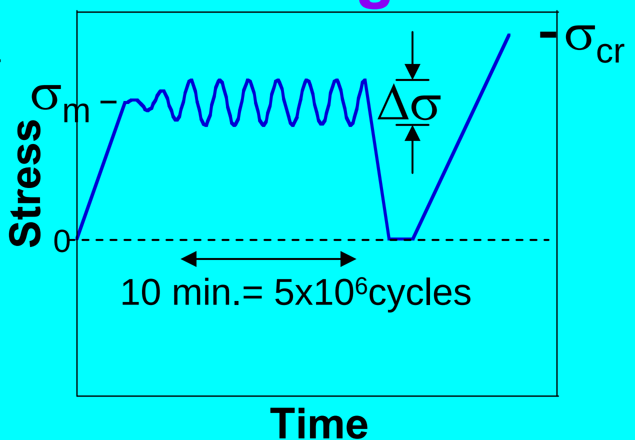

High T Hold/Mono

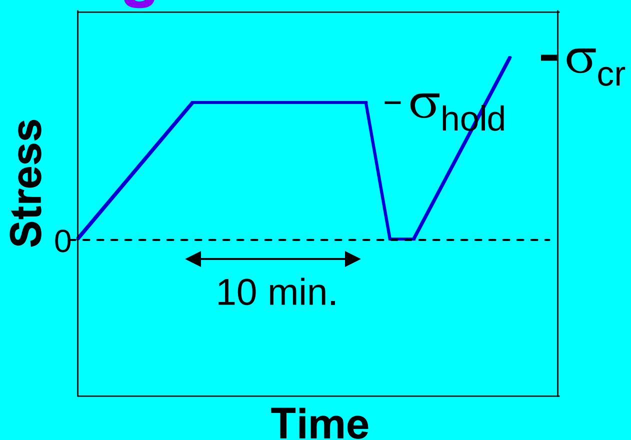

Increasing Amplitude Fatigue
B-doped polysilicon (no sputtered Pd)

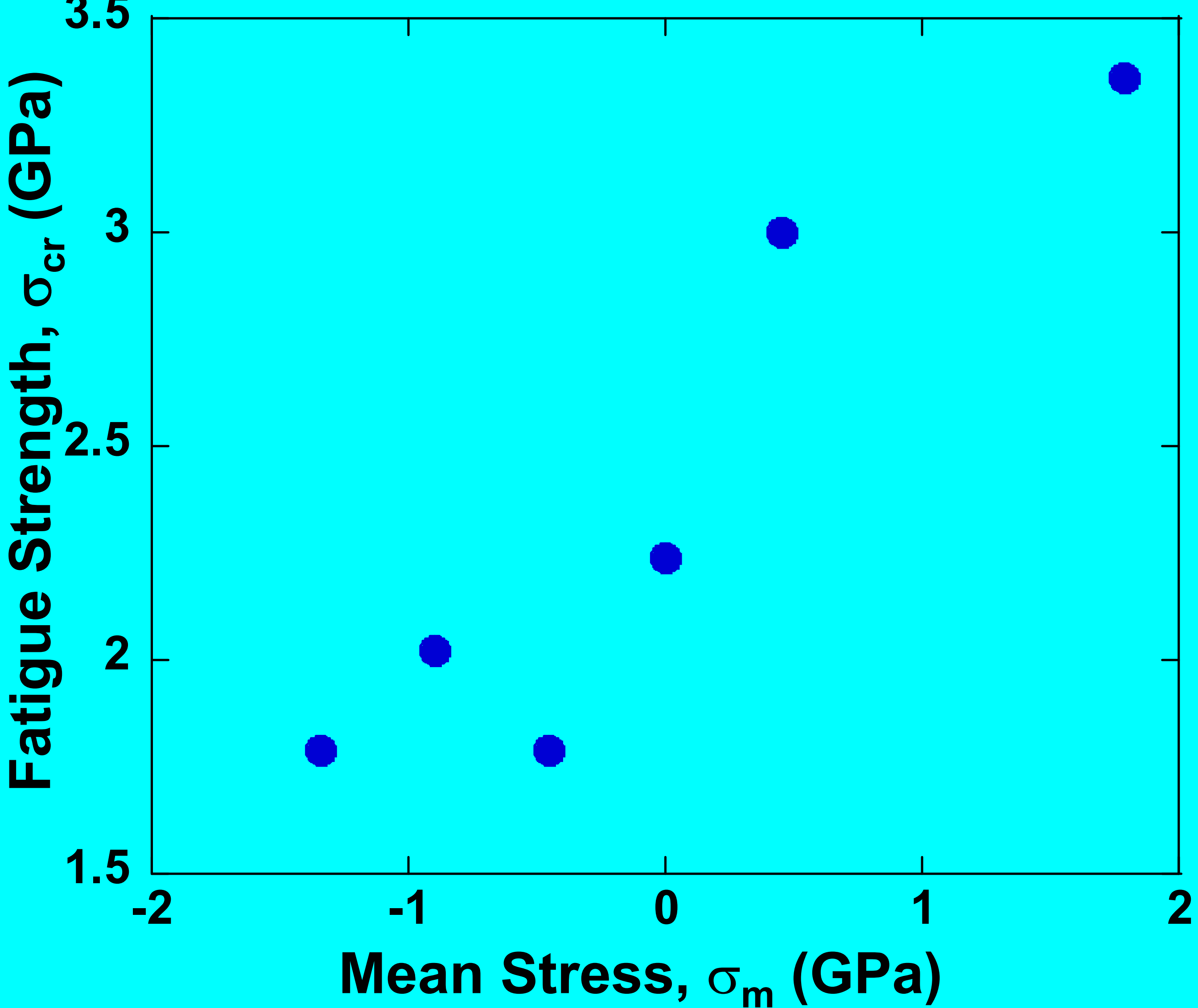

Monotonic Bend Strength
after cycling with a fixed (low) amplitude

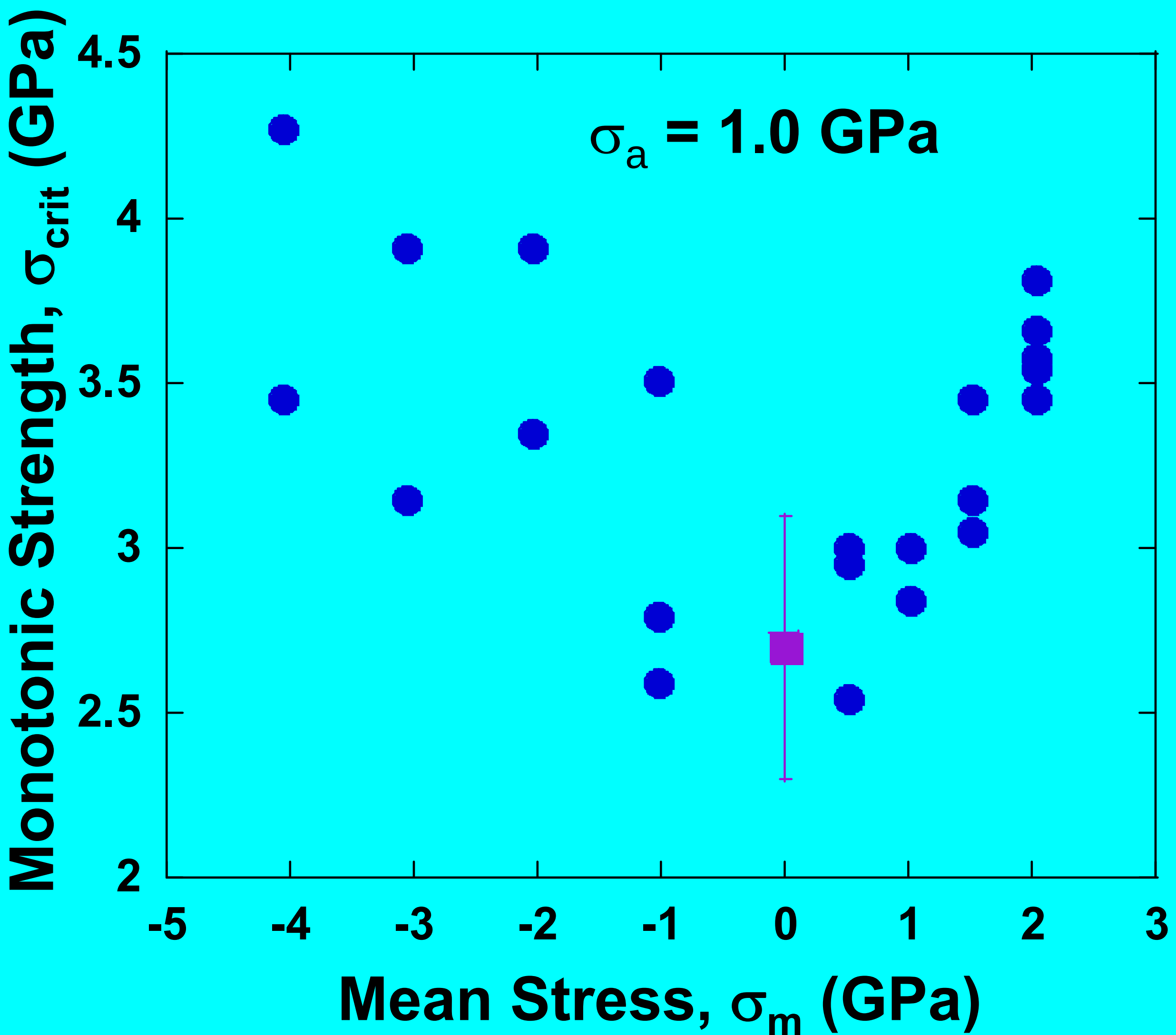

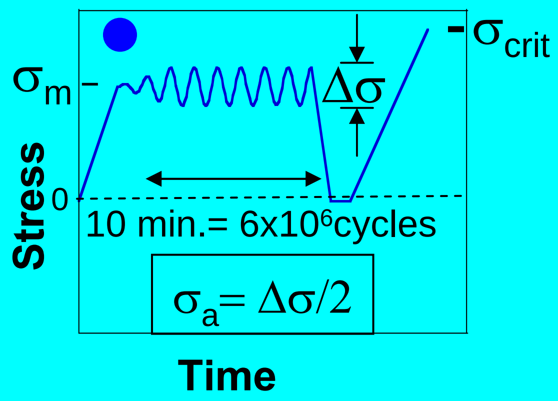

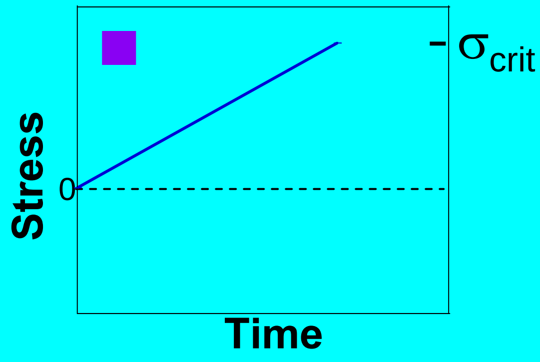

Effects on Monotonic Bend Strength

of mean stress σ_m, and fatigue amplitude σ_a

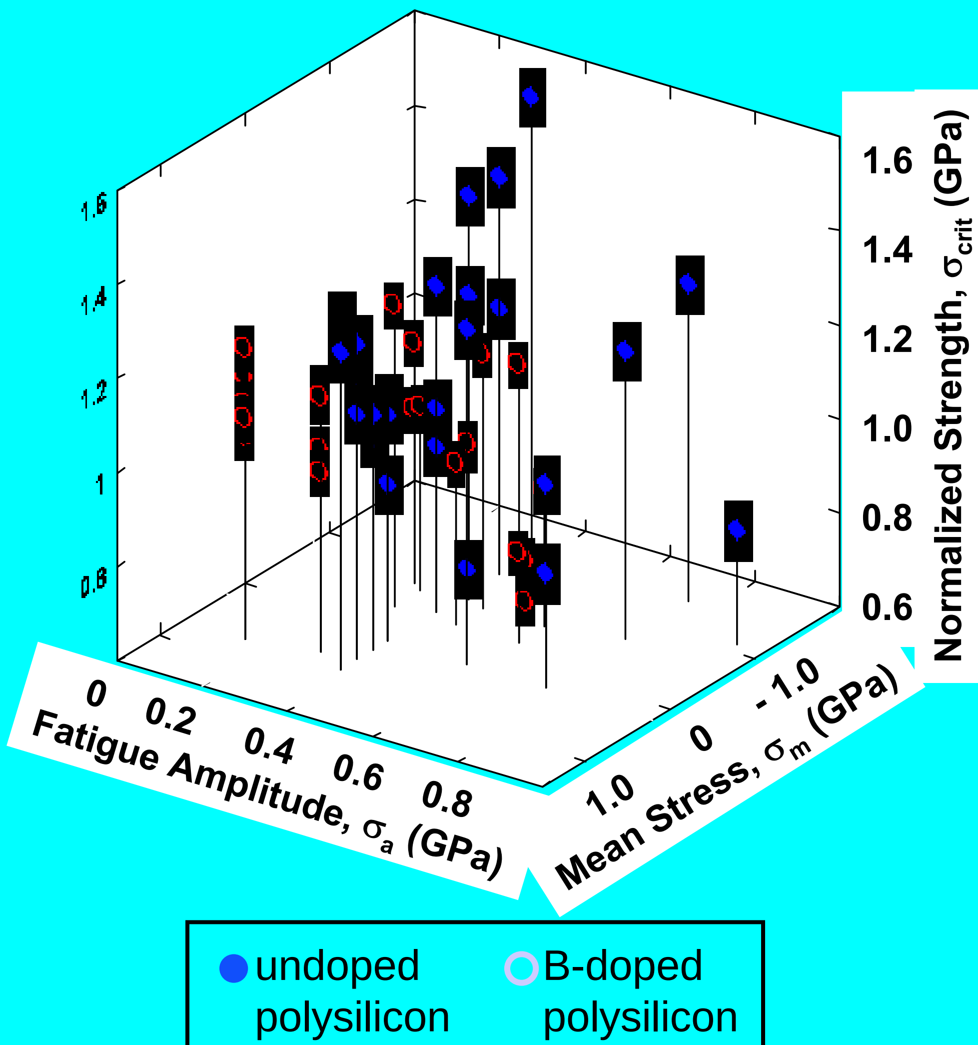

Mean Stress, σ_m (GPa)	Fatigue Amplitude, σ_a (GPa): low	Fatigue Amplitude, σ_a (GPa): high
compressive, high	strengthening	weakening
compressive, low	no effect	weakening
tensile, low	no effect	weakening
tensile, high	strengthening	(not measured)

Mechanical Testing of Collagen Fibers (Nanotechnology)

- **Most abundant protein in the human body.**
- **One of the basic components of bone, ligaments, tendons, teeth, skin.**
- **Collagen monomer:**
  - **Triple helical structure made of three chains of amino acids.**
  - **The monomers assemble into fibrils.**

Collagen Fibrils

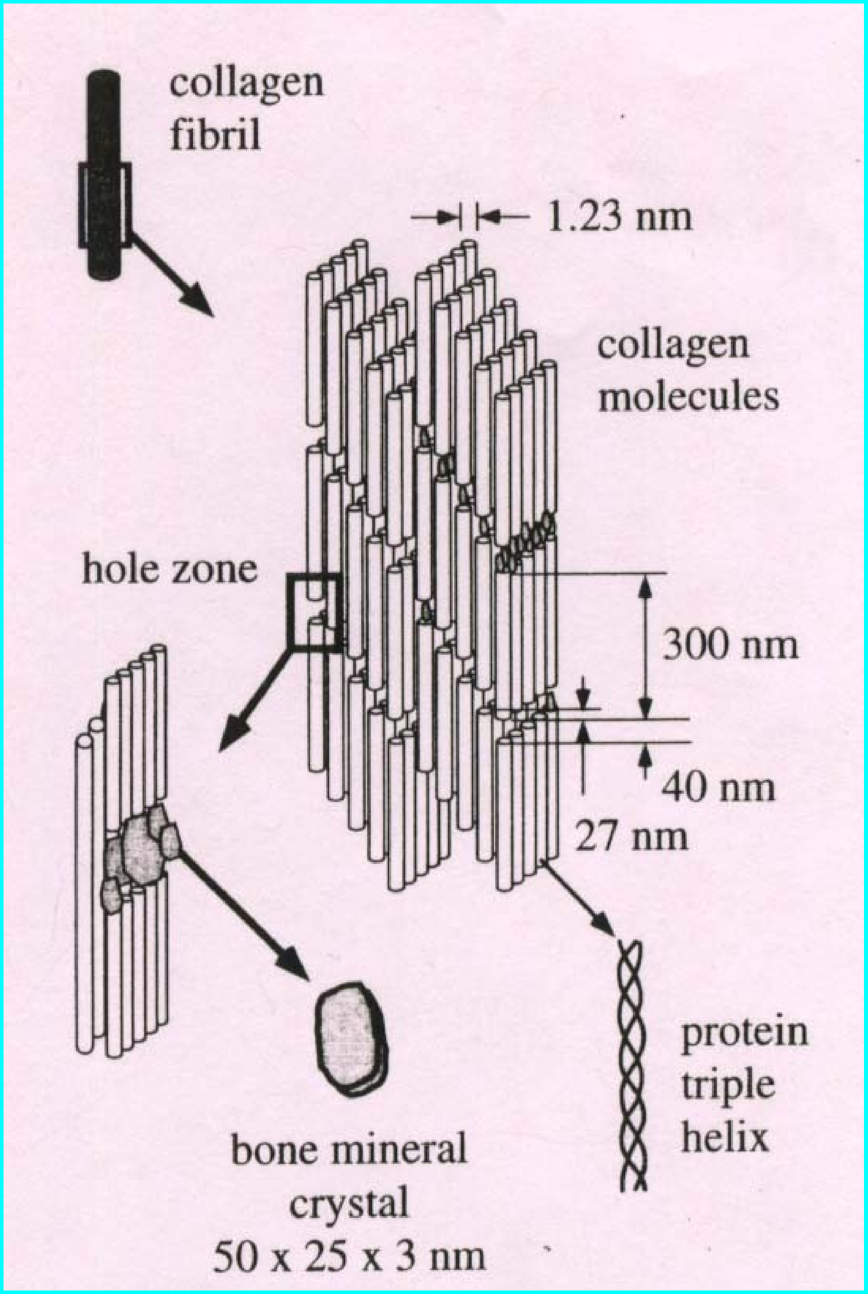

Rho *et al.*, 1998

Hierarchical Structure of Bone

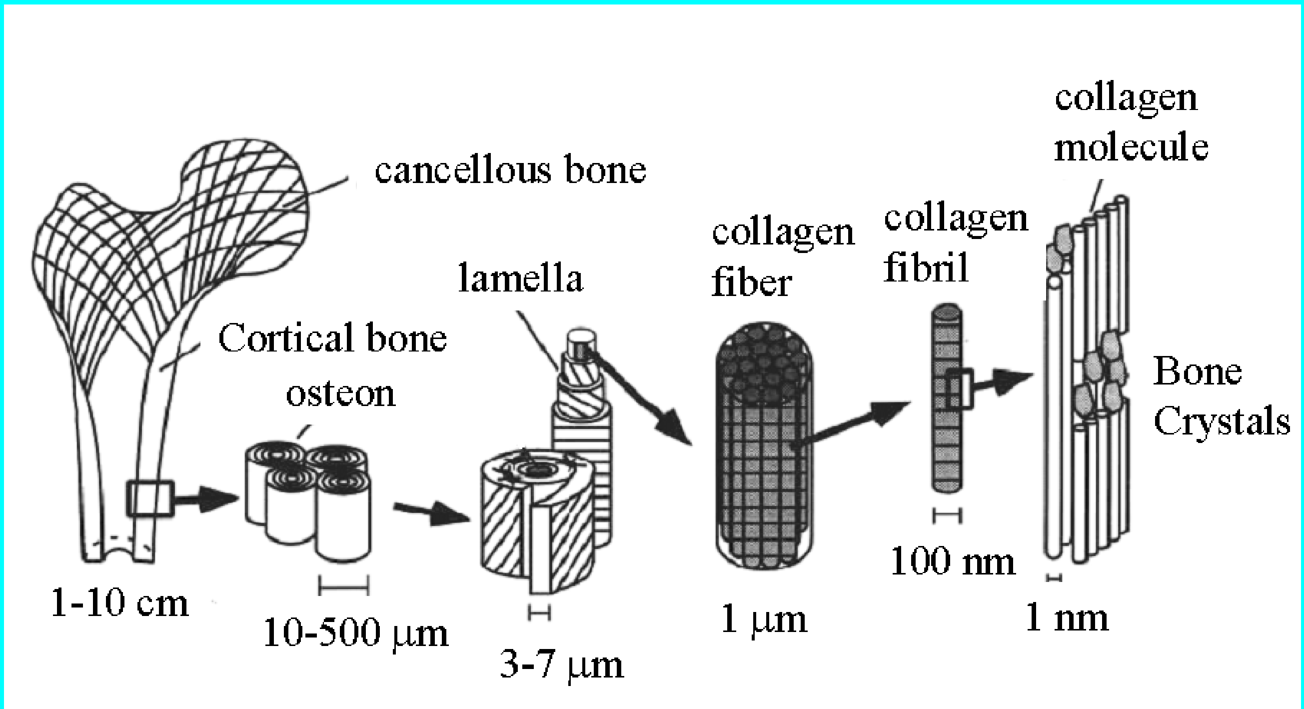

Nanofiber Testing Device

Journal of the Royal Society Interface, 2006.

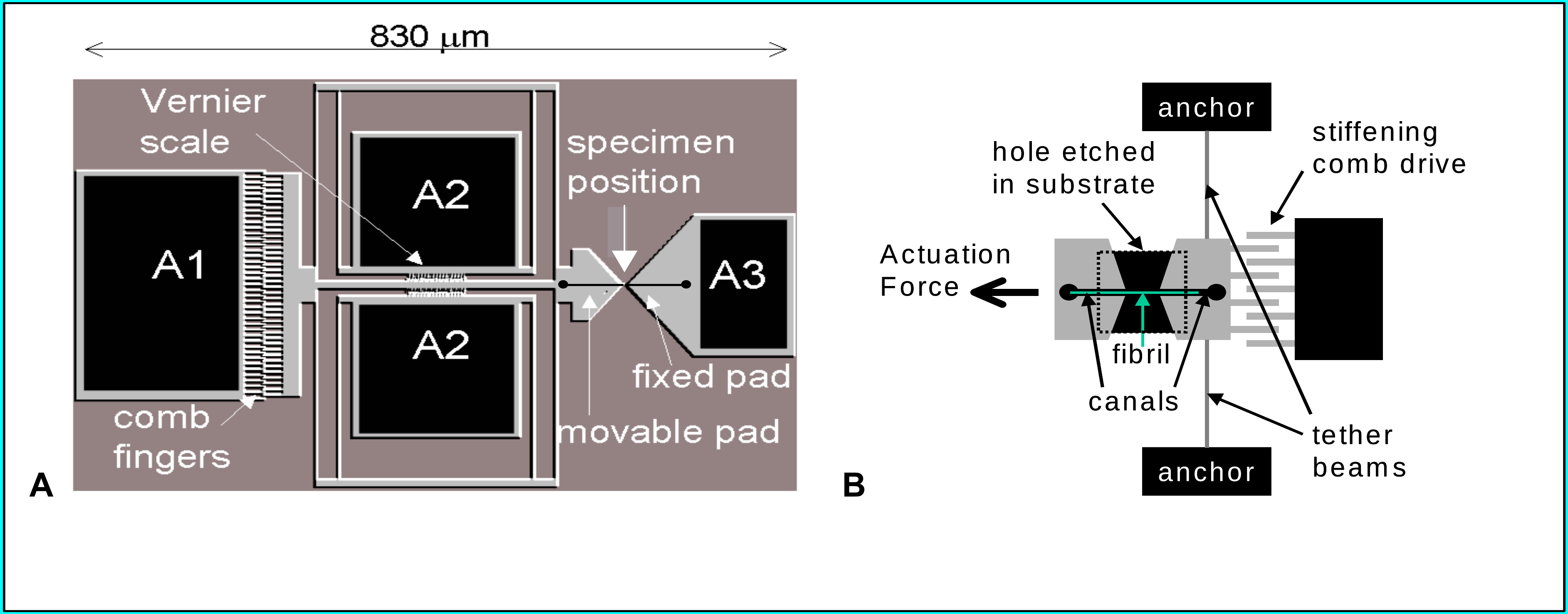

Force: 0.1-100 μN
Displacement: 1-5 μm

Labeling fibrils using fluorescent antibodies

1. Imaging using SEM
2. Labeling

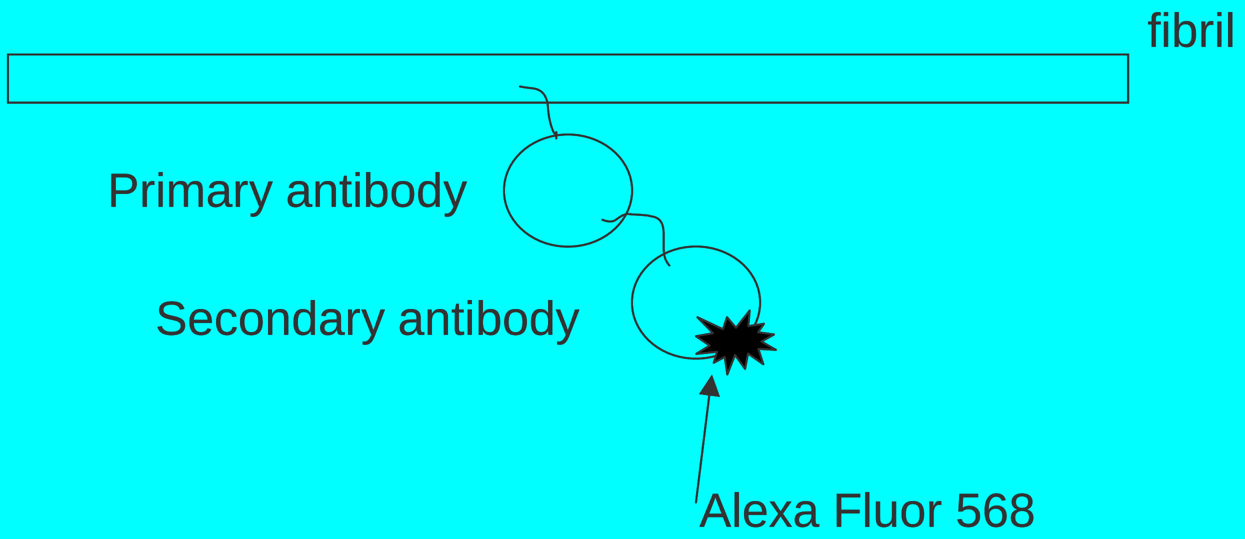

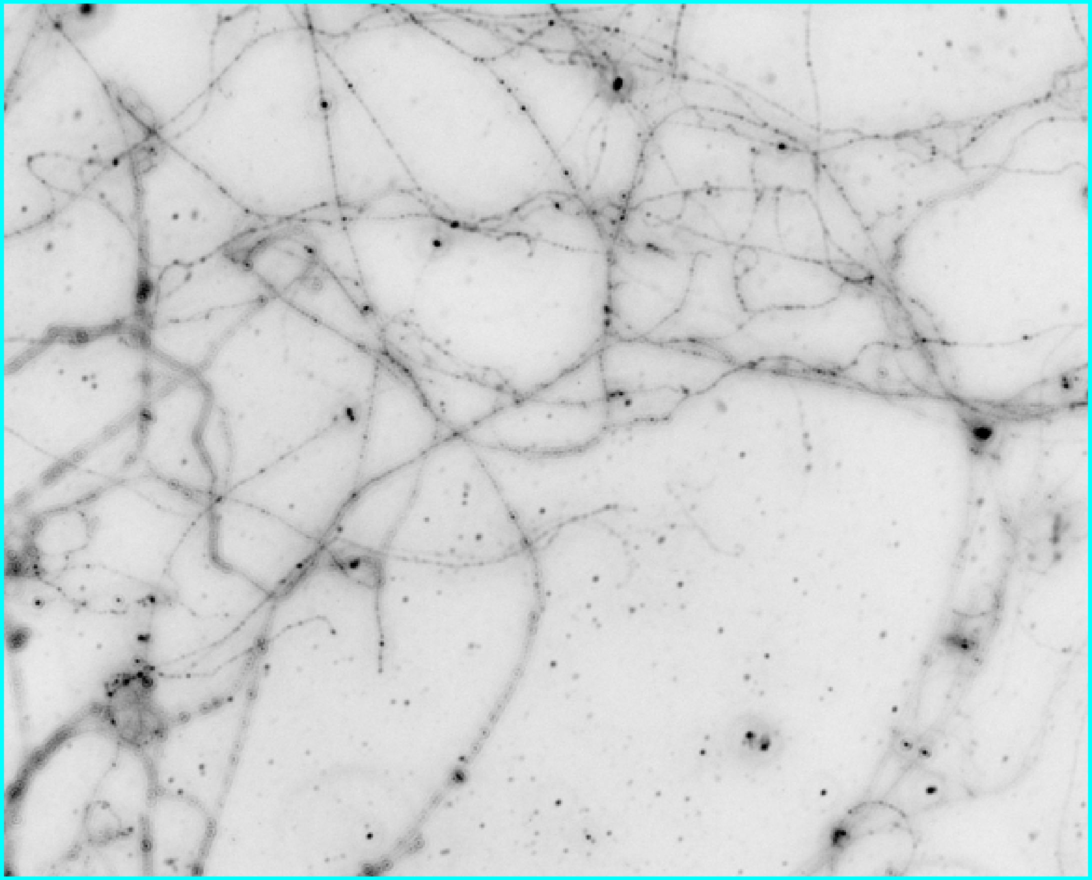

Fluorescently Labeled Collagen Fibers (Negative Image)

Different dilutions of the fibrils were imaged using SEM to determine the appropriate dilution at which individual fibrils were distinguishable. The fibrils were labeled with fluorescent antibodies to achieve contrast and brightness under optical microscope for 5 minutes. Anti-fading agents being tried to allow 30 minutes of manipulation time.

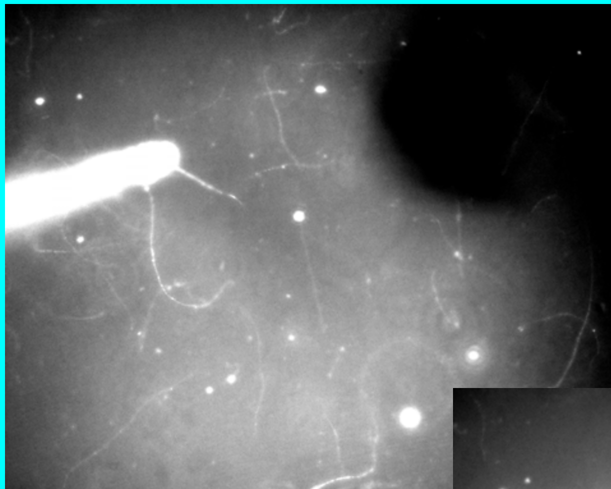

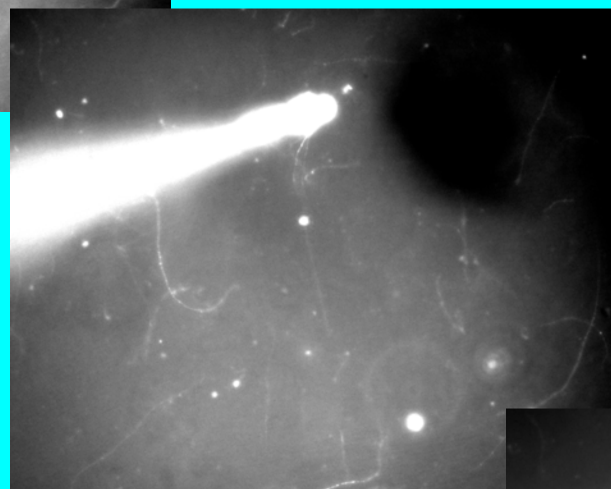

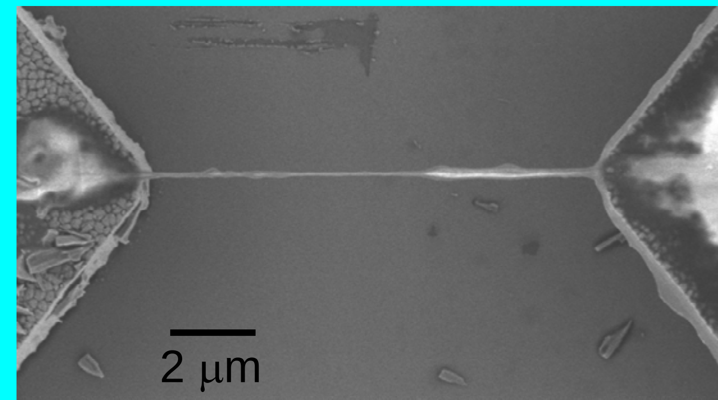

Manipulation using micropipette

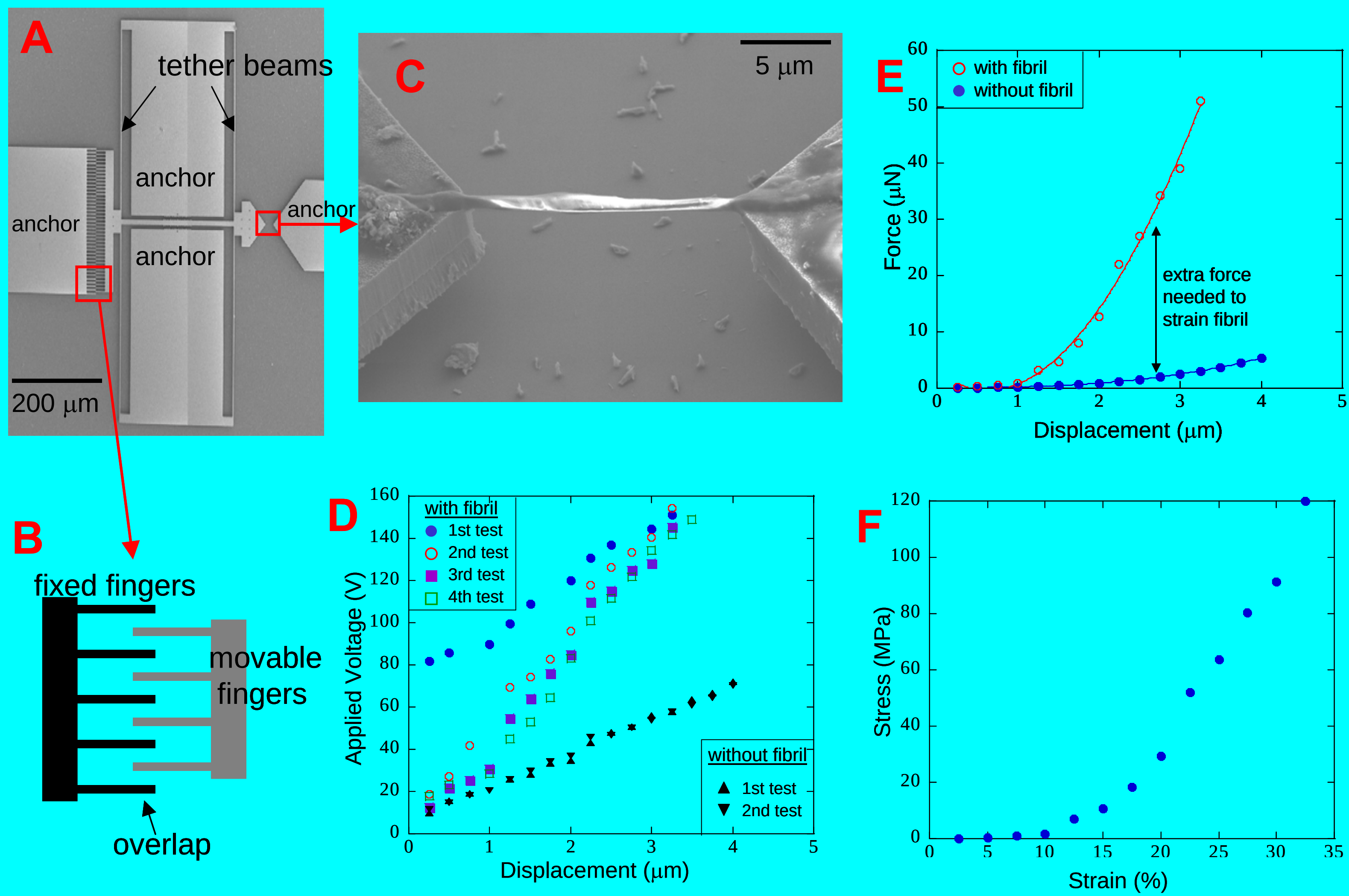

A
tether beams
anchor
anchor
anchor
anchor
200 μm
C
5 μm
E
with fibril
without fibril
Force (μN)
extra force needed to strain fibril
Displacement (μm)
B
fixed fingers
movable fingers
overlap
D
with fibril
1st test
2nd test
3rd test
4th test
without fibril
1st test
2nd test
Applied Voltage (V)
Displacement (μm)
F
Stress (MPa)
Strain (%)